PHASE SEPARATION OF METAL OR METAL-OXIDE MICROPARTICLES IN SOLID POLYMER MATRICES

BY

CINDY LOU FLENNIKEN

A DISSERTATION PRESENTED TO THE GRADUATE COUNCIL
OF THE UNIVERSITY OF FLORIDA IN
PARTIAL FULFILLMENT OF THE REQUIREMENTS
FOR THE DEGREE OF DOCTOR OF PHILOSOPHY

UNIVERSITY OF FLORIDA

1984

To my Family for the wealth of understanding
and encouragement which they provided.

ACKNOWLEDGEMENTS

The author wishes to thank all her committee members for their suggestions and guidance, especially Dr. Eugene P. Goldberg for his constructive criticisms and direction throughout this project and Dr. J. J. Hren for his technical dicussions. Acknowledgement is also made of Dr. R. Tannenbaum's contribution to interpretation of the organometallic chemistry involved in this study. The use of MAIC (Major Analytical Instrumentation Center) facilities and the cooperation of its staff were essential to the research presented in this dissertation.

Warm thanks are also extended to Dr. Henry Catherino in Detroit, Michigan, for his encouragement to pursue graduate studies; to Dr. J. S. Lin for his assistance with the SAXS studies at Oak Ridge National Laboratories; to Ms. Peg Mochel at the Materials Research Laboratory at the University of Illinois for her willing assistance on the electron beam decomposition studies; and to Dr. R. C. Stoufer for his assistance in evaluating the magnetic characteristics of these systems.

A special thank you is extended to Stuart Cheshire and Amy Smith for providing constant encouragement and a warm home environment during the writing of this manuscript. The author wishes to express gratitude and appreciaton to Bill Longo, Jan Stacholy, John Sheets, David Osborn, Jeff Larson, Mindy Donenfeld, Ching-Wang Luo, and Richard Robinson for their friendship, understanding, and assistance.

Thanks go to the faculty and staff for their varied assistance: E. J. Jenkins, Drs. Joe Newkirk, H. C. Aldrich and R. H. Berg III for their assistance with TEM sample preparations and studies; to Guy LaTorre and Frank Sodek, for their varied skills and help; to Mildred Neal for her assistance in literature searches at the Chemistry Library; to the Engineering Publications Department for their excellent graphic works; to and Michelle Smith for her patience in typing this manuscript.

TABLE OF CONTENTS

LIST OF TABLES

LIST OF FIGURES

Abstract of Dissertation Presented to the Graduate Council
of the University of Florida in Partial Fulfillment of the
Requirements for the Degree of Doctor of Philosophy

PHASE SEPARATION OF METAL OR METAL-OXIDE MICROPARTICLES
IN SOLID POLYMER MATRICES

By

Cindy Lou Flenniken

December 1984

Chairperson: Eugene P. Goldberg
Major Department: Materials Science and Engineering

The aim of this study was the synthesis and characterization of polymer composites in which microscopic metal or metal-oxide particles were incorporated by thermal, photolytic, or electron beam decompositions of solid solutions of organometallic complexes in polymers. This study involved the preparation of metal carbonyl solid solutions in polymers and the phase separation decomposition of the organometallic complex to form metal or metal-oxide dispersions of very small particle size (15-250/).

This approach to the preparation of metal-polymer composites may afford unique opportunities for investigating fundamental aspects of nucleation and growth of metal and metal-oxide clusters in the solid state as well as the properties of such microparticles as a function of cluster size, concentration, and environment. Many interesting

catalysis, microelectronics and imaging applications appear possible for metal-polymer composites made by this phase-separation method.

As model systems $Fe(CO)_5$, $Fe_3(CO)_{12}$, and $Co_2(CO)_8$ were studied as the organometallic complexes in the following polymer matrices: bisphenol polycarbonate (PC), polyvinylidene fluoride (PVF_2), polydimethylsiloxane (PSi), polystyrene (PS), aromatic polysulfone (PSF), and polymethylmethacrylate (PMMA). Polymers with varied molecular structures, morphologies, and mechanical properties were selected to assess interactions with active metal species and evaluate effects upon physical properties.

The hydrocarbon solvents used to form the homogeneous metal carbonyl-polymer solutions and the chemical structure of the polymer were shown to significantly affect chemical interactions with the organometallic complexes and to influence the morphologies and properties of the composites. The microparticles produced were observed to be a function of matrix polymer interactions as evidenced by the formation of FeF_2 and FeS in PVF_2 and PSF. The reactive carbonyl species formed during the solid state decomposition was shown to interact with the matrix to crosslink the polymer in the case of PVF_2 or even promote degradation in the case of polycarbonate. Solid state decomposition of carbonyls were faster than in solution. IR extinction coefficients were also found to decrease in solid polymer matrices presumably due to more restricted vibrational freedom.

By clarification of the variables which govern the solid state decomposition chemistry, it is anticipated that this phase separation technique may be improved to afford more precise control of the decompositions and the resulting composite compositions.

1. INTRODUCTION

Electronic devices and materials derived from unique polymers will become increasingly important technologically (1). Current electronic materials applications often involve metals, chalcogenides, ceramics, and other inorganic substances combined with polymers which function primarily in an electrically passive manner as insulators or dielectrics. Depending upon the application, the utility of available electronically active materials may be limited by factors such as weight, fragility, fabrication problems, corrosion, scarcity, and high cost. The trend in high mechanical strength materials has been toward filled or composite polymers. Advantages commonly associated with polymeric materials include high strength-to-weight ratios, toughness, low cost, molecular tailoring of desired properties, and the ease of fabrication into complex shapes. Our objective in this research has therefore been to explore opportunities for preparing novel metal-polymer composites with special interest in obtaining materials with unusual electronic or mechanical properties.

Metal-polymer composites are conventionally prepared by physically mixing metal or metal oxide powders with a polymer and fabricating mixtures by extrusion or molding into materials containing large metal or metal oxide particles dispersed in the polymer matrix. Particle size and shape, volume loading of filler, fabrication technique, specific

gravity of the metal versus the polymer, and compatibility (surface interactions) of the polymer with the metal are important factors affecting the properties of such conventional metal-polymer composite systems.

Fine dispersions of metals in a polymer matrix could combine the interesting electrical properties of metals with the useful mechanical and thermal properties (such as strength, rigidity, high softening temperature, and good corrosion resistance) of polymers to produce a variety of new technologically significant materials (2). Applications for such compositions include (a) photorecording and microcircuitry materials--by selective formation of free metallic species in polymer matrices by special control of phase separations; (b) magnetic materials for magnetic recording or magneto-optical switching devices; (c) polymers of high mechanical modulus and/or electrical conductivity; (d) metal-polymer catalysts.

In contrast to conventional composites or filled polymer compositions, which are prepared by dispersion of particles or fibers in a polymer matrix, this study has involved the preparation of metal carbonyl solid solutions in polymers and the phase separation decomposition of the organometallic complex to form metal or metal oxide dispersions of very small particle size. This novel preparative method has been shown to yield microscopic metal or metal oxide particle dispersions by thermal, photolytic or electron beam decompositions of the solid solutions of organometallic complexes in polymers. The nascent metal species or organometallic intermediates created by UV photolysis, thermal, or electron beam treatments in a polymeric matrix are highly reactive species. This study has been aimed at

understanding chemical reaction pathways as well as the structure and properties of the complex composite products.

The growing number and variety of organometallic complexes that can serve as reagents in selective organic synthesis reactions is a very exciting aspect of contempory synthetic chemistry (3). Many metal carbonyl cluster complexes have been prepared in recent years (4), and extensive studies of the intramolecular chemistry and ligand exchange reactions (5) of these complexes have been carried out. Less is known about the details of reactions in which metal-metal bonds in clusters are formed and broken, but the information which is available (4) indicates that such reactions may be quite useful in developing new transition metal systems for use in synthetic and catalytic processes.

Most metal carbonyls produce very labile complexes upon photolytic or thermal treatments. Frozen gas matrices have most commonly been used to study the labile intermediates (metal carbonyl fragments) generated by insitu photolysis of parent molecules (6, 7). It has been proposed that the driving forces for cluster complex decomposition arises from the expulsion of a molecule of relatively stable mononuclear metal carbonyl, leaving behind a coordinatively unsaturated intermediate which (in the absence of other reagents) oligomerizes to form a higher coordinatively saturated cluster (8). This suggests that in the presence of organic ligands such decompositions might give rise to active catalysts. In fact, numerous metal complex catalysts have been attached to crosslinked polymer supports (9). Though the insoluble catalysts are easily separated from reaction mixtures (unlike their homogeneous analogs), difficulties with such polymer-bound catalysts

systems occur. Changes in activity and selectivity due to the altered ligand environment have been observed.

In order to relate unstable species observed in a rigid matrix (frozen gas matrix) to possible photochemical mechanisms in solution, it has been very useful to study reactions in a variety of matrix media and at different temperatures. Polymers have provided organic photochemists with convenient and inexpensive matrices for trapping relatively unstable luminescent intermediates and free radicals at temperatures between 80-350°K (10, 11). However, the use of polymer matrices for studying decompositions of metal carbonyls has been limited probably because solute IR bands are generally much broader than those exhibited by the frozen gas matrices. Nevertheless, the chemical structure of a polymer may be readily varied to study the interaction of reactive metal carbonyls in an inert matrix or one in which functional groups of the polymer may react with the labile carbonyl fragments.

In spite of the many studies on a great variety of ligands much fundamental quantitative kinetic and thermodynamic information is still lacking regarding the simplest interconversions of the metal carbonyls and the active metallic species they produce on decomposition. This is also the case for reactions of polynuclear metal carbonyl cluster compounds with CO and for reactions in which carbonyls act as homogeneous catalysts or catalyst precursors (12). In this study we have sought to understand how such active species may react with (and in the presence of) a polymeric matrix, solvents, the atmospheric environments, and with each other. Reaction with polymer chains may lead to degradation or crosslinking of a polymer matrix whereas interactions of active species with each other and the atmosphere may create small

metal or metal oxide clusters. A complex relationship must exist between such active organometallic species and the molecular structure of the polymer matrix.

As model systems for studying the synthesis and properties of metal-polymer composites prepared by solid state phase separation, $Fe(CO)_5$, $Fe_3(CO)_{12}$ and $Co_2(CO)_8$ were used as the organometallic complexes with the following polymers: bisphenol polycarbonate (PC), polyvinylidene fluoride (PVF_2), polydimethylsiloxane (PSi), polystyrene (PS), aromatic polysulfone (PSF) and polymethylmethacrylate (PMMA). Polymers with varied molecular structures, morphologies and mechanical properties were selected to assess interactions with active metal species and to evaluate effects upon physical properties.

This approach to the preparation of metal-polymer composites, as already suggested, may afford unique opportunities for investigating some fundamental aspects of nucleation and growth of metal and metal oxide clusters in the solid state as well as the properties of such microparticles. The resulting metal containing polymers may prove interesting as catalysts, magnetic or conducting polymers, semi-insulators, and microelectronic materials (13).

2. BACKGROUND

2.1 Conventional Metal-Polymer Composites

Polymeric composite materials play an increasingly important role in meeting the materials needs of today's technological society because of their light weight strength, flexibility, toughness, and ability to be readily formed into intricate shapes (1). The fillers may be of a variety of materials (glass, metal, cellulose) and structures (fibers, powders, beads).

Metal-polymer composites are conventionally prepared by physically mixing metal or metal oxide powders with a polymer and fabricating mixtures by extrusion or molding into materials containing relatively large metal or metal oxide particles dispersed in the polymer matrix. Particle size and shape, volume loading of filler, fabrication technique, specific gravity of the metal versus the polymer, and compatibility (surface interactions) of the polymer with the metal are important factors affecting properties of such conventional composite systems. It is not easy to control dispersion homogeneity and aggregation in such blended composites.

The concept of polymer reinforcement using fibers is important, but there are relatively few examples of metal-polymer composites of this type. Fiberglass or graphite fiber-reinforced plastics are two commonplace examples. More currently, boron-reinforced epoxy composites are in development for jet engine and fuselage components and even as complete aircraft wings (14).

Another type of composite technology is paints made conductive by polymer suspension of small metallic particles in a polymer latex or solution (acting as carrier fluid and binder). The silver or carbon conductive paints used in electron microscopy to conduct the electron beam current away from the sample to prevent beam damage are examples of this form of metal-polymer composite. Magnetic recording tapes also represent metal-polymer composite technology. Modern recording tapes call for the coating of fine uniform dispersions of oriented particles (which exhibit high coercivity) onto thin polymeric films. Particles of iron oxide, γ-Fe_2O_3, were first used in the 1930's as magnetic recording materials (15). A list of the most recently improved particles used for this purpose include Fe_2O_3-Fe_3O_4 compositions, cobalt-modified iron oxides and chromium dioxide. The desire to increase the coercivity of these materials corresponds to more attractive magnetic properties but seem also invariably to be associated with thermal, mechanical, or chemical instability (16).

The focus of this research has been upon the preparation and characterization of metal-polymer composites; more specifically, a novel phase separation method has been investigated to create a homogeneous dispersion of small metal or metal-oxide particles in a solid polymer matrix. Such fine dispersions of metals in polymer matrices could combine the useful electronic and magnetic properties of metals with the mechanical and thermal properties (such as strength, rigidity, high softening temperature, and good corrosion resistance) of polymers to produce a variety of new and interesting materials (2).

2.2 Metal-Polymer Composites by Solid State Phase Separation

The aim of this study was to prepare metal-polymer composites by a phase separation method to create a homogeneous dispersion of metal or metal oxide in a solid polymer matrix. The approach used was to dissolve organometallic complexes in polymer solutions, cast films and then decompose the organometallic-polymer films using thermal, photolytic or electron beam energy (see Figure 1). This method of preparation should overcome many of the difficulties associated with mechanically blended composites and provide a better understanding of organometallic complex chemistry.

Nascent metallic species created by UV photolysis or by thermal or electron beam decomposition in a polymer matrix should be highly reactive (17, 18). The primary process is the photochemistry of simple carbonyls is the formation of a coordinatively unsaturated species $M(CO)_{n-1}$ (19).

$$M(CO)_n \xrightarrow{h\nu} [M(CO)_{n-1}]^* \longrightarrow M(CO)_{n-1} + CO$$

Continued irradiation often leads to further carbonyl abstraction. Stabilization of these intermediates may be brought about:

a) by recombination with CO to form $M(CO)_n$

b) by reaction with a metal carbonyl:

$$M(CO)_{n-1} + m\ M'_x(CO)_y \longrightarrow M(CO)_{n-1}[M'_x(CO)_y]_m$$

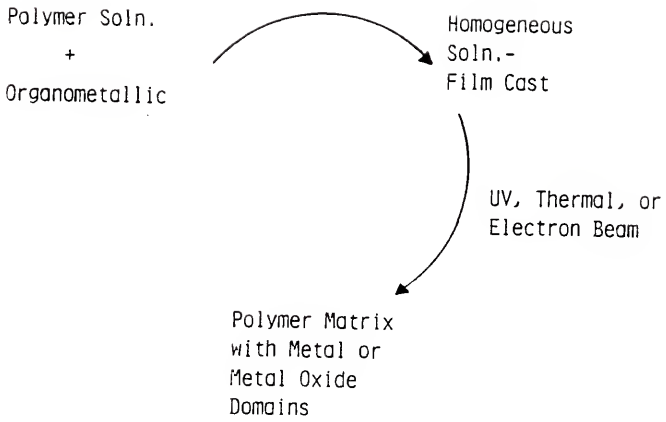

Figure 1. Concept for Producing Metal-Polymer Composite Films.

c) by addition of a ligand L having n- or π-donor properties:

$$M(CO)_{n-1} + L \longrightarrow LM(CO)_{n-1}$$

d) by reaction with a molecule X-Y according to

$$M(CO)_{n-1} + X\text{-}Y \longrightarrow (CO)_{n-1}M \begin{matrix} X \\ \diagdown \\ Y \end{matrix}$$

The emphasis of this research has been directed to process c where the ligand is a polymeric system (polymer and solvent). In this case the metal ions/radicals may follow several pathways of reaction: (a) interaction with remnant solvent to produce further photosensitive complexes (20), (b) attachment to the polymer, a process that can lead to various polymer degradation, crosslinking, or metal attachment processes, and (c) aggregation of metal species to form very small microcluster.

These processes may occur and be significantly influenced by reducing or oxidative atmospheres. The chemistry of the system (i.e. the relative importance of each process) is determined by the structure of the solid polymer matrix (molecular weight, crystallinity and polarity), remnant solvent and its structure, and by the rate of the decomposition process as compared to the diffusion time of the active metal species and gases through the solid polymer matrix (21).

2.3 Chemistry of Metal Carbonyls

2.3.1 Disproportionation Reactions of Metal Carbonyls

The metals of group VII and VIII (iron and cobalt) are known to react with strong n-donars to form ionic metal carbonylates in a

so-called "base reaction" (19, 22, 23). This reaction is shown below for both $Fe(CO)_5$ and $Co_2(CO)_8$ with dimethylformamide (DMF).

$$(1)\quad 5\ Fe(CO)_5 + 6\ DMF \xrightarrow[85^0C]{} [Fe(DMF)_6][Fe_4(CO)_{13}] + 12\ CO$$

$$(2)\quad 3\ Co_2(CO)_8 + 12\ DMF \longrightarrow Co^{II}(DMF)_6[Co(CO)_4]_2 + 8\ CO$$

$Fe_3(CO)_{12}$ is not observed to undergo this disproportionation reaction with DMF. The base reaction is of interest to our study because PVF_2 is soluble only in DMF for our film casting technique. If the resultant cation-anion complex is treated with an acid (hydrogen donor), metal hydrides are formed. Compounds of transition metals (M) with M-H bonds are of critical importance in many catalytic reactions (24). The first known complexes with M-H bonds were in fact the hydrido carbonyls $H_2Fe(CO)_4$ and $HCo(CO)_4$ made in the 1930's by W. Heiber. The hydrido cobalt tetracarbonyl has been demonstrated to react with styrenes having various alkyl substituents (bound either to the α- or β-position of styrene) in hydroformylation and hydrogenation reactions (25). These reactions appear to be subject to steric effects of the substituents.

2.3.2 Metal Carbonyl Reactions with Monoolefins

One aspect of metal carbonyl chemistry pertinent for consideration here is the interaction with isolated double bonds. Molecular orbital theory suggests that a double bond will coordinate with the metal in a manner similar to carbon monoxide (24, 26). The substitution of one CO by a double bond would therefore produce a complex containing the C=C group: i.e. $Fe(C{=}C)_4$. Indeed, in recent literature, there are several

reports concerning the formation of olefin-iron tetracarbonyl complexes. The first example was the preparation of acrylonitrile iron tetracarbonyl from acrylonitrile and $Fe_2(CO)_9$ (27). The same complex may also be obtained with $Fe(CO)_5$ upon irradiation (28). This suggests that $Fe(CO)_5$ is first converted to $Fe_2(CO)_9$ and then reacts with the double bond. The x-ray data for this complex shows that the iron atom is bonded to the C=C group rather than to the -C≡N or the nitrogen atom (29).

Kirch and Orchin (30) observed the oxo reaction of dicobalt octacarbonyl with olefins to form aldehydes proceeds by an olefin cobalt hydrocarbonyl intermediate. It has further been established that the rate of the oxo reaction is inversely proportional to the carbon monoxide partial pressure. As discussed earlier in this text, the cobalt hydrocarbonyl may be prepared under CO by disporportionation with dimethylformamide according to the equation

$$3\ Co_2(CO)_8 + 12\ DMF \longrightarrow 2\ Co(DMF)_6\ [Co(CO)_4]_2 + 8\ CO$$

$$Co(DMF)_6[Co(CO)_4]_2 + 2\ HCl \longrightarrow 2\ HCo(CO)_4 + CoCl_2 + 6\ DMF$$

Dubois and Garrou (31) observed that $Co_2(CO)_8$ catalyzed reaction of acrylonitrile with CO/H_2 in methanol is both temperature and ligand sensitive. The selectivity and activity of cobalt catalytic complexes can be altered dramatically by the presence of ancilliary ligands such as amines and phosphines (32). It has also been shown that when monoolefins of various structures are heated with iron carbonyl, geometrical and positional isomerization occurs (33) and that small

amounts of polar substances appear to promote this isomerization (34). Through variation in solvent systems, it was concluded that this isomerization also occurred via the iron carbonyl hydrides. It is well known that iron carbonyl hydrides are active catalysts for hydrogenation and isomerization of olefins (35, 36) as are the cobalt carbonyls (37, 38).

2.3.3 Metal Carbonyl Reactions with Conjugated and Nonconjugated Dienes

The most common feature of $Fe(CO)_5$ chemistry is its interaction with conjugated or nonconjugated dienes, with the formation of the $Fe(CO)_3$ moiety. Diene-iron carbonyl complexes were first prepared by two entirely different synthetic methods. In 1930, Reihlen and coworkers (39) obtained butadiene-iron tricarbonyl by reaction of butadiene with iron pentacarbonyl, and in 1953 Reppe and Vetter (40, 39) reported the formation of organoiron compounds (since shown to be diene-iron carbonyl complexes) following reaction of acetylene with iron carbonyls. The diene-iron carbonyl complex was further investigated by Hallam and Pauson in 1958, and was found to resist hydrogenation and not to undergo Diels-Alder type reactions (41). Spectroscopic and chemical evidence led to the suggestion that the butadiene molecule remained essentially intact in the organoiron complex. Furthermore, it was shown that an analogous compound, 1,3-cyclohexadiene-iron-tricarbonyl could be prepared in a similar manner from 1,3-cyclohexadiene and $Fe(CO)_5$. It was therefore concluded that the diene system adopted a cis arrangement

of double bonds within the complex rather than trans. The following structure was proposed:

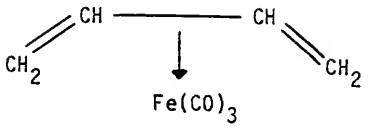

The butadiene structure is assumed to be nearly planar, with the iron atom lying below this plane approximately equidistant from the four carbon atoms of the diene system. The nature of the diene-iron bonding was presumed to involve interaction of the Fe atomic orbitals with molecular orbitals of the diene system as a whole. The structure is therefore more analogous to π-bonding in ferrocene (24) than to δ-type interactions implied by Reihlen (39). The conjugated diene system was considered to be essential for the formation of iron derivatives of this type.

It is now known that conjugated dienes and α,β-unsaturated carbonyls add hydrogen under oxo conditions (42) and were further demonstrated with isoprene by Kirch and Orchin. In 1961 Arnet and Pettit (43) and Stone et al. (44) reported a reaction involving the rearrangement of non-conjugated dienes to corresponding conjugated isomers of diene-iron tricarbonyl compounds following treatment with iron carbonyls [$Fe(CO)_5$ and $Fe_3(CO)_{12}$, respectively]. This was confirmed by Whitesides and Neilan (45) and postulated to proceed by metal hydride intermediates. Butadiene-$Fe(CO)_4$ and butadiene-$[Fe(CO)_4]_2$

have also been prepared from butadiene and $Fe_2(CO)_9$ (46). In these complexes, one of the carbon double bonds is π-bonded to the Fe atom. The butadiene-$Fe(CO)_4$ complex reacts with HCl to form the 1-methyl-π-allylchloroiron tricarbonyl complex, possibly through intermediate formation of a methyl-π-allyl-$Fe(CO)_4$ cation (46,47).

Interesting correlations exist between the electronic structure of the carbonyl groups for various diene-iron tricarbonyl complexes. Cationic ligands shift the C=O infrared absorption frequencies to higher values (48,49,50,51). In butadiene-iron tricarbonyl itself, there are two regions of carbonyl absorption (52), a narrow intense band at 2053 cm^{-1} and a broader band which is resolved into two maxima at 1985 and 1975 cm^{-1} (53). In analogous derivatives the gross structure of these bands is retained. However, positions shift according to the nature of the ligand (24,54).

The majority of diene-iron tricarbonyl complexes have been made by direct reaction of dienes with one of the three common iron carbonyls [$Fe(CO)_5$, $Fe_2CO)_9$ and $Fe_3(CO)_{12}$], either by simply heating the reagents together or by photochemical reaction. Using $Fe(CO)_5$, a temperature of 120-160°C is required and reactions are conducted in sealed tubes. In equivalent reactions using $Fe_3(CO)_{12}$, the products isolated are (with very few exceptions) diene-iron tricarbonyls (53).

The previously mentioned work with diene systems has demonstrated the reaction chemistry of iron carbonyls and opened the door to further interesting work for incorporating organometallics into polymers and for polymer synthesis. Indeed, reactions of chromium, molydenum, tungsten, and iron polyhalogenated organic compounds have been used to initiate the free radical polymerization of vinyl monomers (34).

2.3.4 Metal Carbonyl Reactions With Halides

Halogenated hydrocarbons have been found to be involved in reactions with metal carbonyls either as oxidizing agents (55,56) or entering as additional molecules (57,58) besides producing substitution products (59). Metal carbonyl chemistry in the presence of halides is of great importance for our consideration as we have selected methylene chloride as a polymer solvent. Iron pentacarbonyl reacts with organic halides if two conditions are met. First, the halide must be activated by at least one, and preferably two, groups such as cyano, phenyl or halogen (in decreasing order of effectiveness). Second, there must be at least two halogens on the same carbon atom or in very close proximity to each other. For example, dichlorodiphenylmethane $[(C_6H_5)_2CCl_2]$ reacts readily with $Fe(CO)_5$ (55) according to the following reaction

$$2\ Fe(CO)_5 + 2\ (C_6H_5)CCl_2 \longrightarrow 10\ CO + 2\ FeCl_2 + (C_6H_5)_2C{=}C(C_6H_5)_2$$

Furthermore, 1,2-dichloro-1,1,2,2-tetraphenylethane, even though it does not have geminal halogen atoms, reacts readily with $Fe(CO)_5$ according to the following reaction

$$Fe(CO)_5 + (C_6H_5)ClC\text{-}CCl(C_6H_5)_2 \longrightarrow 5\ CO + FeCl_2 + (C_6H_5)_2C{=}C(C_6H_5)_2$$

Molecular models of this halide reveal that the halogens (in the rotamer with the closest proximity of halogens) are as close as in a geminal dihalide and it is perhaps not surprising that reaction occurred. In no case does reaction occur with monohalogenated compounds, even when the halide is as strongly activated as that in triphenylmethyl chloride.

Another type of reaction leads to the formation of iron complexes of the general form $FeCl_2L_2$ or $FeCl_3L$, where L stands for ligands such as formamide, n-methylformamide, aniline, benzamide, acetamide, triphenylphosphine and triphenylarsine (59,60). All three iron carbonyls [$Fe(CO)_5$, $Fe_2(CO)_9$, $Fe_3(CO)_{12}$] react with these various ligands in the presence of chloroform to form halide adducts of the type $FeCl_2L_2$ or $FeCl_3L$. Solvents such as carbon tetrachloride, tetrachloroethane, and benzylchloride lead to similar oxidation reactions. Dichloroethane and methylene chloride lead to partial decomposition giving rise to impure compounds. The organic ligands which form $FeCl_2L_2$ complexes are formamide, methylformamide and acetamide, whereas those which form the $FeCl_3L$ complex are aniline, benzamide, triphenylphosphine and triphenylarsine. All ligands which have phenyl groups give rise to an iron complex of higher oxidation state.

The formation of complexes of the type $FeCl_2L_2$ or $FeCl_3L$ by the reaction of iron carbonyl with various ligands in the presence of halogenated hydrocarbons may be described by the following reaction mechanism. A substituted carbonyl complex of the type $Fe(CO)_4L$ forms and reacts with halogenated hydrocarbons to give rise to a halide complex. To verify this, $Fe(CO)_4L$ was allowed to react with chloroform, and the halide complex was obtained. In order to establish the reaction mechanism, Singh and Rivest (59) tried unsuccessfully to isolate the product formed from the oxidation reaction in chloroform. Therefore, they replaced the chloroform with diphenyldichloromethane and allowed this to react with $Fe(CO)_4(AsPh_3)$. They could then isolate

tetraphenylethylene and the halide complex. A possible mechanism for the reaction, therefore, can be suggested:

$$Fe(CO)_5 + 2\ L \longrightarrow Fe(CO)_3L_2 + 2\ CO$$

$$2\ Fe(CO)_3L_2 + 2\ (C_6H_5)_2CCl_2 \longrightarrow 2\ FeCl_2L_2 + (C_6H_5)_2C{=}C(C_6H_5)_2 + 6\ CO$$

In view of the foregoing, the decomposition of metal carbonyls in polymers of differing molecular structures (and using different mutual film casting solvents) may be expected to lead to significant differences in polymer interactions and decomposition chemistry. Polymers with different backbone structures and side chain groups were therefore studied to help explain the different physicochemical interactions which might occur with iron pentacarbonyl and other organometallic complexes.

Present electonically active materials are composed primarily from a variety of metals, semi-metals, ceramics and other inorganic substances with polymers used in the the electrically passive manner as insulators or dielectrics. Though synthetic polymers are generally regarded as electrically passive, the last two decades have seen the development of plastic conductive fibers (61,62). This has been achieved by mixing a high-modulus aramid polymeric solution with an organic metal solution from which fibers are spun. To increase conductivity, the fibers have been doped with iodine.

Yet another area of development is the use of metal polymer composites in novel circuitry applications. Printed circuit boards are commonly made by the photoetching process. Material losses are great

and the process is extremely complicated (high cost, low yield). Tabei et al. (63) investigated a new, much simpler process in which metal salts of organic acids are coated on an insulating substrate. When irradiated with UV light in a pattern of the desired circuit, metal ions (silver) are liberated so as to deposit the metal atoms to form aggregates. Electroless plating on the pattern is carried out with the deposited silver metal functioning as the nuclei for plating. This is a simple process to form printed circuits and can be applied to other fields such as photographic material, inlaid work, and photomasks.

2.4 Related Studies

Aside from the more conventional metal-polymer composites, there are other functions which compositions of metals and polymers may serve. There is also an active interest in the magnetic properties of particles small enough to contain single domains when there is no applied magnetic field. Magnetic fluids, or ferrofluids, exhibiting this characteristic are colloidal suspensions of ferro- or ferrimagnetic particles. This base of knowledge is of interest in our studies in that it provides an understanding of the interactions that may occur between small magnetic particles and the carrier fluid (the polymer matrix). In addition, carbonyls decomposed in the presence of organic ligands have been demonstrated to be active catalysts for acetylene trimerizations. Polymers also provide organic photochemists with a convenient matrix for isolating unstable and air sensitive organometallic complexes and clusters for study.

2.4.1 Ferrofluids and Other Colloidal Dispersions

There is an active interest in magnetic properties of stable dispersions of subdomain magnetic particles--ferrofluids. Particles

that are small enough, on energetic grounds, to contain but one domain without an applied magnetic field are termed subdomain (64). Ferrofluid chemistry is of interest in this metal-polymer composite study in that it provides an understanding of the interaction between the small magnetic particles and their dispersant in terms of concentration, dispersant chemical structure and surfactants.

A magnetic fluid or ferrofluid is a dispersion of ferro- or ferrimagnetic particles in a carrier fluid. The particles are coated with long chain surfactant molecules which prevents formation of agglomerates via the short range van der Waals interactions (65). Ultrafine particles (100 Å diameters) are used to reduce the longer range interactions between magnetic particles. The magnetic response of a ferrofluid is due to the coupling of response in individual magnetic particles with a substantial volume of the surrounding carrier liquid (66). Thus, when a magnetic field is applied to a ferrofluid this force is transmitted not only to the particle but also to the associated liquid phase. Coupling of these magnetic particles to the bulk liquid phase is accomplished by the use of surfactants (compounds with functional groups which adsorb onto the particle and still are solvated by the carrier liquid). A typical compound is oleic acid--a molecule containing a polar carboxylic end group that absorbs on the particle surface and a hydrocarbon moiety that is similar to the dispersing medium in chemical structure (66). By proper choice of stabilizing agents, magnetic properties may be conferred to a wide variety of liquid mediums. Depending on the structure and molecular weight of the dispersing agent and selected solvent, the effective thickness of the sheath may be varied from 30 to 1000 Å (67,68). It is the solvated

sheath which is responsible for the stability of very small particle suspensions.

The concept for preparing uniform dispersions of metals by phase separation in media of low dielectric constants is suggested by some metal colloidal literature. For example, thermolysis of transition-metal carbonyls in fluids under an inert atmosphere is a well known technique for the preparation of pure metal powders and a widely used process for the preparation of ferromagnetic cobalt particle dispersion (21,69). In 1966, Hess and Parker (21) thermally decomposed dicobalt octacarbonyl in solutions of polymer dispersants to form stable colloids of discrete particles which were separated by polymer coatings. In their work, they studied a large number of purified, uninhibited polymer and solvent systems. High concentrations of dicobalt octacarbonyl to polymer were used (typically 75 wt%). Dicobalt octacarbonyl (23 g) was dissolved in an organic solvent (188 ml). This solution was placed in a three-necked round-bottomed flask equipped with stirrer and condenser. Sufficient polymer was added to yield desired metal-to-polymer ratios and the system closed and stirred 5 minutes. The contents were then rapidly heated to achieve decomposition of the carbonyl. Carbon monoxide evolution was monitored and when it ceased the reaction mixture was cooled with continued stirring. These solutions were then film cast onto Mylar to 0.1-0.2 mm thickness and dried with infrared lamps. Magnetic properties were measured with a B-H meter with a 2000 gauss field strength. Electron photomicrographs of a 1:10 dilution of the cobalt particle sample to solvent were used to measure particle size.

Preparation of single-domain ferromagnetic cobalt particles with good magnetic properties depends on a delicate balance between

dispersant polymer, solvent and the growing metal particle. Hess and Parker concluded that variation of polymer composition, molecular weight and solvent affects particle size and colloid stability. They specifically observed that the most successful polymers are linear addition polymers of high molecular weight having relatively nonpolar backbones with pendent polar groups (i.e. amides) every 200 or so backbone carbon atoms. Stabilization of the cobalt particles results by adsorption of the polar group of the polymer to the metal particles to form a film which sterically hinders carbonyl decomposition at the metal surface, thereby retarding particle growth. The solvents for these systems should be less polar than the most polar groups in the polymer to minimize competition with the polymer-metal particle interaction. Though a number of condensation and addition polymers can act as the dispersant, Thomas (69) observed that polymers containing a relatively large percentage of highly polar groups promote the growth of smaller particles and that higher polymer concentrations produce a similar trend.

Hess and Parker's method was successfully applied to the preparation of small iron particles by Griffiths et al. (70) in polymer solutions. The macromolecules reportedly act as dispersing and stabilizing agents for the iron. Stable colloidal dispersions (50-100 A) of zero valent iron were obtained by thermolysis of low concentrations of $Fe(CO)_5$ in polymer solutions. All specimen preparation and manipulation were carried out in a nitrogen atmosphere. Magnetic measurements were made on a vibrating sample magnetometer. Diffraction and morphological characterization were accomplished using a electron microscope. Exposure of dispersions to

the atmosphere decreased the observed magnetic moment due to formation of an oxide film on the particles. Chlorinated solvent based dispersions were observed to generate chlorine which destroyed the γ-Fe_2O_3 spinel film passivity and promoted reaction with water to give β-FeOOH.

In 1979, Smith and Wychick (71) prepared stable colloidal dispersions (50-150 Å) of zero-valent iron by the thermolysis at 130-160°C under argon of $Fe(CO)_5$ in dilute solutions of functional polymers. The kinetics of the decomposition were monitored by following rates of CO evolution. Infrared spectral analysis was used to follow the progress of the reaction and GLC to determine either relative concentrations of $Fe_2(CO)_9$ and $Fe(CO)_5$. Completion of the thermolysis reaction yielded a strongly superparamagnetic Fe^0 dispersion. The percentage of iron in final dispersions was determined colorimetrically or by atomic absorption. Magnetic properties were evaluated using a vibrating sample magnetometer and transmission electron microscopy used to determine particle size. A "locus control" formalism of particle nucleation and growth was proposed to describe the formation of these colloidal dispersions (71). It was suggested that the polymer served as a catalyst for the decomposition of the metal carbonyl and induced particle nucleation. Selected polymer systems were termed "active" because the initial and overall rate of decomposition of $Fe(CO)_5$, as determined by the rate of CO evolution, was much faster in the presence of the active polymers (those with an amine function) than in solvent alone.

Using the refluxing technique of Hess and Parker, Berger and Manuel (72) noted that treatment of polybutadienes with iron carbonyl resulted in formation of polymers containing tricarbonyl complexes. Hampton's infrared analysis technique (73) was used to show the distribution of free double bonds remaining. The infrared spectra exhibited a pair of carbonyl stretching frequencies in the 2000 cm^{-1} region characteristic of tricarbonyl (conjugated diene) iron complexes. A combustion analysis for iron showed 20 wt% $Fe(CO)_3$. The complexing reactions for the polybutadiene were done with either iron pentacarbonyl or triiron dodecacarbonyl as the reagent in xylene or benzene, respectively. They observed substantial molecular weight breakdown in the recovered polymer when a hydrocarbon alone is used as solvent and that this could be avoided by addition of small amounts of polar nonacidic solvents (alcohol, ketone, or ether). Basic solvents and high temperature favored this incorporation of the iron carbonyl groups into the polymer to produce ferromagnetic products with enhanced thermal stability.

Chantrell et al. (65,74) studied the effect of dilution on the stability of a ferrofluid consisting of cobalt particles in toluene. The cobalt/toluene ferrofluid was prepared by the thermal decomposition of dicobalt octacarbonyl (using the method of Hess and Parker) with sodium dioctyl sulphosuccinate as surfactant (to stabilize the resultant colloidal dispersion and control particle size). Magnetic measurements were made at room temperature on a vibrating sample magnetometer. This data indicates the superparamagnetic character of the cobalt/toluene ferrofluid. The particle size distribution parameters were calculated from the low and high field magnetic behavior and found to be 50 Å.

The long term gravitational stability of the original cobalt/toluene fluid and commercial ferrofluid was tested and the change in concentration profile found to be negligible for both over a 50 day period. In order to test the dilution stability of the cobalt/toluene fluids, several toluene dilutions were prepared from the original fluid. The concentration profile clearly shows apparent instability of the fluid with the formation of larger aggregates of particles on dilution of the ferrofluid. Chantrell et al. proposed that this instability is due to a disturbance of the balance which must exist between the adsorbed surfactant on the surface of the particles in order to maintain the equilibrium between adsorbed and free surfactant. They concluded, therefore, that when making measurements on ferrofluids in large applied fields the magnitude of the field induced aggregation should be measured.

2.4.2 Organometallic Complexes as Catalysts

Another aspect of interest in composite chemistry is the use of organometallic complexes that serve as reagents in selective organic synthesis reactions (3). The feasibility of this was demonstrated by Vollhardt (8) in 1975 with the photochemical decomposition of η^5-cyclopentadienyl-cobalt dicarbonyl in the presence of organic ligands to produce active catalysts for acetylene trimerization at temperatures lower than that normally required. Further information is available which indicates such reactions may be quite useful in developing new transition metal systems for use in synthetic and catalytic processes. However, with various ligands much fundamental quantitative kinetic and thermodynamic information concerning metal carbonyls is still lacking in the literature (12,19,60).

Dispersed metal crystallites have been formed by thermal decomposition of metal carbonyl complexes anchored on both organic and inorganic supports (75). Derouane and Nagy (76) report that adsorption of $Ni(CO)_4$ on various oxide materials followed by thermal decomposition leads to the formation of stable, porous metallic crystallites. The interaction of the carbonyl with the support, the nature of the decomposition mechanism and resulting catalytic activity of the products warrant further investigation. These systems are capable of leading to improvements with respect to preparation of multimetallic catalysts by direct clustering of metals in a zero-valent state.

Metal-containing polymers offer potential utility as catalysts. Organometallic polymers for this purpose may be prepared by derivatizing preformed organic polymers with organometallic functions (77), or by preparing monomers which contain organometallic units and polymerizing these monomers (13,78). Many transition metal complex catalysts have been attached to crosslinked polymer supports. Difficulties with polymer-bound catalyst systems include changes in activity and selectivity due to the altered ligand environment (79); steric constraints imposed by the presence of the polymer structure in the vicinity of the attached complex (79,80); reduced activity due to the thermodynamic exclusion of reactant molecules from the solvent-swollen polymer support phase (81); and intraparticle mass transport effects on the reaction rate since the reactants must diffuse through the solvent-swollen polymer matrix to reach active complexes therein (79,81).

With regard to hydrocarbon media, it has been found that appropriate modification of alkyl methacrylates can result in outstanding dispersants for use in automotive lubricants (82). A better

understanding of the chemistry of these systems is provided in the literature and is relevant to this study. Fontana and Thomas (83) found that incorporation of 17 mole % N-vinyl-2-pyrrolidone (VP) into polylauryl methacrylate (PLMA) increased the adsorbed surface layer on silica to 200 Å (relative to 30 Å for samples without VP). They proposed that this thicker film results from preferential adsorption of the smaller number of more strongly polar pyrrolidone groups.

In a similar study, Fontana (84) was able to quantitatively demonstrate this surface adsorption phenomenom (via infrared spectroscopy) for a 20:1 mole ratio of alkyl methacrylate-polyglycol methacrylate copolymer (PAM-PG). The copolymer molecular weight was approximately 310,000 as determined from intrinsic viscosity measurements. Polyglycol methacrylate was the acting dispersant. Details of the determination of the pertinent extinction coefficients and calculations of adsorbed ester segments are described in a previous publication (83). The data demonstrate the exclusion of ester segments from attachment to the surface because of preferential adsorption of the polyglycol ether segments. Thus, the resultant polymer configuration is more extended away from the surface and aids in stabilizing the colloidal dispersion by virtue of its polar substituents.

2.4.3 Metal-Polymer Composites Prepared by Adsorption of Metal Carbonyl Solution onto Films

De Paoli (10,11) found that by incorporating the unstable metal carbonyls by adsorption into polymers he could work with them at ambient conditions without the inconvenience of cryogenic temperatures. He also noted that, in addition, the active carbonyl intermediates exhibited higher mobility and a higher local concentration of reagents in a polymer matrix. He used PTFE and PE (0.2 and 1.0 mm thick,

respectively) as matrices to study (via infrared spectroscopy) the photochemical products and reaction of $Fe(CO)_5$ with olefinic ligands (such as ethylene, acrylic acid, methylacrylate, butadiene, isoprene, norbornadiene). De Paoli felt that saturated hydro- or fluorocarbon polymers would not absorb the radiation used to induce the photochemical carbonyl process, and thus would not hinder the reaction nor themselves be degraded.

The sorption of $Fe(CO)_5$ in the polymer was carried out by soaking the film in a 10% solution of it in degassed hexane. This was followed by an ethanol wash under an inert atmosphere to prevent oxidation of iron pentacarbonyl on the surface. Sorption of the second reagent was achieved 1) for liquids, by soaking for the time required to saturate it, and 2) for gases, irradiation in an immersion well filled with the gas.

De Paoli noted that once iron pentacarbonyl was trapped inside the matrix it did not oxidize during the time required for IR experiments. Photochemical decompositions of the $Fe(CO)_5$ composites was done using a Philips HPK-125 W lamp with Vycor filters and an adapted Phillips HPLN-125 W lamp with Pyrex filters. Reactions were followed with a double beam IR spectrophotometer with control films used as references. To study the photo-fragments of $Fe(CO)_5$, irradiated films directly in the IR spectrophotometer. De Paoli observed that after 1 to 2 hours of visible light irradiation PTFE films treated with $Fe(CO)_5$ and butadiene produced spectra corresponding to butadiene iron tricarbonyl (ν_{CO}= 2060, 1995 cm^{-1}) and bis(butadiene) ironmonocarbonyl (ν_{CO}= 1985 cm^{-1}). Experiments with isoprene produced similar results. He observed that the IR spectra of these films did not change after one

week at ambient conditions or even after pumping air though them. Even heating the films containing dieneiron tricarbonyl compounds to 160°C produces no spectra changes. PTFE films pretreated with $Fe(CO)_5$ and irradiated in an immersion well filled with ethylene for 45 minutes show no absorptions due to $Fe(CO)_5$, only four peaks at 2092, 2029, 2014 and 1993 cm^{-1} (corresponding to substitution of one carbon monoxide by an ethylene).

Experiments with low density polyethylene (which is highly amorphous) allowed for higher degrees of carbonyl sorption. Irradiation for three minutes of PE films pretreated with $Fe(CO)_5$ and norbornadiene produced four new IR bands: 2098, 2032, 2020 and 2010 cm^{-1} as well as a band at 1730 cm^{-1}. Continued irradiation led to an increase in the 1730 cm^{-1} band while the others vanished. These four initial bands correspond to $(n^2\text{-NBD})Fe(CO)_4$ while the 1730 cm^{-1} absorption corresponds to a carbonyl inserted into a dimer of NBD.

Photolysis of PE-$Fe(CO)_5$-MMA for one minute shows complete disappearance of the ν_{CO} band of $Fe(CO)_5$ and the formation of four new bands at 2098, 2032, 2020 and 1996 cm^{-1}. These bands correspond to the compound methylacrylate-iron tetracarbonyl, a compound of the type $Fe(CO)_4L$. Further photolysis does not produce additional changes.

In solution the photochemical substitution of carbon monoxide in $Fe(CO)_5$ is assumed to follow an S_N1 type mechanism (19) and to decay to the very reactive $Fe(CO)_4$ species. De Paoli assumed this species to also to be formed in the polymer matrices. UV treatment of a PE-$Fe(CO)_5$ film showed two new absorptions at 2063 and 1973 cm^{-1} and the still remaining $Fe(CO)_5$ band at 1998 cm^{-1}. Kinetic measurements indicated a first order rate constant of 6.5 and 2.5 x 10^{-3} sec^{-1}, respectively.

The bands at 1973 and 1998 cm^{-1} are assigned to the photo-fragment $Fe(CO)_4$ and the other to a product of further fragmentation, probably $Fe(CO)_3$ (11).

De Paoli suggested that the molecules of iron pentacarbonyl are lodged in close proximity within the amorphous sites of the polymers, yet are sufficiently mobile for reaction to occur between the carbonyl and methylacrylate (or other second reagent) and to allow relatively rapid desorption of the CO out. De Paoli, however, assumed that there was no chemical effect of irradiation upon the polymer and hence that there was no interaction between the matrix and reactive carbonyl species. Literature (2,85,86,87), however, states that photolytic degradation of polymers does occur--thus UV stabilizers are often added to polymers to be exposed to an external environment. This suggests that radical species may have been formed within the polymers themselves which would also be open to reaction with the carbonyl.

Galembeck (88) also introduced metal carbonyls into polymer films by soaking the latter in ethanol solutions containing 10% iron pentacarbonyl for a period depending on the degree of crystallinity of the polymer. He observed that sorption of $Fe(CO)_5$ by polytetrafluorinated ethylene (PTFE) films 0.2 mm thick followed by insitu oxidation gives iron oxide-PTFE and that upon exposure to sunlight the $Fe(CO)_5$ treated PTFE forms $Fe_2(CO)_{12}$ dimer (89). He determined the original PTFE films to be 65% crystalline using x-ray diffraction. He irradiated samples left soaking for various periods of time in the carbonyl in the beam of a slide projector under which conditions the nonvolatile $Fe_2(CO)_{12}$ was formed. Complete oxidation of samples was then allowed to occur in air for three days. This was

followed by heating at 105°C to eliminate unreacted traces of $Fe(CO)_5$ (as indicated by IR). Following a wash in 1N sulfuric acid and ethanol and air drying, iron oxide content was determined gravimetrically. Iron oxide content ranged from 0.34 to 1.50% (w/w).

Particle size was determined using transmission electron microscopy. Samples were mechanically sliced and electron bombarded under vacuum in the TEM to achieve adequately thin samples for transmission. This procedure led to the depolymerization of the PTFE with evaporation of monomeric C_2F_4. Particles were observed to be rather uniformly distributed and spherically shaped with diameters of 15 to 80 Å. Size of the particles did appear to increase slightly for higher concentrations of iron oxide. Optical adsorption measurements were done using a photoacoustic technique. These measurements indicate the formation of two characteristic volume distributions of iron oxide particles in these PTFE composite materials, namely the 36 and 44 Å average diameter sizes.

2.4.4 Metal-Polymer Composites Prepared by Casting of Metal Carbonyl-Polymer Solutions

Cassen et al. (90) and Hitam et al. (91) used a solvent-casting technique to prepare metal carbonyl-polymer films. Hooker and Rest also tried the sorption technique but observed that a more uniform concentration of the carbonyl could be obtained throughout the polymer matrix by using this solvent-casting technique (92). They noted that chromium, molybdenum, and tungsten hexacarbonyls in polyvinyl chloride (PVC) showed broader and shifted carbonyl bands (between 1980 and 1974 cm^{-1}) suggesting a polymer-solute (THF) interaction. The generation of pentacarbonyl fragments and photoreversal are analogous to reactions observed in hydrocarbon glasses and frozen gas matrices.

They prepared 0.8 and 2.7 wt% solutions of PVC (0.5 g each) in 1,2-dichloromethane and tetrahydrofuran (THF), respectively. To each solution 4 mg of hexacarbonyl was added and the resulting solution poured into petri dishes. Samples were stored in the dark and allowed to dry overnight. This produced films approximately 40 μ thick. A water cooled mercury arc lamp was used as the photolysis source with samples at a distance of 12 cm. Filters were used to achieve irradiation at specific wavelengths: filter A, $\lambda < 350$ nm; filter B, $\lambda > 400$ nm.

Both IR and UV-visible spectra were used to follow the photolysis of these films. Figure 2 shows the IR spectra of UV irradiated $W(CO)_6$-PVC films. The photoreactions of the Group VI metal hexacarbonyls observed in PVC films were studied by Hooker and Rest. New IR bands appeared at 2074, 1929 and 1887 cm^{-1} with reduction in the parent band. A very slow reversal of the reaction occurred when the polymer was left in the dark for several days. $W(CO)_6$ films cast from dichloromethane also showed the same effect but with IR bands at a higher wavenumbers (2080, 1932, and 1888 cm^{-1}). In contrast, however, thermal reversal of the reaction in this film occurred after only a few minutes. These reactions are summarized in Figure 3. Similar results were observed for the UV irradiation of $Cr(CO)_6$ and $Mo(CO)_5$ films, although these hexacarbonyls were regenerated in the dark more quickly than the tungsten analogue.

Evidence for residual THF in films cast from this solvent was found when polymer bands were subtracted out of the spectra. Films cast from dichloroethane solution showed only a band at 1728 cm^{-1} for ketones. These bands did not disappear with irradiation (see Figure 2).

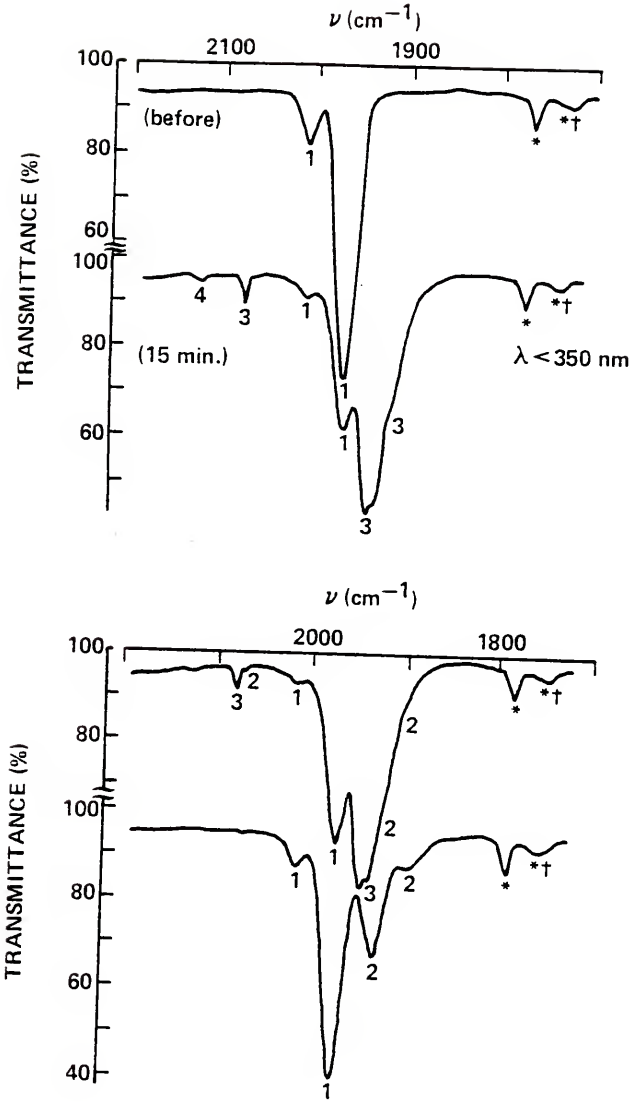

Figure 2. Infrared Spectra from an Experiment with $W(CO)_6$ in a PVC Film (Cast From THF): (a) Before Photolysis, at 12°K; (b) after 15 min. Photolysis, (λ<350 nm); (c) as (b) then Warming to 120°K and (d) as (c) then Further Warming to Room Temperature Bands Marked 1, 2, 3, and 4 are for $W(CO)_6$, $W(CO)_5(THF)$, $W(CO)_5$ and Free CO, Respectively. Bands Marked (*) and (+) are for Oxidized F Residues and Chloroketones, Respectively (92).

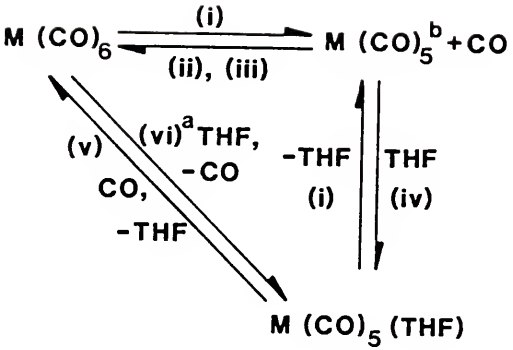

[a] Reaction observed in solution

[b] Unstable species observed in other low temperature matrices

Figure 3. Photoreactions of Group VI Metal Hexacarbonyls in PVC Films: (i) $\lambda<350$ nm at 12°K; (ii) hv $\lambda>400$ nm at 12°K; (iii) Warming to 200°K; (iv) Warming Between 100 and 200°K; (v) Thermal Reaction Above 200°K; (iv) $\lambda<350$ nm at 298 K°(92).

respectively and a broad but well resolved ν_{CO} band at higher wavenumbers. The bands are broad even when only 0.2 wt% of carbonyl is present in the polymer matrix, suggesting that significant polymer solute interactions exist. Lowering the temperature of the polymer films made the IR spectra of the hexacarbonyls slightly sharper, but no significant shift in band positions was noted. The ν_{CO} band at higher wavenumbers, which has been observed for metal hexacarbonyls in various hydrocarbon glasses at 77°K, probably results from site symmetry effects or from some distortion of the carbonyl molecules trapped in amorphous sites of the polymer matrix. For Group VIB metal hexacarbonyls, McIntyre (93) suggested the mechanism of the photochromic reaction to be

$$M(CO)_6 + h\nu \longrightarrow M(CO)_6^* \longrightarrow \underset{\text{(yellow)}}{M(CO)_5} + CO \qquad (1)$$

$$M(CO)_5 + D \rightleftharpoons M(CO)_5D \qquad (2)$$

$$M(CO)_5 + CO \longrightarrow M(CO)_6 \qquad (3)$$

D = charge donor

Experiments with both degassed and nondegassed solutions demonstrated the sensitivity of the rate of reaction (3) to traces of oxygen. Cyclohexane was checked with mass spectroscopy for impurities which would interfere with the reaction. Polystyrene films (0.05 cm thick) containing 1 wt% $Cr(CO)_6$ were prepared by casting from a

methylethyl ketone solution onto quartz plates in the dark. Photolytic decompositions were performed. McIntyre assumed a second-order rate law for reaction (3), the fading reaction, on the basis of the good linear plots of $1/A_t$ vs time. Exact extinction coefficients were not determined due to the extensive overlap of all absorption bands of $Cr(CO)_6$ and $Cr(CO)_5$, but a minimum value of ε = 1000 liter/mole·cm was suggested. The values of k/ε (rate constant/extinction coefficient) were 0.317 and 0.00025 for cyclohexane and polystyrene as solvent, respectively. This large difference is attributed to the greatly decreased mobility of CO in polystyrene relative to cyclohexane.

Massey and Orgel (94) dissolved $M(CO)_6$ (M = Cr, Mo or W) in a polymethylmethacrylate solution. With evaporation of the solvent and UV irradiation, the polymer assumed the color of the $M(CO)_5$ fragment (yellow). The $M(CO)_6$ complex was observed to regenerate with time in the dark. They further observed that the $M(CO)_5$ fragments in the PMMA matrix appeared to be stabilized by the oxygen donating groups in the polymer itself. This is supported by the work of Hooker and Rest (92) wherein the "naked" pentacarbonyl intermediates were not observed in a PVC matrix which contains no oxygen donator. The same technique was used by McIntyre (50) to study the flash-photolysis of $Cr(CO)_6$ in a polystyrene matrix. He also observed the thermal back reaction to regenerate $Cr(CO)_6$ but noted that it occurred at a rate much slower than in solution.

2.5 Metal-Polymer Composites by Phase Separation

2.5.1 Polymer Matrices Selected for Preparation of Metal-Polymer Composites

As model systems for studying the preparation of metal-polymer composites by solid state phase separation, we selected $Fe(CO)_5$, $Fe_3(CO)_{12}$ and $Co_2(CO)_8$ as the organometallic complexes and the following polymers: bisphenol polycarbonate (PC), polyvinylidene fluoride (PVF_2), polystyrene (PS), aromatic polysulfone (PSF), polymethylmethacrylate (PMMA) and polydimethylsiloxane rubber (PSi), (see Figure 4). Some of the criteria for selecting these polymers were

1. Commercially available and soluble thermoplastic polymers to facilitate sample preparation and analysis.
2. Mutual solubility of polymer and organometallic complex in common organic solvents.
3. Polymers exhibiting high melting and glass transition temperatures, preferably above the decomposition temperature of the metal carbonyl to be used.
4. Polymers with varied molecular structures, morphologies, and mechanical properties to assess interactions with active metal species and evaluate effects upon physical properties.

Polycarbonate (LEXAN®, 131-111, $\bar{M}_v$= 323,000) is soluble in benzene and polyvinylidene fluoride (Polyscience, Inc., $\bar{M}_v$= 119,000) is soluble in dimethylformamide. We knew from preliminary studies (95,96) that in the PC system both thermal and photolytic decompositions $Fe(CO)_5$ led to significant polymer-Fe interactions which were accompanied by severe

POLYCARBONATE (PC)

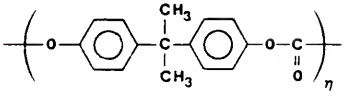

POLYSULFONE (PSF)

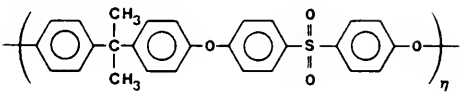

POLYSTYRENE (PS)

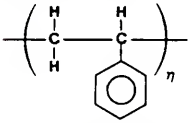

POLYMETHYLMETHACRYLATE (PMMA)

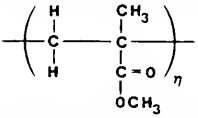

POLYVINYLIDENE FLUORIDE (PVF_2)

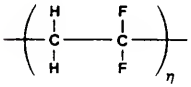

POLYDIMETHYLSILOXANE (PSI)

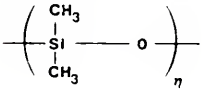

Figure 4. Polymers Selected For Metal-Polymer Composite Studies.

degradation of the polymer. The PC system may in fact be of interest for photoresist applications.

PVF_2-$Fe(CO)_5$ composites were initally studied in some detail in this laboratory by S. Reich and found to produce ferrimagnetic materials upon thermolysis due to formation of submicroscopic α-Fe and γ-Fe_2O_3 particles (97). The PVF_2-iron composites may be of interest for magnetic recording applications. The decomposition of $Fe(CO)_5$ in PVF_2 leads to some fluorine abstraction by Fe and slight crosslinking of the polymer yielding insoluble but tough, strong, magnetic polymer composite films. The PC and PVF_2 systems represent extremes of $Fe(CO)_5$-polymer chemistry. Other polymer media produce various degrees of Fe-Fe versus Fe-polymer bond formation. Investigation of polymers of differing molecular structures and the analysis of the products obtained with each polymer were undertaken to help establish mechanistic pathways for decompositions of $Fe(CO)_5$ and other organometallic complexes in polymeric matrices.

2.5.2 Organometallic Complexes Selected for Preparation of Metal-Polymer Composites

Sufficient literature is available concerning the incorporation of both Group VII and Group VIII metal carbonyls into various polymers to make the prospects of further studies interesting. However, for this research project we have limited our work to include $Fe(CO)_5$, $Fe_3(CO)_{12}$ and $Co_2(CO)_8$ (see Figure 5). These carbonyls were selected because of their availability, lower toxicity relative to other carbonyls (i.e., nickel) and because there exists a large body of knowledge concerning their thermal and photolytic decomposition reactions, though less information is available on the kinetics of these reactions. It was of interest to study the solid-state decomposition of mono- and trinuclear

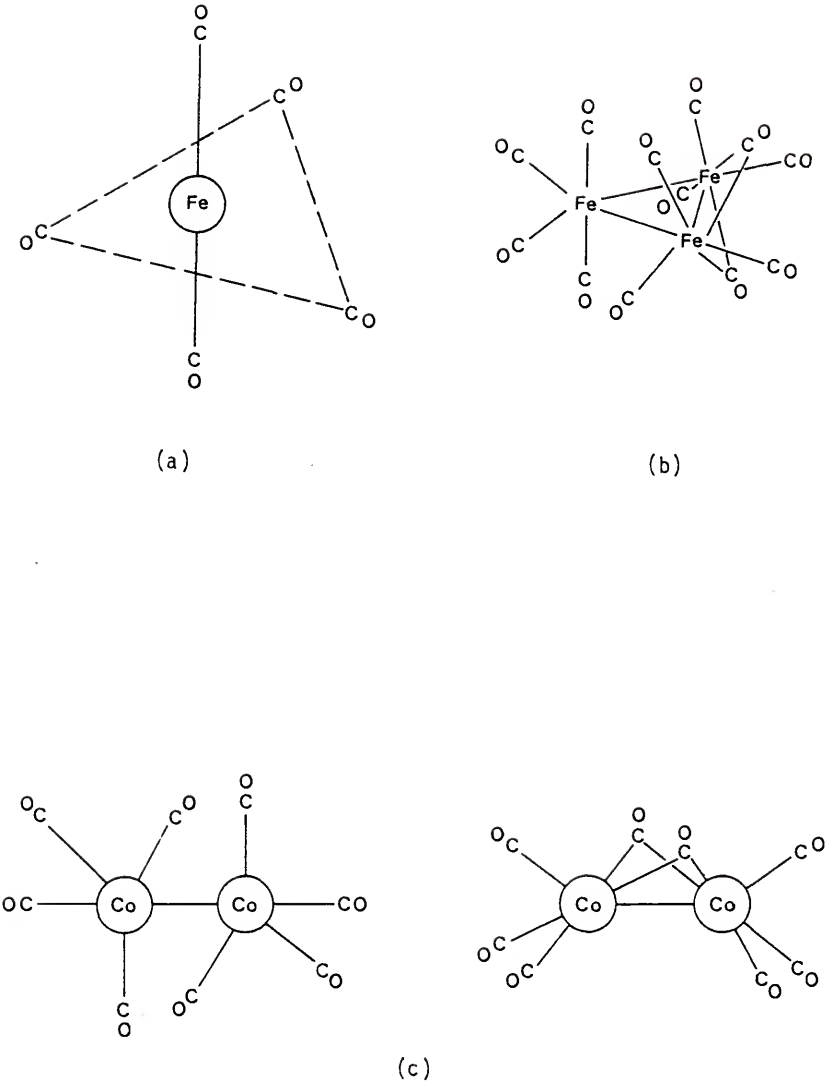

Figure 5. Proposed Chemical Configuration of (a) $Fe(CO)_5$, (b) $Fe_3(CO)_{12}$ and (c) $Co_2(CO)_8$.

iron carbonyls in order to compare differences in decomposition products and consequent interaction with the matrix polymer. Both $Fe(CO)_5$ and $Co_2(CO)_8$ exhibit good solubility in organic solvents, a necessity in these polymer systems. The study and comparison of the metal carbonyl decompositions in solid polymers were pursued to ellucidate the mechanistic pathways and kinetics of these reactions.

3. EXPERIMENTAL

3.1 Preparation of Iron Pentacarbonyl-Polymer Films

3.1.1 Polycarbonate (PC)/$Fe(CO)_5$/Methylene Chloride

Polycarbonate pellets (10.0 g) and 43.9 ml methylene chloride (Fisher Reagent) were mixed 24 hours at room temperature and ambient atmosphere with a Teflon stir bar on a magnetic stir plate in a 50 ml glass-stoppered erlenmeyer flask. Methylene chloride used for solvation of the polymer was dried using molecular sieve pellets (Matheson, Coleman & Bell). Iron pentacarbonyl (Alfa Products, Thiokol/Ventron Division) was filtered through filter paper circles (Whatman 7.0 cm, qualitative 4) into a foil covered test tube. Then 1.0 ml was added dropwise to the above erlenmeyer, now completely covered with aluminum foil. This solution of iron pentacarbonyl and polymer in methylene chloride was mixed for approximately five minutes and then film cast onto sheets of glass using a 0.005" or 0.020" steel doctor blade. Resultant films contained 13.0 wt. % added $Fe(CO)_5$. Films containing 9.1, 4.6, 2.3, and 1.1 wt. % added $Fe(CO)_5$ in polycarbonate were prepared to determine the extinction coefficient of $Fe(CO)_5$ in a polycarbonate matrix. All films were analyzed to determine the actual $Fe(CO)_5$ retained and found to contain 9.3, 6.8, 2.6, 1.3, and 0.44 wt. % $Fe(CO)_5$, respectively.

3.1.2 Polystyrene (PS)/$Fe(CO)_5$/Methylene Chloride

3.1.2.1 Polystyrene/$Fe(CO)_5$/methylene chloride preparation in air

Polystyrene beads (5.0 g) and 21.6 ml methylene chloride were mixed 24 hours in a 50 ml glass-stoppered erlenmeyer flask. Methylene chloride was dried as for the polycarbonate films. Iron pentacarbonyl was filtered through Whatman filter paper circles into a foil covered test tube. Then 0.6 ml was added dropwise to the above (now foil covered) erlenmeyer. This solution of iron pentacarbonyl and polymer in methylene chloride was mixed approximately five minutes and then cast twice onto glass using a 0.005" steel doctor blade (with a brief drying between layers). Resultant films contained 10.7 wt. % added $Fe(CO)_5$ in PS. Films containing graduated levels of $Fe(CO)_5$ were also prepared to determine an extinction coefficient for $Fe(CO)_5$ in a PS matrix. Added versus actual wt. % (respectively) iron pentacarbonyl in PS were shown to be 10.7 vs. 1.6, 9.2 vs 1.41, 7.3 vs. 1.31, 5.9 vs. 1.03, 3.8 vs. 0.99, and 2.1 vs. 0.71 wt. % $Fe(CO)_5$.

3.1.2.2 Polystyrene/$Fe(CO)_5$/methylene chloride preparation in H_2

Polystyrene beads (8.03 g) and 34.7 ml methylene chloride were mixed for 24 hours in a 50 ml glass-stoppered erlenmeyer flask. This produced a 15 wt. % solution weighing 53.7 g. This solution was divided into two portions of 24.3 g each for use as the composite polymer solution (A) and as the control polystyrene solution (B). The remaining 5.1 g was used for preparation of TEM grids by the dilution technique. Solution A plus 10 ml methylene chloride was placed in a 1000 ml round-bottom three-necked flask fitted with a 2-way gas adapter and equipped with a magnetic stir bar and placed over a magnetic stir plate (see Figure 6). This closed gas-vacuum system was set-up within a hood.

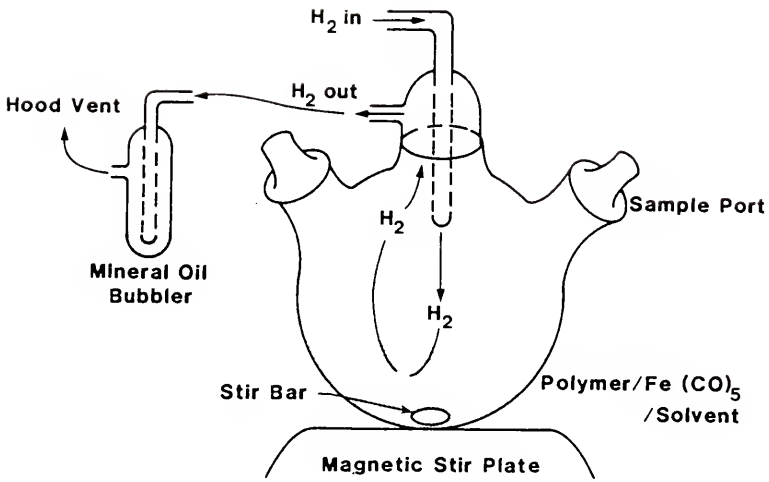

Figure 6. Schematic for Preparation of Composites in a Closed Environment.

Solution A was then mixed under a 10% H_2-argon environment for approximately 3 hours. Iron pentacarbonyl was filtered through a Whatman filter paper circle into a foil covered test tube and 0.22 ml added to solution A while positive gas pressure was maintained. This $Fe(CO)_5$-PS-methylene chloride solution was then mixed under the H_2 atmosphere foil covered for approximately 15 minutes. The magnetic stir bar was then removed. The flask was next turned at an angle and the solution rotated to coat the interior of the flask walls. This was continued with H_2-argon gas flow (~2 psi) for 20 to 30 minutes until a sufficiently viscous film was cast upon the walls. Gas flow was continued for 2 to 3 hours and then this reaction vessel placed in a glove box purged with the same H_2-argon environment. The film was then removed from the 1000 ml flask and stored within the glove box in darkness until needed. Control films were prepared from solution B in the same manner but without the addition of $Fe(CO)_5$.

3.1.3 Polysulfone (PSF)/$Fe(CO)_5$/Methylene Chloride

3.1.3.1 Polysulfone/$Fe(CO)_5$/methylene chloride preparation in air

Polysulfone pellets (7.5 g) were added to methylene chloride (32.6 ml) in a 50 ml glass-stoppered erlenmeyer flask. This solution was mixed 24 hours with a Teflon stir bar on a magnetic stir plate. The methylene chloride was dried with molecular sieve (as for the polycarbonate system). Iron pentacarbonyl was filtered as before and 0.50 ml added dropwise to the foil-covered polysulfone solution and stirring continued for approximately 5 minutes. Thin films were cast from this solution onto sheet glass using an 0.005" doctor blade. Films containing 16.7 added wt. % $Fe(CO)_5$ were produced. Films

containing 9.1, 7.7, 5.9, 4.0 and, 2.0 added wt. % $Fe(CO)_5$ in PSF were prepared to determine the extinction coefficient of $Fe(CO)_5$ in a PSF matrix. All films were analyzed to determined the actual $Fe(CO)_5$ retained and found to contain 2.1, 1.8, 0.4, 0.3, 0.26, and 0.11 wt % $Fe(CO)_5$, respectively.

3.1.3.2 Polysulfone/$Fe(CO)_5$/methylene chloride preparation in H_2

Polysulfone beads (3.77 g) and 16.2 ml methylene chloride were mixed for 24 hours in a 50 ml glass-stoppered erlenmeyer flask. This produced a 15 wt. % solution weighing 25.1 g. This solution was divided into two portions of 13.7 (A) and 9.0 g (B) for use as the composite polymer solution and as the control polysulfone solution, respectively. The remaining 2.4 g was retained for preparation of TEM grids. Solution A and 10 ml methylene chloride was placed in a 100 ml round-bottom three-necked flask equipped with a magnetic stir bar and placed over a magnetic stir plate (refer to Figure 6). Solution A was then mixed under 10% H_2-argon gas for approximately 3 hours. Iron pentacarbonyl was filtered through a Whatman filter paper circle into a foil covered test tube and 0.15 ml added to solution A while positive gas pressure was maintained within the flask. This $Fe(CO)_5$-PSF-methylene chloride solution was mixed under the H_2 environment for approximately 15 minutes. At this point, it was observed that very thick films would be produced by casting all this composite solution in one 100 ml round-bottom flask so 6.7 g was transferred to another 100 ml round-bottom flask (equipped as before) via a 90° fritted glass elbow adapter. Some sample solution (1.4 g) was lost in the tube during transfer. The magnetic stir bar was then removed and the flasks rotated while at an angle to coat the interior wall. This was continued until

films were cast and then allowed to dry under a slow flow of H_2 for two to three hours. Gas inlet and outlet valves were then closed and the reaction vessel placed in a glove box purged with the same gas atmosphere and films removed and stored under H_2. Control films were prepared from solution B in the same manner but without the addition of $Fe(CO)_5$. All films were dried and stored in the dark within the glove box.

3.1.4 Polydimethylsiloxane (PSi)/$Fe(CO)_5$/Methylene Chloride

Uncrosslinked polydimethylsiloxane elastomer (3.02 g) and 10 ml methylene chloride were vortexed (speed control No. 6) for 5 minutes in a 50 ml glass-stoppered flask. Vigorous and short mixing times were used because the polysiloxane is a one component room-temperature vulcanizing elastomer. Filtered iron pentacarbonyl (0.5 ml) was added dropwise to the above (now foil covered) erlenmeyer. This solution was mixed 5 minutes and poured into glass petri dishes and allowed to dry and vulcanize in the dark. All petri dish bottoms used for the polysiloxane studies were coated with Sigma Cote® (Sigma Chemical Co.) to prevent adhesion of the elastomer to the glass. Resultant films contained 20 wt. % added $Fe(CO)_5$ in polysiloxane. Films were analyzed for iron following pyrolysis (since crosslinking renders it insoluble) and found to contain < 0.1 wt. % $Fe(CO)_5$ in PSi as evidenced by the low absorption in the IR carbonyl stretching region and by its lack of the characteristic brown-yellow carbonyl color.

3.1.5 Polymethylmethacrylate (PMMA)/$Fe(CO)_5$/Benzene

PMMA pellets (5.0 g) and 32.2 ml benzene (Fisher Reagent) were mixed for 48 hours at room temperature in an erlenmeyer flask. The

benzene was dried using molecular sieve pellets. Higher loadings of iron pentacarbonyl were used for the PMMA studies, primarily because iron analysis of composite PMMA films indicated that less iron pentacarbonyl was retained in the PMMA film (in comparison to polycarbonate composites). This may be due to loss of the carbonyl with the benzene solvent during drying of the films. Filtered iron pentacarbonyl was added dropwise to a foil covered flask of PMMA-benzene solution and mixed for five minutes. This solution was used for film casting. PMMA composite films with initial loadings of 43, 37, 31, 23 and 11 wt. % $Fe(CO)_5$ were prepared by dropwise addition of 2.5, 2.0, 1.0 and 0.4 ml $Fe(CO)_5$, respectively. As before, all films were analyzed for iron content to determine the actual $Fe(CO)_5$ concentration retained. The final concentrations were found to be 0.8, 0.5, 0.4, and 0.2 wt. % $Fe(CO)_5$ retained, respectively.

3.1.6 Polyvinylidene Fluoride (PVF_2)/$Fe(CO)_5$/Dimethylformamide (DMF)

Two methods were used to produce PVF_2 films for 1) TEM studies and 2) kinetic and SAXS studies. Films for TEM were prepared as follows: PVF_2 pellets (10.0 g) and 94.8 ml N,N-dimethylformamide (Fisher Reagent) were mixed for six days in a flask. Filtered iron pentacarbonyl (4.1 ml) was added dropwise to a covered flask of PVF_2-DMF. This solution was cast onto hot glass (110°C) and held at this temperature for 1 hour. This was followed by heating for 24 hours at 140°C. This procedure simultaneously volatilized the DMF and decomposed the carbonyl. For kinetic studies, solutions of $Fe(CO)_5$-PVF_2-DMF were prepared and film cast at room temperature and dried for 48 hours. Though poor quality films resulted, they were adequate for kinetic

studies. Actual $Fe(CO)_5$ content was determined to be approximately 5 wt. % by pyrolysis of the composite films followed by iron analysis.

3.2 Preparation of Triiron Dodecacarbonyl-Polymer Films

3.2.1 Polystyrene $Fe_3(CO)_{12}$/Methylene Chloride

Polystyrene beads (1.0 g) and 10.0 ml methylene chloride were placed inside a CO purged glove box (LABCONCO) and mixed 12 hours at room temperature in Teflon stoppered 16 X 125 mm test tubes. Molecular sieve pellets were used to dry the organic solvent. Triiron dodecacarbonyl (0.0796 g) was solvated with methylene chloride in a 25 ml glass-stoppered volumetric flask (carbon monoxide gas was bubbled through solvent prior to carbonyl addition). This $Fe_3(CO)_{12}$ solution was mixed in the CO atmosphere of the glove box for approximately one-half hour. Then 2.5 ml of the $Fe_3(CO)_{12}$ solution was added to the PS solution and mixed on a Vortex Genie under CO. Good quality films were cast by pouring this entire solution into a petri and drying under CO. Resultant films contained 0.79 added wt. % $Fe_3(CO)_{12}$ but iron analysis indicates a 0.72 actual wt. %. In a similar manner, four more polystyrene-methylene chloride solutions were prepared and 2.0, 1.5, 1.0 and 0 ml of the same $Fe_3(CO)_{12}$-methylene chloride solution added to obtain 0.63, 0.48, 0.32, and 0 wt. % added $Fe_3(CO)_{12}$ in films. Analyses indicates 0.57, 0.45, 0.28, and 0 wt. % actual $Fe_3(CO)_{12}$ in resulting films, respectively.

3.2.2 Polycarbonate $Fe_3(CO)_{12}$/Methylene Chloride

Polycarbonate pellet (1.25 g) and 15.0 ml methylene chloride were mixed 24 hours at room temperature with a Teflon stir bar on a magnetic stir plate in a 50 ml glass-stoppered erlenmeyer flask. Molecular sieve

pellets were used to dry the solvent prior to mixing with PC pellets. Triiron dodecacarbonyl (0.06 g) was solvated in 7.5 ml methylene chloride in a foil covered erlenmeyer prior to addition to the PC-methylene chloride solution. Following a five minute mixing period, this composite solution was film cast twice onto glass with an 0.005" steel doctor blade. Films were dried and stored in the dark. Resultant films contained 4.6 added wt. % $Fe_3(CO)_{12}$ but crystals were observed within these films even prior to decomposition. To prevent the formation of the triiron dodecacarbonyl crystals within films, concentrations were lowered and preparation done under CO.

Polycarbonate beads (1.0 g) and 10.0 ml methylene chloride were placed inside a CO purged glove box (LABCONCO) and mixed 12 hours at room temperature in Teflon stoppered 16 x 125 mm test tubes. Molecular sieve pellets were used to dry the organic solvent. Triiron dodecacarbonyl (0.0796 g) was solvated with methylene chloride in a 25 ml glass-stoppered volumetric flask (carbon monoxide gas was bubbled through solvent prior to carbonyl addition). This $Fe_3(CO)_{12}$ solution was mixed in the CO atmosphere of the glove box for approximately one-half hour. Then 1.5 ml of the $Fe_3(CO)_{12}$ solution was added to the PS solution and mixed on a Vortex Genie under CO. Good quality films were cast by pouring this entire solution into a petri and drying under CO. Resultant films contained 0.48 added wt. % $Fe_3(CO)_{12}$ (iron analysis indicates a 0.52 actual wt. %). In a similar manner, three more polycarbonate-methylene chloride solutions were prepared and 1.0, 0.5 and 0 ml of the same $Fe_3(CO)_{12}$-methylene chloride solution added to obtain 0.32, 0.16, and 0 wt. % added $Fe_3(CO)_{12}$ in films. Analyses indicate 0.33, 0.24, and 0 wt. % actual $Fe_3(CO)_{12}$ in resulting films.

respectively. Evidently, the solution was more concentrated than assumed - possibly due to volatilization of the methylene chloride.

3.2.3 Polysulfone/$Fe_3(CO)_{12}$/Methylene Chloride With Added Surfactant

The solubility of $Fe_3(CO)_{12}$ (Aldrich Reagent) in methylene chloride was determined to be about 3.4 g/liter at room temperature. If this concentration was used in the initial methylene chloride solution added to the polymer, crystals were observed to form during the evaporation of solvent and resulting increase in concentration of the $Fe_3(CO)_{12}$. Surfactants were used in an attempt to remedy this problem and thus lead to the formation of homogeneous $Fe_3(CO)_{12}$-polymer films. $Fe_3(CO)_{12}$ (0.18759 g) and 0.01 g Pluronic F68 (a nonionic polyethylene oxide-polypropylene surfactant) were brought up to a 50 ml volume with methylene chloride and mixed in a foil covered volumetric. A 25 ml portion of this solution was added to an erlenmeyer flask and 1.0 g polysulfone added. This composite solution was foil covered and mixed approximately 1 hour. Following this, the dark green mixture was film cast with a 0.005" doctor blade four times onto glass (i.e. 0.020" thickness prior to drying). These films were dried and stored in the dark. Apparently homogeneous green films resulted. Control polysulfone films were the same as those prepared for polysulfone-$Fe(CO)_5$ studies as Pluronic F68 surfactant does not show an absorbance in the IR carbonyl absorption region.

An identical composite solution was prepared as discussed above but with the addition of 2.0 ml DMF in place of Pluronic. This was done also in an attempt to affect the solubility of the $Fe_3(CO)_{12}$. This technique enabled higher loadings of the $Fe_3(CO)_{12}$ to be achieved without precipitation of iron carbonyl crystals, though heating

necessary to volatilize the DMF also volatilized some of the $Fe_3(CO)_{12}$ added. Of 51 wt. % added $Fe_3(CO)_{12}$, only 6 wt. % was retained.

3.2.4 Polystyrene $Fe_3(CO)_{12}$/Methylene Chloride With Added Surfactant

A 25 ml solution of $Fe_3(CO)_{12}$ in methylene chloride was added to a 50 ml erlenmeyer flask and 1.0 g of polystyrene and 2 ml DMF added. Again the solution was mixed and then cast four times onto glass with 0.005" doctor blade. It was then dried and stored in the dark. Control films were prepared in the same manner as those prepared for the polystyrene-$Fe(CO)_5$ studies.

3.3 Preparation of Dicobalt Octacarbonyl-Polymer Films

3.3.1 Varied Loadings of $Co_2(CO)_8$ in Polystyrene/Methylene Chloride Prepared Under CO

Polystyrene beads (1.2 g) and 5.4 ml methylene chloride were mixed 24 hours at room temperature with a Teflon stir bar on a magnetic stir plate in a 50 ml glass-stoppered erlenmeyer flask. Molecular sieve pellets were used to dry the organic solvent. Dicobalt octacarbonyl (0.38 g) was solvated in 10 ml methylene chloride under a CO atmosphere in a three necked, round bottomed flask (as shown in schematic 3.1.2.2 for H_2 atmosphere). The PS-methylene chloride solution was then added to this reaction flask while positive CO pressure was maintained. This composite solution was mixed under the CO atmosphere for approximately 15 minutes and then transferred to a glove box purged with CO. Films were cast by pouring approximately 6 ml of the composite solution into petri dishes and drying under CO (exchanged 2 time daily). However, better quality films were obtained by allowing a constant CO flow in the reaction flask while rotating it. The composite solution became

increasingly more viscous as solvent volatized and was deposited upon the walls of the flask to produce good quality films of 23.1 added wt. % $Co_2(CO)_8$ for our study. The CO gas flow was continued until films were dry. They were then sealed under this CO environment until analyzed. Weight per cent loadings of 16.7, 13.0, and 9.1 were also prepared in this manner with the addition of 1.0, 0.75, and 0.5 g $Co_2(CO)_8$, respectively.

Polystyrene beads (1.0 g) and 10.0 ml methylene chloride were placed inside a CO purged glove box and mixed 12 hours at room temperature in a Teflon stoppered 16 X 125 mm test tube. Molecular sieve pellets were used to dry the organic solvent. Dicobalt octacarbonyl (0.18 g) was solvated in 15.0 ml methylene chloride under a CO atmosphere in a 25 ml volumetric flask. Carbon monoxide was slowly bubbled through the solvent for approximately one-half hour prior to addition of $Co_2(CO)_8$. The solution of methylene chloride and $Co_2(CO)_8$ was mixed in the CO purged glove box for approximately one-half hour. It was noted that not all the $Co_2(CO)_8$ went into solution, possibly due to decomposed dicobalt octacarbonyl. Then 4 ml of this $Co_2(CO)_8$ solution was added to the PS-methylene chloride solution and mixed under CO. Films were cast by pouring this entire solution into a petri dish and drying under CO. Resultant films contained 4.5 wt. % added $Co_2(CO)_8$ but cobalt analysis indicated a 1.1 actual wt. %. In a similar manner, four more polystyrene-methylene chloride solutions were prepared and 3, 2, 1 and 0 ml of the same $Co_2(CO)_8$-methylene chloride solution added to obtain 3.5, 2.3, 1.2, and 0 wt. % added $Co_2(CO)_8$. Analysis indicated 0.9, 0.7, 0.3, and 0 wt. % actual $Co_2(CO)_8$ in resulting films, respectively.

3.3.2 $Co_2(CO)_8$ in Polystyrene/Methylene Chloride Prepared in H_2

Sample preparation was done as for the PS-$Co_2(CO)_8$ composites cast in CO with the exception that 10% H_2-argon was slowly passed through the system. Films of theoretical wt. % $Co_2(CO)_8$ were cast by rotating the flask while H_2-argon gas was slowly passed through the closed system. Films were dried and stored in this H_2 atmosphere.

3.3.3 Polystyrene/$Co_2(CO)_8$/Methylene Chloride Sandwich Preparation (to Evaluate Oxygen Diffusion Rate)

Polystyrene beads (5.0 g) and 22.0 ml methylene chloride (Mallinkrodt Reagent) were mixed 24 hours at room temperature with a Teflon stir bar on a magnetic stir plate in a 50 ml glass-stoppered erlenmeyer flask. As for the polycarbonate systems, molecular sieve pellets (Matheson, Coleman & Bell) were used to dry the methylene chloride for solvation of polymers. This solution was divided into two equal portions, both in stoppered 50 ml erlenmeyers with Teflon stir bars. Both polystyrene-methylene chloride solutions were placed in a glove box (LABCONCO) purged with carbon monoxide following evacuation. $Co_2(CO)_8$ (0.6361 g) was weighed into a test tube (16 x 125 mm) in air and immediately purged with CO in the glove box. The $Co_2(CO)_8$ was added to one of the PS-methylene chloride solutions to give 20.3 wt. % $Co_2(CO)_8$ in polystyrene. This solution was mixed approximately 5 minutes.

Mixing and casting of the polystyrene and $Co_2(CO)_8$-polystyrene solutions were done in a carbon monoxide environment. The $Co_2(CO)_8$-PS sandwich films were prepared by first casting a polystyrene film onto glass, then a layer of $Co_2(CO)_8$-PS sandwich films were prepared by first casting a polystyrene film onto glass, then a layer of $Co_2(CO)_8$-PS and finally another polystyrene layer (see Figure 7). An 0.005" steel

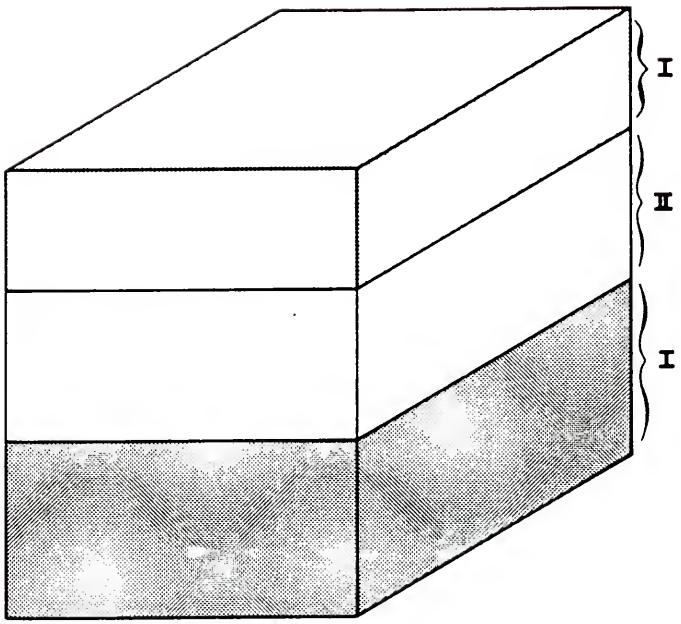

I = Polystyrene protective layer of varying thickness

II = Polystyrene containing 20% Co

Figure 7. "Sandwich" O_2 Barrier Concept for Polystyrene-$Co_2(CO)_8$ Films.

doctor blade was used for each layer and a five minute drying period was allowed between casting of layers. This sandwich was then removed from the glass and stored in a 3-necked round bottom glass flask in a CO environment. A control polystyrene film was prepared in the same manner but with a center layer of polystyrene. A similar sandwich of thicker polystyrene "bread" was prepared by using a 0.020" doctor blade for both outer polystyrene layers. This $Co_2(CO)_8$-PS film, however, dried more slowly so was not removed from the glass but left under CO in the glove box overnite to dry. Good quality, yellow-colored films were obtained in both cases.

3.3.4 Preparation of $Co_2(CO)_8$ in Polyvinylidene Fluoride (PVF_2)/ Dimethyl Formamide (DMF)

Dicobalt octacarbonyl (~0.2 g) was solvated in 10 ml DMF. A pink color developed with the evolution of gas (probably CO) on the glass interface and formation of black precipitate. To this still bubbling solution, approximately 1.0 g of PVF_2 beads was added and mixed. This solution was cast into petri dishes, covered and stored under CO for 5 days. Drying was not complete at this time so the sample was placed in air to more rapidly volatilize the remaining DMF.

3.4 Preparation of Iron and Cobalt Carbonyl-Polymer Films

3.4.1 Polyvinylidene Fluoride $Fe(CO)_5$-$Co_2(CO)_8$/Dimethylformamide Prepared in CO

Polyvinylidene fluoride (4.00 g) and 38.3 ml DMF were mixed for six days in a 50 ml erlenmeyer flask. $Co_2(CO)_8$ (0.5 g) was added to 15 ml DMF in a 100 ml round bottom three necked flask with 2 psi CO gas flow through (see Figure 6) and stirred. Filtered iron pentacarbonyl (0.34 ml) was added dropwise with mixing to this $Co_2(CO)_8$-DMF solution. Next 30 g of the PVF2-DMF solution (3.0 g PVF2) was added with mixing and gas

flow continuted. The remaining PVF_2-DMF solution was used to prepare control samples. This solution of PVF_2-cobalt/iron carbonyl in DMF was then heated to 160°C to volatilize the solvent. By angling and rotating the flask a film was produced on the interior wall. Films theoretically contained 12.5 wt. % $Fe(CO)_5$ and 12.5 wt. % $Co_2(CO)_8$ in PVF_2. Films were stored in CO and in the dark until analyzed.

3.4.2 Polysulfone $Fe(CO)_5$-$Co_2(CO)_8$Methylene Chloride Preparation in CO

Polysulfone (8.03 g) and 34.7 ml methylene chloride were mixed for 24 hours in a 50 ml erlenmeyer flask. $Co_2(CO)_8$ (0.33 g) was added to 15 ml methylene chloride in a 100 ml round bottom flask with CO gas flowing through and stirring. Filtered iron pentacarbonyl (0.22 ml) was added dropwise to the cobalt solution. Next, 20.1 g of the PSF-methylene chloride solution (3.0 g PSF) was added to this CO gas purged system and mixed for approximately 10 minutes. The gas flow was then slightly increased and the flask angled and rotated to cast a film on the interior wall. Films of 10 added wt. % $Fe(CO)_5$ and 10 added wt. % $Co_2(CO)_8$ were formed. They were stored in the dark and in CO until analyzed.

3.5 Preparation of Control Films

Appropriate polymer controls were prepared by eliminating the addition of iron pentacarbonyl to identical polymer-solvent solutions. All cast films were foil covered during drying and storage to prevent photolytic decomposition of the carbonyl in composite films and for experimental consistency in the control samples.

3.6 Quantitative Metal Analysis of Metal Carbonyl-Polymer Films

3.6.1 Standard Curve For Vogel's Iron Analysis

A variation of Vogel's 1,10-phenanthroline iron analysis technique (98) was used for the composite iron analysis, thus a comparable standard curve was prepared. Dimethyl formamide (DMF) was selected as the solvent for the composite and control polymers because it is not only a good polymer solvent, but also water soluble as are the reagents for Vogel's method. For the standard curve, two solutions were prepared: an Fe solution (A) and a control (or reference) solution (B). A 2.5 ml volume of the Fe standard (prepared according to Vogel) was added to a 50 ml volumetric flask - A. No Fe standard was added to the control - B. The standard iron solution was prepared (as directed by Vogel) from 0.7030 g ammonium iron sulfate (Matheson, Coleman & Bell) dissolved in 100 ml water. Five ml of 1:5 sulfuric acid was added and a dilute solution of potassium permanganate (0.604 g/300 ml) was run in cautiously until a slight pink color remained after stirring well. This was diluted to 1 liter and mixed thoroughly (final solution: 1 ml = 0.1001 mg Fe).

Next, 5.0 ml of 10% hydroxylammonium chloride, (Fisher Reagent) 0.7 ml 0.2 M sodium acetate (Fisher Reagent) and 4.0 ml of 1,10-phenanthroline (Fisher Reagent) were added to both flasks. Solutions were vortexed after each addition. Finally, both flask A and B were brought up to 50 ml volume with DMF and again mixed. After standing for one half to one hour both solutions were filtered through Whatman glass fiber filters. The Fe solution A contained 5.01×10^{-3} mg Fe/ml solution.

Next, a dilution series of the Fe solution A in DMF was prepared as shown in Table 1 and the UV absorbance at 396 nm measured in quartz curvettes. Solution B was used as the reference. These data are plotted in Figure 8. A linear curve fitting for the data shows 0.999 correlation.

3.6.2 Vogel's 1,10-Phenanthroline Method for Iron Analysis

The actual weight percent of iron in the untreated films was determined by Vogel's 1,10-phenanthroline method. This method measures the UV absorption at 396 nm of dissolved samples. Absorption was compared to a standard curve (see section 3.6.1) to quantify total iron. Sample for this analysis were prepared by dissolving 0.02-0.10 g of the composite film in 15 ml dimethylformamide in a 25 ml volumetric flask. After solvation of the polymer, the following were added: 2.5 ml of 10% hydroxylammonium chloride 2.5 ml 0.2M sodium acetate to adjust pH to 3.5± 1.0, and 2.0 ml 1,10-phenanthroline solutions were vortexed (Vortex-Genie, Scientific Industries) after each addition. This solution was then brought up to 25 ml with dimethylformamide and again mixed. After standing 1 hour (to develop full color), the solution was filtered through a Whatman 934-AH glass fiber filter to remove the precipitated polymer and the UV absorption at 396 nm of the filtrate was measured in quartz cuvettes. Appropriate control polymer films prepared in the same manner were used as a reference.

Selected iron polymer samples were also analyzed by atomic absorption (Perkin-Elmer 460 AA Spectrophotometer with iron hollow cathode lamp and air-C_2H_2 flame) to verify values obtained by Vogel's method. The use of Soil Science's AA Spectrophotometer and Frank Sodek's assistance is gratefully acknowledged. Samples were prepared

Table 1. Preparation of Dilution Series for Standard Iron Concentration Curve.

Fe Soln. a ml	Control Soln. b ml	Added* DMF ml	Corresponding mg Fe/ml	A_{UV}(396 nm)
0	2	0	0	0
2	0	0	5.01×10^{-3}	0.281
2	0	1	3.34×10^{-3}	0.180
2	0	2	2.50×10^{-3}	0.132
2	0	4	1.67×10^{-3}	0.091
2	0	6	1.25×10^{-3}	0.064

*vortexing after additions

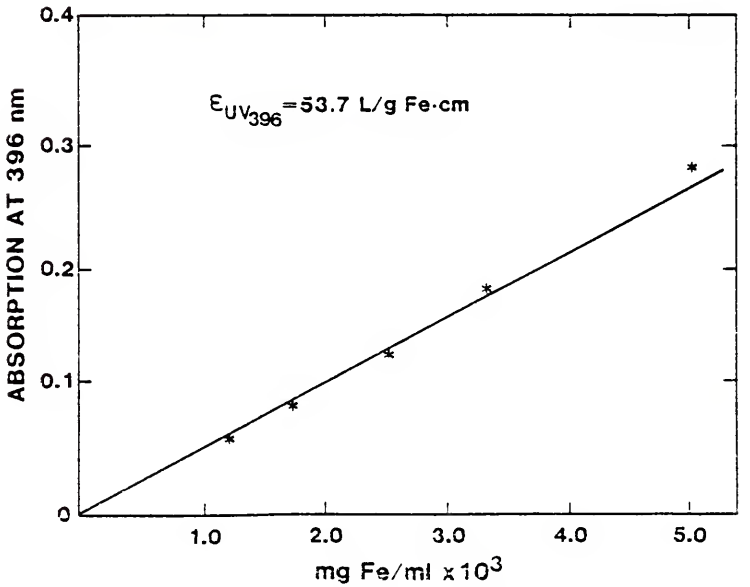

Figure 8. Iron Standard Curve in Dimethyl Formamide.

both by 1) solvation in DMF and also 2) as for Vogel's iron analysis. Iron standards of 0, 5 and 10 ppm Fe were also prepared in a similar fashion; however, a commercial iron standard (Scientific Products--1000 ppm) was used with the respective additions of 0, 0.125, 0.250 ml of this standard as measured with a microburette. Comparison of these values (from the DMF solvation and from Vogel's chemical medium) indicate that only slight amounts of iron are retained in the precipitated polymer thus similar values were obtained in both instances.

3.6.3 Pyrolytic Technique for Atomic Absorption to Quantitate Iron and Cobalt Content

The PVF_2 iron carbonyl composites were observed to be insoluble in DMF and other solvents. Thus, an ashing technique suggested by Smith and Wychick (71) was used to liberate the iron from the crosslinked polymer matrix. Samples of composite and control films (0.03 g) were weighed into platinum crucibles. This was followed by ashing at 600°C for one hour in a muffle furnace (Sybron Thermolyne, Model 1-6028). After cooling, samples for colorimetry were prepared by extracting the iron from the hydrocarbon medium with 100 ul (Clay Adams Autopipettor) of concentrated HCl (Fisher Reagent). This was then followed by Vogel's 1,10-phenanthroline iron analysis. To verify this value, a wet digestion procedure (99) followed by atomic absorption analysis (100) was done by Galbraith Laboratories. Similar values for iron in PVF_2 films were obtained from both techniques. The polysiloxane composites were also insoluble and were therefore analyzed by Galbraith Laboratories in this same manner.

Cobalt-polystyrene films were also analyzed by Galbraith Laboratories. Again samples were wet digested in a Carius furnace followed by atomic absorption analysis for cobalt.

3.7 Determination of Extinction Coefficient of Metal Carbonyls in a Polymer or in a Solution

The IR carbonyl stretching absorption at approximately 2000 cm^{-1} of composite films was measured prior to metal analysis. Iron or cobalt concentrations in the metal carbonyl-polymer samples were then determined either by Vogel's 1,10-phenanthroline method or by atomic absorption as previously described. Using the IR absorption observed at the 2000 cm^{-1} carbonyl stretching region, the iron concentration (as determined either from atomic absorption or from Vogel's 1,10-phenanthroline method), and Beer's Law (Abs = εdc), the extinction coefficient, ε, for each metal carbonyl was calculated as a function of solid polymer and carbonyl concentration.

3.8 Solid State Decomposition Methods for Metal Carbonyl-Polymer Systems

3.8.1 Thermal Decomposition of Metal Carbonyl-Polymer Systems

Thermal decompositions were carried out in a temperature controlled vacuum oven (National Appliance) with controlled atmosphere capability. Decomposition times and temperatures were varied for kinetic measurements. Temperatures were varied from 118°C to 142°C with measurement times dependent upon rate of decomposition (a function of temperature).

For selected systems, it was of interest to follow the thermal decomposition kinetics under a 10% H_2-argon atmosphere. For these

studies, small (100 ml) three-necked round-bottomed flasks were equipment as shown in Figure 9. This flask was placed in an oil bath within a hood. Films were placed in vials and these vials placed into the round bottom flasks and decompositions carried out at various temperatures. Decompositions of the $Co_2(CO)_8$ samples under an N_2 atmosphere could be done simply by placing them within the closed chamber (purged with N_2) of the Nicolet MX-1, FTIR.

3.8.2 Photolytic Decomposition of Metal Carbonyl-Polymer Systems

Photolytic (UV) decompositions were performed using a 100 watt mercury arc lamp (Ealing Optics Corp.) or a 75 watt xenon lamp (Ealing) mounted on an optical bench with a quartz water filter between the sample and source to avoid heating by infrared radiation (see Figure 10). UV irradiance and time were varied. A WG 305 filter (Schott Optical) was used to limit the UV radiation to wavelengths greater than 305± nm. Irradiance at the sample (for distances of 30 to 50 cm from the source) were measured with a radiometer/photometer system (EG & G, Electro-Optics Model 550).

3.8.3 Gamma Radiation Decomposition of Metal Carbonyl-Polymer Systems

In this study, gamma radiation was explored as a means to decompose metal carbonyl complexes within the solid polymer matrix. A cobalt (measured to emit 600 curie in 1975) source was selected for this purpose. Film samples (0.016 cm thick) were placed on microscope slides within Coplin jars (see Figure 11). These containers were placed 2 inches from the gamma radiation source and times of exposure varied from 0 to 72 hours. Samples treated in this manner were $Fe(CO)_5$-PC, $Fe_3(CO)_{12}$-PC and $Fe_3(CO)_{12}$-PS.

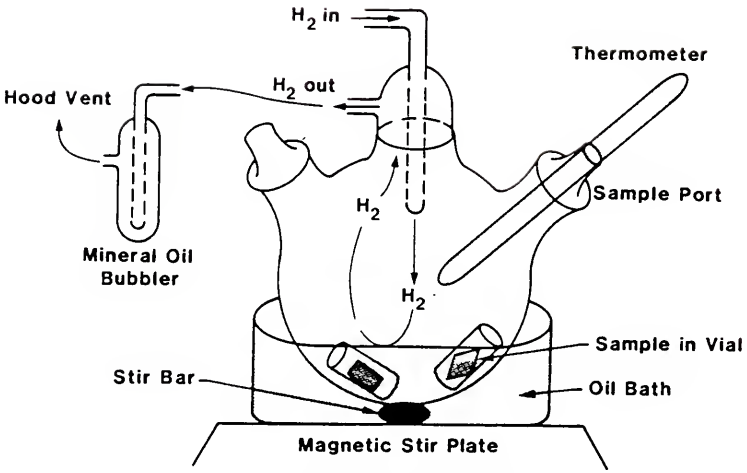

Figure 9. Apparatus for Thermal Decomposition of Metal Carbonyl-Polymer Systems in Closed Environment.

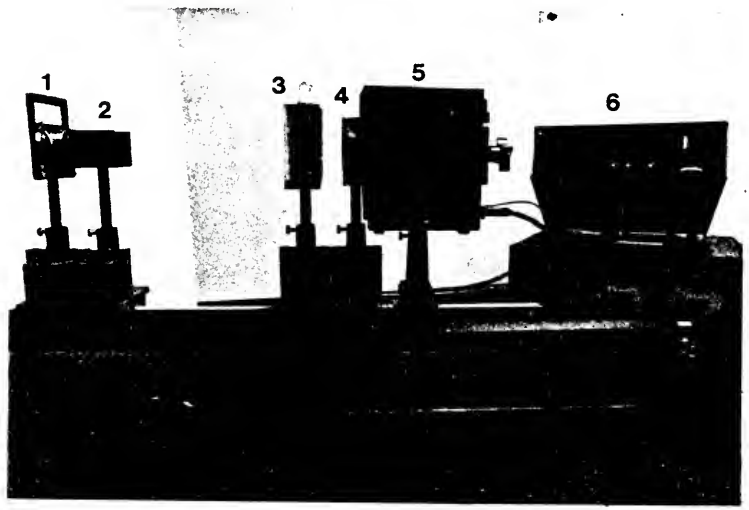

Figure 10. UV Irradiation Assembly 1. Sample, 2. WG 305 Filter, 3. Quartz Water Filter, 4. Collimating/Focusing Lens, 5. UV Source and 6. Radiometer/Photometer.

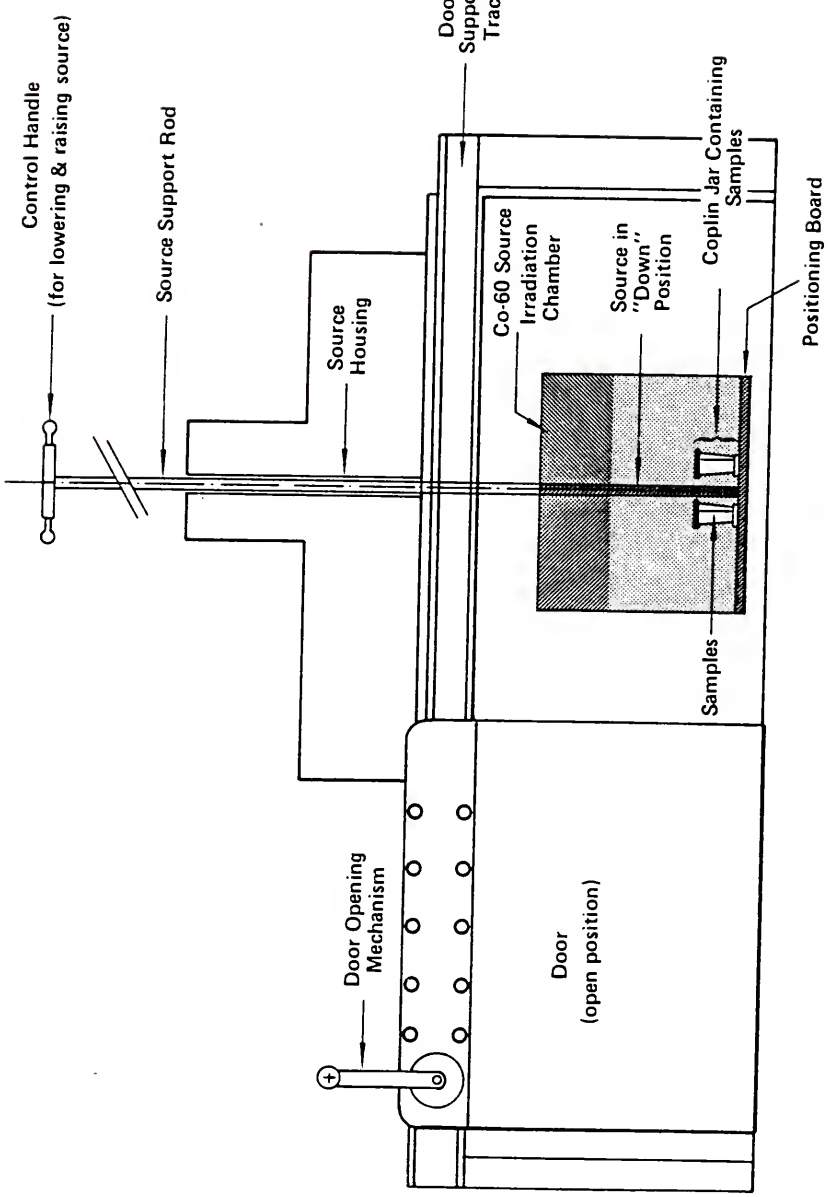

Figure 11. Schematic Drawing of Co-60 Source, Department of Radiation Biology, University of Florida.

3.8.4 Electron Beam Decomposition of Metal Carbonyl-Polymer Systems

Electron beam decompositions were done using both a JEOL JSM-35C scanning electron microscope (SEM) and a VG-HB5 STEM both with a 100 KeV tungsten field emission tip. Electron beam decomposition studies were initially conducted on the JEOL JSM 35C SEM. Samples of polycarbonate and 5 and 10 wt. % $Fe(CO)_5$ polycarbonate films, typically 0.004 to 0.015 cm thick, were mounted on 1 inch aluminum SEM stumps with double sticky tape and conductive carbon paint on the edges. No carbon or gold was sputtered onto these samples to aid conduction of current off. A variety of voltages ranging from 10 to 30 KeV, exposure times up to 10 minutes, magnifications, working distances, aperatures, and scanning modes were tried as well as variations in iron carbonyl loadings. Carbonyl decomposition was observed under the conditions discussed below.

The filament was saturated and the 30 KeV electron beam focused on a blank SEM stump with 0° tilt. The x and y coordinates were noted in order to properly center sample later. Both 39 and 15 mm working distances were used to vary magnification of the sample from 10 to 20 times, respectively. The voltage was then turned off, with the filament condensor left in the saturation position, and the 5 wt. % added metal carbonyl-polymer sample placed in the beam chamber. Aperatures were pulled out, gun bias set to 3 and the beam blanking device then switched on followed by the voltage. At onset of timed exposures, the beam blanking device was turned off and sample scanned (irradiated) in Photo mode 9/9. Specimen current and lens settings were recorded so that the energy absorbed by the sample could be determined (see Appendix A for calculation).

Electron beam decompositions were also conducted at the University of Illinois Materials Research Laboratory. The willing and capable assistance of Ms. Peg Mochel in these electron beam decomposition studies was greatly appreciated. The VG-HB5 STEM has the capability of electron beam writing via a very slow scanning rate and small (12 A) beam size. The electron focal spot on the sample in a scanning electron microscope is quite small to provide good spatial resolution. As a result, the current in the electron beam hitting the sample is small, of the order of 10^{-9} ampere or less (101).

Thin samples of polysulfone and polysulfone with 30 wt. % loadings of $Fe(CO)_5$ were prepared by the dilution technique as described in Section 3.1.1 and stored in darkness. A magnification of 100,000X and applied voltages of 60 and 100 KeV were used to treat these thin samples. With this STEM, a beam blanking device was not used. Initial focusing was simply done at high magnification (to limit the area of decomposition on the grid), then the grid region changed when decomposition was to be followed. With these increased voltages, shorter times could be used to achieve decomposition.

3.9 Kinetics for Decomposition of Metal Carbonyls in Solid Polymer Matrices

Infrared absorption bands (Perkin-Elmer 283B Infrared Spectrophotometer and Nicolet MX-1 FTIR) at 1996 and 645 cm^{-1} (carbonyl stretching and bending, respectively) were observed to change during decomposition of the $Fe(CO)_5$-polymer films. The 1996 cm^{-1} band was used to follow the kinetics of the decompositions. Kinetics for thermal and UV decompositions and activation energies for the thermal decomposition reactions in composite films were determined. The willing cooperation

of Guy LaTorre was greatly appreciated in studies using the Nicolet MX-1, FTIR.

Rate constants for each decomposition temperature (or specific energy input from the UV source) were calculated based upon the assumption that each absorbance measured could be correlated to a given concentration of $Fe(CO)_5$. A concentration could be evaluated using the extinction coefficient as determined in section 3.8. Thus, the remaining concentration of $Fe(CO)_5$ in the polymer treated at a given temperature T for time t was calculated. Assuming thermal decomposition kinetics follows a first-order mechanism, the slope of a linear curve fitting of x (time t) versus y (Ln concentration) will be the decomposition rate constant k, at the temperature T. Furthermore, by plotting the natural logarithm of each rate constant versus the reciprocal of each respective temperature T, the slope is observed to be the activation energy for the decomposition kinetics for $Fe(CO)_5$ in a polymeric matrix (102). For $Co_2(CO)_8$-polymer and solvent systems decomposed under N_2, second-order kinetics was observed. Thus, by plotting:

$$\ln \frac{A}{A_o(A_o-A)} \text{ vs. time t, where}$$

A = concentration of reactant A at time t

A_o = initial concentration of reactant A

One may determine the rate constant for this reaction from the slope of this curve.

For photolytic decompositions, the kinetics of the decomposition must be viewed differently. An activation energy was estimated by

plotting the rate versus energy of photolytic source at a given distance or versus the inverse of this distance squared. The value for the activation energy arrived at in this manner may still be compared with that achieved for thermal decomposition data though the units differ.

3.10 Kinetics of Carbonyl Decomposition in Solution

3.10.1 Thermal Decomposition of $Fe(CO)_5$ in Ethyl Benzene Solution

Fifty ml of ethyl benzene (Matheson Coleman & Bell Reagent) were placed in a foil-covered 100 ml three-neck flask. Filtered iron pentacarbonyl (0.13 ml) was added to the ethyl benzene and stirred with a magnetic stir bar. This reaction vessel was fitted with a condenser (to limit volatilization) and stoppers (to allow for sampling) and placed in a heated oil bath (see Figure 12). Decompositions were measured at 70, 90, 110 and 130°C and followed by infrared spectroscopy in sealed demountable NaCl liquid cells. An ethyl benzene reference was used. Noack's (103) extinction coefficient of 8000 1 $mol^{-1}cm^{-1}$ was used for determination of $Fe(CO)_5$ concentration in the ethyl benzene solution.

3.10.2 Thermal Decomposition of $Fe_3(CO)_{12}$ in Ethyl Benzene Solution

Fifty ml of ethyl benzene (Matheson Coleman & Bell Reagent) were placed in a foil covered 100 ml three-necked flask. Triiron dodecacarbonyl (0.12 g) was added to the ethyl benzene and stirred with a magnetic stir bar. The reaction vessel was fitted with a condenser (to limit volatilization) and stoppers (to allow for sampling) and placed in a heated oil bath (see Figure 12). Decompositions were followed at 82 and 110°C by infrared spectroscopy in sealed demountable NaCl liquid cells. An ethyl benzene reference was used. An extinction

coefficient of 12,650 l/mol cm was used for determination of $Fe_3(CO)_{12}$ concentration in the ethyl benzene solution.

3.10.3 Photolytic Decomposition of $Fe(CO)_5$ in Ethyl Benzene Solution

Fifty ml of ethyl benzene were placed in a foil-covered 100 ml beaker. Filtered iron pentacarbonyl (0.13 ml) was added to the ethyl benzene and stirred with a magnetic stir bar. This beaker was then covered with a quartz water filter to prevent evaporation of the solvent yet allow the passage of UV light. It was then placed in line with the UV source and the foil removed and shown below (Figure 13).
The UV source was placed above the solution to remedy interference of carbonyl decomposition products deposited upon the container walls with irradiation of the solution. The distance from source to sample was varied and the respective photometric energies measured at each distance to quantitate an activation energy.

3.11 Microscopic Characterization of Composite Film Morphology

Electron diffraction patterns from a field emission gun of a transmission electron microscope (JEOL Model 200CX STEM and Philips Model 301 TEM) and photomicrographs were used to study the compositions and morphology of metallic particles. Samples were prepared by two methods.

For those, TEM samples to be thermally decomposed in air the dilution technique provided sample grids of satisfactory quality. A 0.1% solution of the polymer-carbonyl mixture in appropriate solvent was applied dropwise to carbon coated (100 A thick) TEM grids. The thin films produced on the grids were then treated to decompose them. Better quality and more representative samples were found to be produced by microtoming. For this procedure, composite films were embedded in epoxy

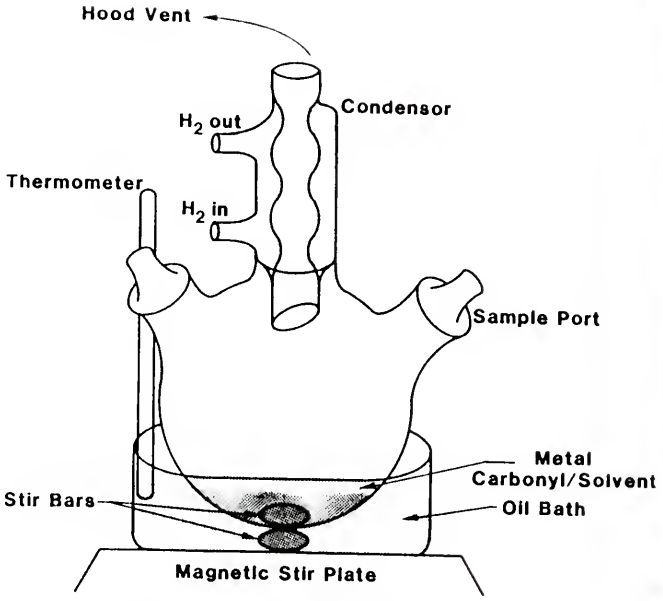

Figure 12. Apparatus Used for Thermal Decomposition of $Fe(CO)_5$ in Ethyl Benzene Solution.

Figure 13. Apparatus for Photolytic Decomposition of $Fe(CO)_5$ in Ethyl Benzene.

resin. The best embedding medium was found to be an equal ratio mixture of solution A: solution B (Solution A and B prepared according to instructions in Epon 812 Kit BU 013 055T-Baltzers). Embedded composites were then ultramicrotomed (LKB Ultratome) at a speed of 5 mm/sec and floated off on water onto formvar coated TEM grids. The assistance of Drs. R. H. Berg III, and H. C. Aldrich was greatly appreciated in developing a successful microtoming technique for these composites.

Samples were allowed to dry and then carbon coated (100 Å). This TEM sample preparation technique was found to be well suited to these composite films decomposed in closed gas environments (CO or H_2). Composite films were examined further by optical microscopy (Zeiss) and scanning electron microscopy (JEOL Model 35C-SEM) with electron energy dispersive spectra capabilities.

3.12 Small Angle X-ray Scattering Experiments to Measure Particle Size Distribution

Quantitative small angle x-ray scattering (SAXS) experiments to measure particle size and size distribution as well as changes in polymer crystalline morphology were performed on the 10 meter SAXS facility at the National Center for Small Angle Scattering Research (NCSASR) at the Oak Ridge National Laboratory. This apparatus features (Cu Kα radiation at 34.0 KV and 40 mA) pinhole collimation of the incident beam (1620 mm apart), a 2-dimensional position sensitive detector, and a mini-computer based data acquisition and analysis system (see Figures, 14 and 15). The distance between sample and the two-dimensional position-sensitive proportional counter was 515 cm. All data were corrected for background scattering, cosmic radiation, detector sensitivity, variations in incident beam intensity, sample transmission

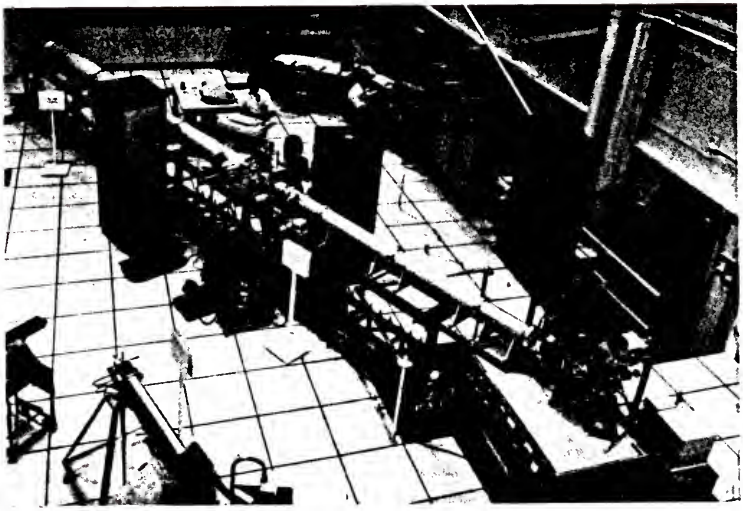

Figure 14. Photograph of Small Angle X-Ray Scattering Facility at Oak Ridge National Laboratory

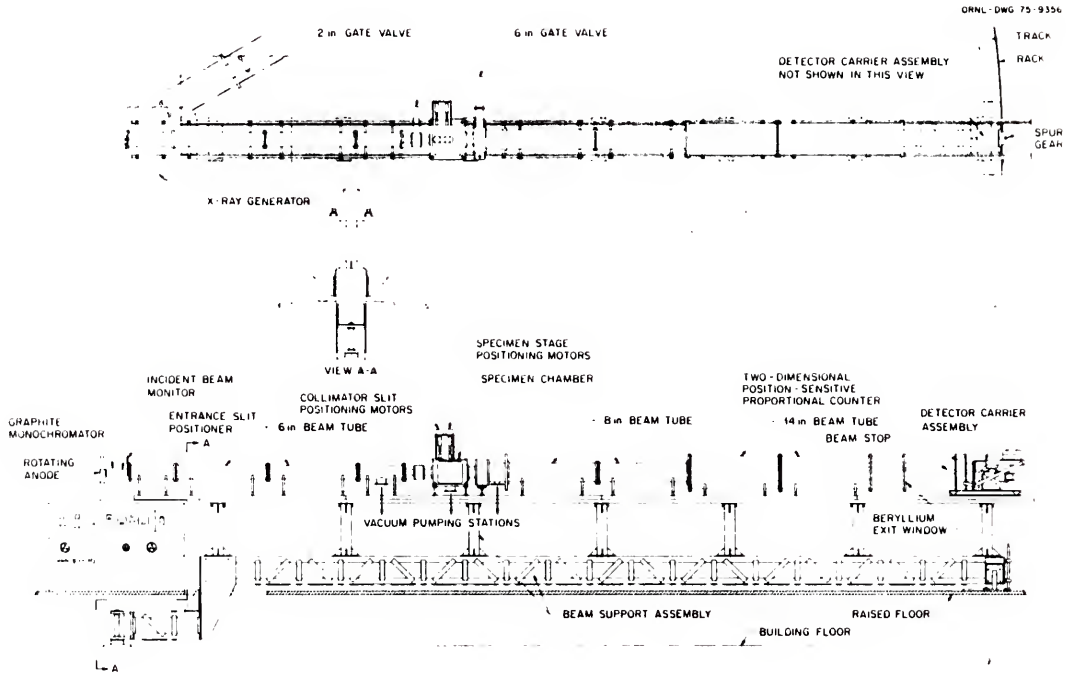

Figure 15. Schematic of SAXS Facility Used at Oak Ridge National Laboratory.

coefficient and exposure time. Fully corrected data are presented as two-dimensional contour plots of intensity versus scattering angle and Guinier plots of log intensity versus scattering angle. Small angle x-ray scattering studies required samples approximately 0.7 mm thick. Metal carbonyl-polymer films cast to this thickness and then treated to decompose the carbonyl were observed the bubble as CO was evolved. Thus, thin films were prepared and treated to decompose the carbonyl. This was followed by grinding of the samples (as done for magnetic measurements--see Section 3.14) and then pressing at 10,000 pounds for 5-10 minutes in an infrared KBr pellet die (without KBr) at ambient temperature to achieve the proper sample thickness necessary for SAXS studies.

The assistance of Dr. J. S. Lin with SAXS studies and the use of Oak Ridge National Laboratory facilities is gratefully acknowledged. Studies were performed at the National Center for Small Angle Scattering Research which is funded by National Science Foundation Grant No. DMR-77-244-58 through Interagency Agreement No. 40-637-77 with the Department of Energy (DOE) and was operated by the Union Carbide Corporation under Contract No. W-7405-eng-26 with the DOE.

3.13 Determination of Average Magnetic Susceptibility of Metal-Polymer Composites by the Guoy Method

A convenient way of making molar magnetic susceptibility measurements is by means of a Guoy magnetic balance illustrated in Figure 16 (104). An electromagnet establishes a field H_0 and one measures the resulting change in weight of a sample. The sample is contained in a tube which is suspended between the pole pieces of a magnet, with the bottom of the sample at centerline. This tube is

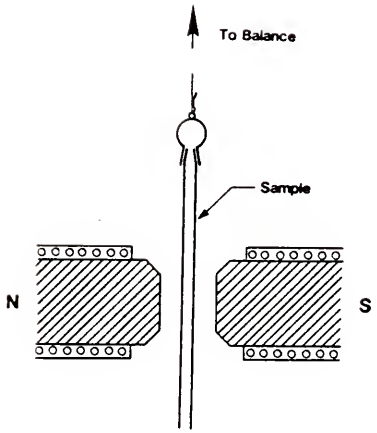

Figure 16. The Guoy Balance.

attached to a sensitive balance and one measures the change in pull that occurs when the magnetic field is applied. If the sample is diamagnetic (i.e. the induced field opposes the external magnetic field), the magnetic field within it is less than H_0 (M/H_0 is negative and M = magnetization). A paramagnetic sample shows the reverse effect (the induced field aids the external one) so that M/H_0 is positive.

Thus far, the possibility of an interaction between the mangetic moments of adjacent atoms has been neglected. This is a reasonable procedure to follow when the atoms have closed outer shells. However, transition metal atoms (like Fe, Co, and Ni) and ions have characteristically incomplete d and f shells and these unpaired electrons can interact with similar electrons in neighboring (adjacent) atoms. This phenomenum is termed ferromagnetism and commonly results in much larger intensities of magnetization. Ferromagnetism is rare in nature though technologically important. Paramagnetism is common among the transition group elements and diamagnetism is a universal property of matter.

3.13.1 Sample Preparation for Magnetic Susceptibility Measurements

Thermally treated composite and control samples (approximately 5 g) were first chopped in a Waring Commercial Blender (Model No. 31BL92) followed by grinding (Arthur H. Thomas Gear-Cutter) to achieve small particle sizes. This comminuated material was then sieved to select particles of somewhat uniform size suitable for magnetic susceptibility measurements. Particles passing through Tyler No. 28 but not through Tyler No. 48 (595 mm and 300 mm, respectively) were found to be suitable for this purpose. Selected polymer samples (i.e. PVF_2) found to be too tough for comminuation by this process were further ground in a mortor

and pestle with liquid nitrogen. To reduce sample loss due to static charge, it was observed that ground samples could easily be collected if wetted with ethanol. Samples were dried at 60°C after collection into sample vials.

3.13.2 Guoy Balance for Measurements of Magnetic Properties

The magnetic properties of these composites were measured on a Guoy Balance. Thanks are extended to Dr. Stoufer for his helpful discussions and assistance as well as the use of his Guoy Balance in the Chemistry Department here at the University of Florida.

A Mettler semi-microbalance (Model B6) was used to weigh these sieved samples (0.5 g) in applied fields of 6830 gauss, 5740 gauss and no field environments. This was achieved with a Varian Power Supply (Model V-2300-A) and Current Regulator (Model V-2301-A). Triplicate measurements were made at each field strength for all samples. Normally samples of approximately 0.5 g were used and showed an average deviation of 0.0004 g. Data were corrected for sample holder background in the various fields as well as for matrix polymer effects. Metal content of these samples was measured to directly correlate the magnetic susceptibility of samples to metal content.

3.14 Effect of $Fe(CO)_5$ Decomposition on Polymer Molecular Weight

Intrinsic viscosities ([η]) of polymers and composite compositions were determined using a Ubbelohde 0B viscometer. Solutions of the composite and control polycarbonate, polysulfone and polydimethylsiloxane films were prepared and mixed in dioxane (Fisher Reagent) overnite and then filtered through glass fiber filters just prior to viscosity measurements. Solutions of polystyrene and polymethylmethacrylate composite and control films were prepared in

benzene. Polyvinylidene fluoride composite and control viscosities were measured prior to film casting as a function of time after addition of $Fe(CO)_5$ because the films became insoluble after film casting and decomposition of the organometallic. Measurements were made at 30°C. By plotting x (concentration C of solution in g/dl) versus y (reduced viscosity = specific viscosity/concentration of solution) and extrapolating to C = 0, one can determine the intrinsic viscosity, [n]. The [n] was used to calculate viscosity-average molecular weights, $\bar{M}_v$, using the Mark-Houwink equation (105) and appropriate constants for each polymeric system. This procedure is more clearly described in Appendix B.

4. RESULTS AND DISCUSSION

4.1 Preparation of Metal Carbonyl-Polymer Solid Solutions

The preparation, decomposition chemistry and properties for a number of carbonyl-polymer compositions were studied (see Table 2). A variety of metal carbonyls were selected to study any differences in decomposition pathways and the products formed as well as their interaction with the matrix polymer. By also selecting polymers with various chemical structures, the chemistry of these solid state decompositions may be better understood. The need for mutual solubility of the carbonyl and polymer governs the organic solvent selected for the preparation of films and the chemical interaction of the solvent with the metal carbonyl and polymer was also found to affect the final products. The following discussion summarizes the significant results achieved in this investigation.

4.1.1 Carbonyl-Solvent Interactions Affecting Polymer Films

To produce homogeneous solid solutions of a metal carbonyl in a polymer, they must be comiscible in suitable film casting solvents. It is important to understand any chemical interactions that may occur between the metal carbonyl and solvent to produce active intermediates which may in turn affect the final products. For example, in the system PVF_2-$Fe(CO)_5$, PVF_2 is soluble in DMF which also solvents $Fe(CO)_5$. However, the IR spectrum of $Fe(CO)_5$ in DMF (Figure 17), shows the appearance of a band at 1880 cm^{-1} corresponding to a carbonyl anion.

TABLE 2: Metal Carbonyl-Polymer Systems Studied

Metal Carbonyl Concentration[a]	Polymer	Solvent	Characterization
Wt. % $(Fe(CO)_5$			
0.4 - 6.8	Polycarbonate	CH_2Cl_2	ε, [η], IR
6.8 - 9.3			TEM, [η]
3.0 - 6.8			e^-
6.8			SAXS/Mag, Ea/k
0.1 - 1.8	Polysulfone	CH_2Cl_2	ε, IR
1.8 - 2.1			[η]
2.1 - ~4.0			TEM
~4.0			e^-
1.8			SAXS/Mag, Ea/k
0.7	Polysulfone	CH_2Cl_2 (in 10% H_2)	TEM, Ea/k, IR
0.7 - 1.6	Polystyrene	CH_2Cl_2	ε, IR
1.6			[η], SAXS/Mag, Ea/k
1.6 - ~3.0			TEM
0.9	Polystyrene	CH_2Cl_2 (in 10% H_2)	TEM, Ea/k, IR
<0.1	Polydimethyl-siloxane	CH_2Cl_2	TEM, IR
0.2 - 0.88	Polymethyl-methacrylate	C_6H_6	ε, IR
0.88			[η], TEM
0.88			SAXS/Mg, Ea/k
4.6 - 5.7	Polyvinylidene Fluoride	DMF	ε, TEM
6.5 (added)			[η][c]
4.6			SAXS/Mag, Ea/k
Wt. % $Fe_3(CO)_{12}$			
0.24 - 0.52	Polycarbonate	CH_2Cl_2 (in CO)	ε, Ea/k, IR
0.52			TEM
0.54	Polycarbonate	CH_2Cl_2 (in air)	IR

Table 2: Metal Carbonyl-Polymer Systems Studied (continued)

Metal Carbonyl Concentration[a]	Polymer	Solvent	Characterization
0.28 - 0.57	Polystyrene	CH_2Cl_2 (in CO)	ε, Ea/k, TEM
~1.0	Polystyrene	CH_2Cl_2/DMF	TEM, IR
2.0 - 6.0	Polystyrene	CH_2Cl_2/Pluronic	SAXS/Mag.
~0.3 - 6.0	Polysulfone	CH_2Cl_2/Pluronic	TEM, IR
2.1			SAXS/Mag
~1.0	Polysulfone	CH_2Cl_2/DMF	TEM, IR
Wt. %. $Co_2(CO)_8$			
0.3 - 1.1	Polystyrene	CH_2Cl_2 (in CO)	ε
0.9 - 8.6			Ea/k, IR
4.2 - 8.6			TEM
4.2			SAXS/Mag
8.8	Polystyrene	Ch_2Cl_2(in 10% H_2)	Ea/k, IR
~20 (added)	Polyvinylidene Fluoride	DMF (in CO)	TEM [η][c]
Wt. % $Fe(CO)_5/Co_2(CO)_8$			
7/8 (added)	Polysulfone	CH_2Cl_2 (in CO)	IR, Qualitative only
7/8 (added)	Polyvinylidene Fluoride	DMF (in CO)	Qualitative only

[a] Actual metal carbonyl concentration retained in films. Controls with no added carbonyl also studied.

[b] Legend to characterization of composite systems:

ε = extinction coefficient determinations
[η] = intrinsic viscosity measurements
e^- = electron beam decomposition studies
TEM = transmission electron microscopy and electron energy dispersive data
SAXS/Mag = small angle X-ray scattering studies and magnetic property measurements
Ea/k = activation energy and/or rate constant evaluation via infrared spectroscopy studies
IR = infrared spectroscopy

[c] Viscosity measurements made prior to film casting of solution.

This indicates that a reaction occurs between $Fe(CO)_5$ and DMF; a disproportionation reaction (23, 106).

Similar reactions are also observed to occur between $Co_2(CO)_8$ and DMF, though much more rapidly (63,107). Studies of the disproportionation reaction of $Co_2(CO)_8$ show that the kinetics of this reaction is strongly dependent on the solvent and gaseous environment used (Figure 18). Wender et al. (22) also observed the formation of the anion-cation complex for $Co_2(CO)_8$ in pyridine:

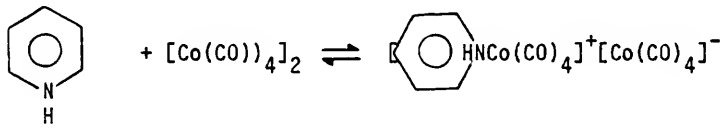

In DMF, $Co_2(CO)_8$ shows a broad amide (N-H stretching) absorption at 3550 cm^{-1} in addition to the carbonyl anion absorption at 1880 cm^{-1}. As noted from the above reaction scheme, the distribution of electron densities about the nitrogen atom would be altered by the presence of the bulky cobalt cation-anion complex. A similar reaction is probable with DMF to produce the observed 3550 cm^{-1} infrared absorption. DMF, an aprotic solvent, is able to solvate cations most strongly through formation of ion-dipole bonds while leaving the anions relatively unencumbered and highly reactive (22,102). Solvation affects the N-H stretching of the DMF. In hexane, like methylene chloride, only the terminal and bridging species are observed with no disproportionation

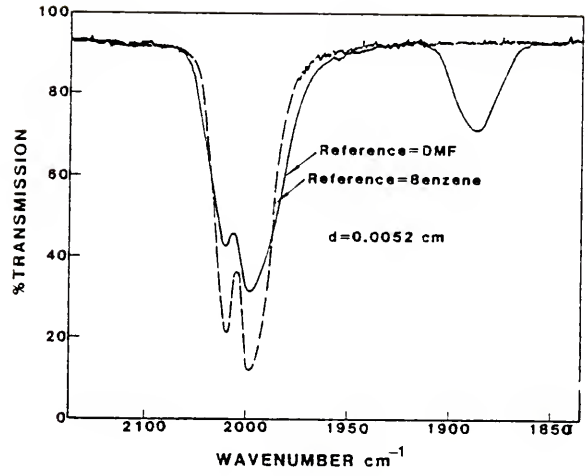

Figure 17. Infrared Spectrum of $Fe(CO)_5$ in DMF and in Benzene.

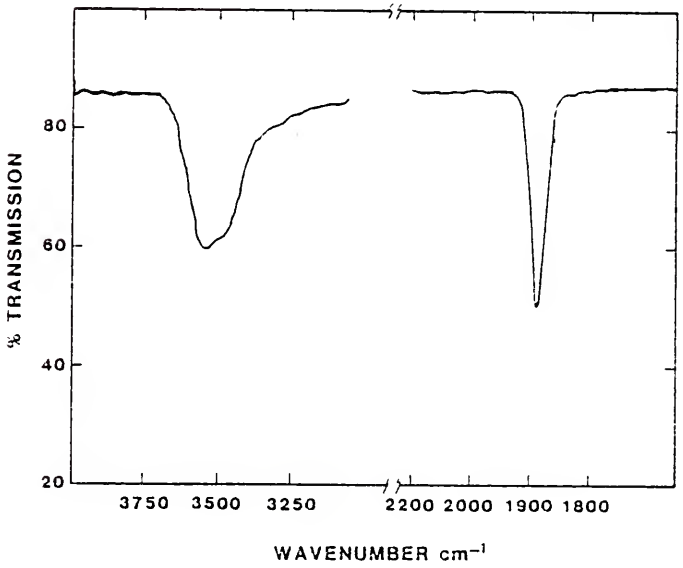

Figure 18. Infrared Spectrum of $Co_2(CO)_8$ in DMF.

reaction occurring (Figure 19). Figure 20 summarizes the disproportionation reactions that may occur between either iron or cobalt carbonyls and DMF. For $Co_2(CO)_8$ in methylene chloride, two major carbonyl peaks are observed: the terminal CO stretch (at 2040 cm^{-1}) and the bridging CO stretching (at 1860 cm^{-1}). These bands are retained though shifted to lower wavenumber in the $Co_2(CO)_8$/PS/methylene chloride composite systems (Figure 21). The bridging CO absorption at 1860 cm^{-1} was used to determine the kinetics of decomposition reactions for these systems.

Though the disproportionation reaction of $Fe(CO)_5$ in DMF is slow, it cannot be neglected in the preparation of PVF_2-$Fe(CO)_5$ composites. The boiling point of DMF is 136°C. Hence, the drying time for the film is quite long at room temperature (2-3 days). There is therefore sufficient time for the carbonyl-solvent reaction as supported by data given in Table 3. Two different PVF_2 film casting methods were compared. The only difference was the length of time during which the iron carbonyl was in contact with DMF. In the "hot" method, the contact time was only 1-2 hours until the film was dry. For the"cold" method, where the film was dried at room temperature, the time was several days. The resulting films were quite different. With the "hot" method, very good, tough, and uniform films were obtained. With the "cold" method, it appears that the polymer was attacked and degraded to some extent thus yielding poorly formed films.

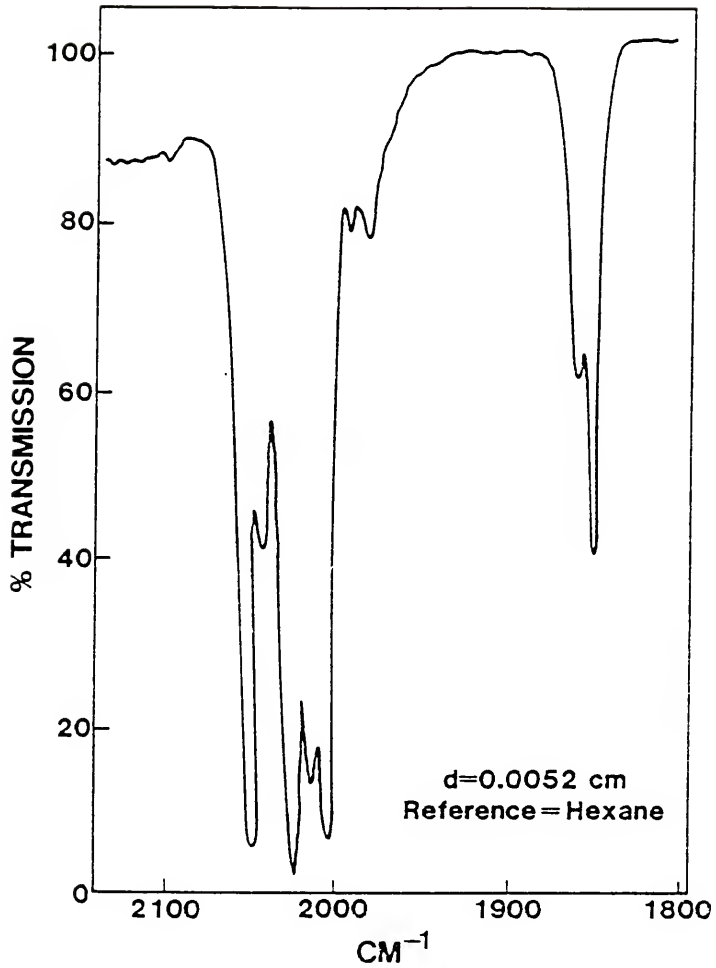

Figure 19. Infrared Spectrum of $Co_2(CO)_8$ in Hexane After Mixing 30 Minutes and in CO.

(1)

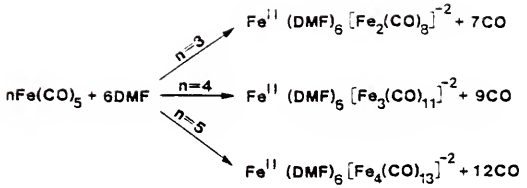

(2)

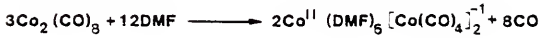

Figure 20. Disproportionation Reactions of Iron (1) and Cobalt (2) Carbonyls in DMF.

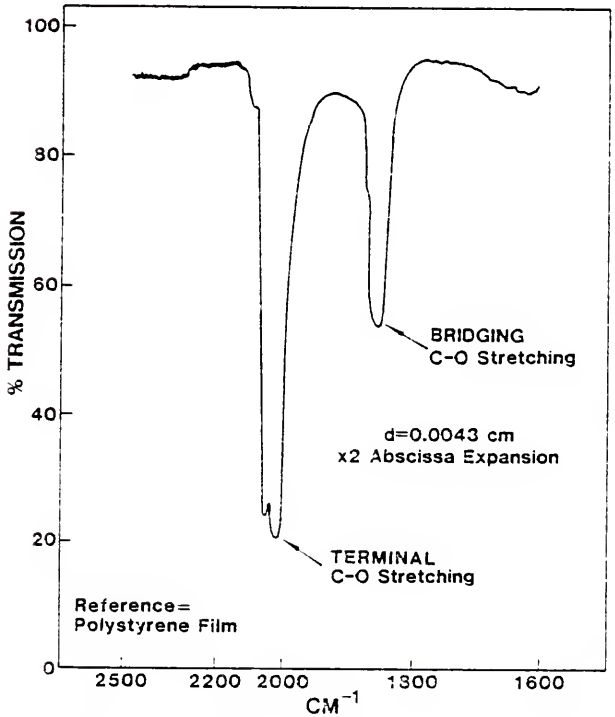

Figure 21. Infrared Spectrum of a 30 wt.% $Co_2(CO)_8$-Polystyrene Film (Cast from CH_2Cl_2).

TABLE 3. Casting Methods for $Fe(CO)_5/PVF_2$/DMF Systems

Solution	Casting Method	Quality of Film	Solubility in DMF	Appearance
PVF_2/DMF	Hot(114°C)	Good	No	Clear
	Cold (R.T.)	Good	Yes	Clear
PVF_2/DMF/$Fe(CO)_5$	Hot	Good	No	Clear
	Cold	Cracked Areas	No	Opaque

As stated earlier, DMF is an aprotic solvent. This type of solvent is very polar and dissolves both organic and inorganic reagents. In dissolving ionic compounds, it solvates cations most strongly leaving the anionic species more available for reaction. Bases are much more basic and nucleophiles more nucleophilic in DMF. Thus, the electronegative fluorine atom becomes more susceptible to abstraction at the elevated temperatures used to devolatilize the aprotic solvent, DMF. It is very interesting that this chemical reaction can lead to crosslinking of the PVF_2 itself and resultant insolubility. In PVF_2-$Fe(CO)_5$ systems, the iron carbonyl anion forms due to the disproportionation reaction. This anionic species is reactive and most probably reacts with the abstracted fluorine atom leading to the formation of FeF_2.

In the PMMA-$Fe(CO)_5$ system, another problem arises. As a rule, it is preferable for the solvent to have a boiling point well below that of $Fe(CO)_5$, 101°C. Therefore, in most of the systems studied, CH_2Cl_2 (boiling point of 40°C) was chosen. There is no interaction between $Fe(CO)_5$ and methylene chloride under the experimental conditions (see Figure 22). It is also of interest to note that no chemical interaction

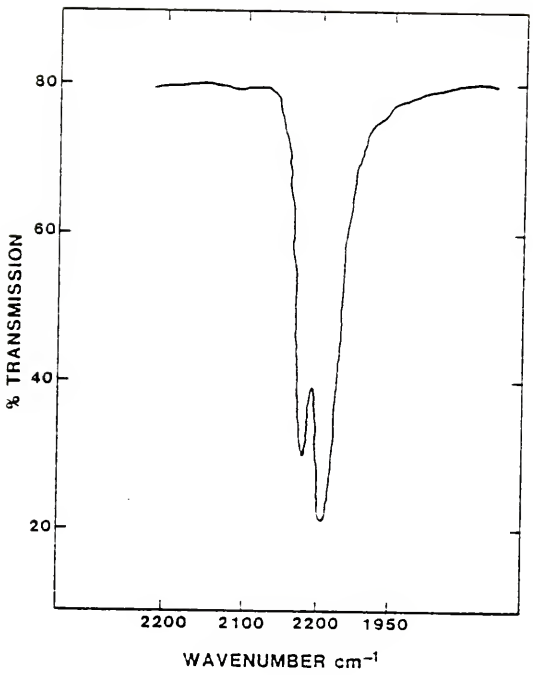

Figure 22. Infrared Spectra of $Fe(CO)_5$ in Methylene Chloride.

between the separate carbonyls for the mixed iron-cobalt carbonyl systems in either DMF or methylene chloride was observed.

As stated previously (59,108), interactions between $Fe(CO)_5$ and chlorinated solvents can occur only when the latter have geminal dihalides and are activated by an electron donor group. This is not the case for CH_2Cl_2. For PMMA-$Fe(CO)_5$, however, CH_2Cl_2 does not solvate PMMA. Benzene was therefore used since it dissolves PMMA and because there is no $Fe(CO)_5$-benzene interaction (see Figure 17). Since the boiling point of benzene is 80°C, $Fe(CO)_5$ evaporation occurs with benzene evaporation during the drying period. As a result, the initial carbonyl concentration decreased significantly during film forming. For example, an initial $Fe(CO)_5$ loading of 40 wt% was found to correspond to an actual loading of less than 10 wt% in the final cast films.

Though $Fe_3(CO)_{12}$ was not observed to undergo a disproportionation reaction in DMF as does $Fe(CO)_5$ (see Figure 23), the low solubility of $Fe_3(CO)_{12}$ in methylene chloride also created some problems in the preparation of homogeneous films (109). This is indicated in the photomicrograph of a $Fe_3(CO)_{12}$-polycarbonate film (Figure 24) prepared from a methylene chloride solution. A solubility limit of 3.4 g $Fe_3(CO)_{12}$/liter methylene chloride was determined in our laboratory. In order to facilitate dispersion, a surfactant (Pluronic--polyethylene oxide-polypropylene oxide) or a few percent of DMF was added. Studies by Chantrell et al. (65) suggest that the use of surfactant molecules containing a polar group that may adsorb to a particle surface and to a hydrocarbon that is similar to the dispersing medium improves the dispersion of ferrofluids. Hess and Parker (21) have also noted that polymers of high molecular weight and relatively nonpolar backbones with

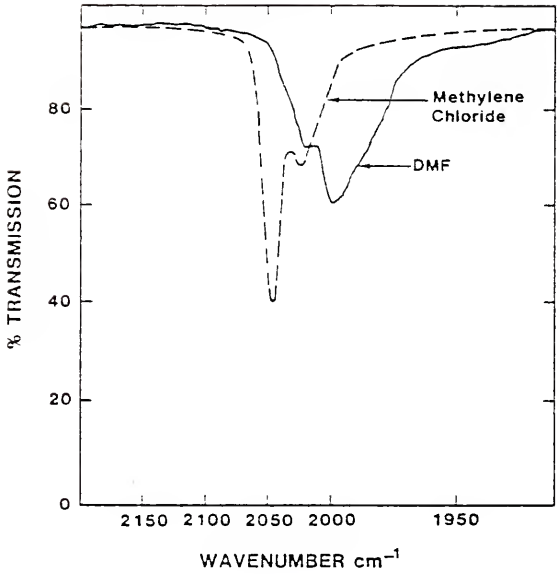

Figure 23. Infrared Spectra of $Fe_3(CO)_{12}$ in DMF and in Methylene Chloride.

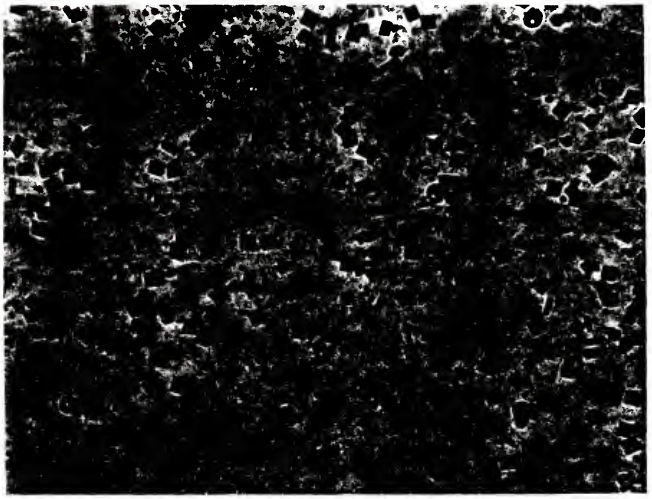

Figure 24. Photomicrograph of $Fe_3(CO)_{12}$-Polycarbonate Film Showing $Fe_3(CO)_{12}$ Crystals.

pendent polar groups (i.e. amides) tend to stabilize colloidal cobalt systems. Our studies indicate that Pluronic surfactant greatly increases the dispersion of $Fe_3(CO)_{12}$ but that phase separation occurs between the polymer matrix and surfactant. Thus, the selection of a polymer more compatible with the surfactant may improve the overall dispersivity of $Fe_3(CO)_{12}$ in polymeric systems.

4.1.2 Photolytic and Oxidative Decomposition Factors Affecting Incorporation of Metal Carbonyls into Polymer Films

A problem arises in the preparation of composite films because many of the metal carbonyls are sensitive to photolytic and oxidative decomposition. The reaction:

$$Fe(CO)_5 \xrightarrow{h\nu} Fe(CO)_4 + CO \xrightarrow{Fe(CO)_5} Fe_2(CO)_9$$

occurs readily upon UV irradiation of $Fe(CO)_5$ (28,110,111). The product of this photolytic process, $Fe_2(CO)_9$, is more susceptibly to oxidation than $Fe(CO)_5$. Though somewhat protected from oxidation within the polymeric matrix, exposure of the films to air and light at room temperature may lead to the formation of iron oxide in a very short time. To prevent this undesired decomposition, $Fe(CO)_5$-polymer films must be shielded at all times from exposure to light and preferably stored in an inert atmosphere. If the first requirement is met, then $Fe(CO)_5$ is not converted to $Fe_2(CO)_9$, and the oxidation of $Fe(CO)_5$ at room temperature is very slow. Thus, UV shielded films can be kept for long periods of time even in air without significant decomposition.

Triiron dodecacarbonyl is a volatile dark green crystalline solid, very sparingly soluble in organic solvents (109). On standing in air,

this carbonyl oxidizes to brown iron(III) oxide. Thus, it is best preserved by storage under nitrogen. Triiron dodecacarbonyl may be formed by three different methods: the action of heat on $Fe_2(CO)_9$, oxidation of the anion $HFe(CO)_4^-$ by various oxidizing agents, and treatment of $Fe(CO)_5$ with triethylamine followed by acidification of the reaction mixture. These preparative methods are briefly mentioned because of their close relationship to the systems in this study. Following incorporation of $Fe_3(CO)_{12}$ into polymer matrices, a greatly reduced oxidation rate was noted. In fact, films could be left for long times (days) in air with only slight carbonyl decomposition.

For $Co_2(CO)_8$, there also is a room temperature oxidation process which occurs in the absence of light:

$$Co_2(CO)_8 \xrightarrow[\text{room temp.}]{\text{air } (O_2)} CoO,\ Co_2O_3$$

Crystalline $Co_2(CO)_8$ is thermodynamcally stable up to 5°C if kept under 1 atmosphere CO, but at 25°C, $Co_4(CO)_{12}$ begins to form (112). Under an inert atmosphere and in solution, decomposition occurs more rapidly and via a $Co_4(CO)_{12}$ intermediate:

$$Co_2(CO)_8 \xrightarrow[50\text{-}70\,^0C]{\text{inert atm } (N_2)} Co_4(CO)_{12} \xrightarrow[90\text{-}100\,^0C]{\text{inert atm } (N_2)} Co + CO$$

Cobalt-polymer films were primarily prepared under a room temperature CO environment to favor the equilibrium of this reaction to the left--towards maintaining $Co_2(CO)_8$.

4.2 Spectroscopic Analysis of Carbonyl-Polymer Compositions

The identification and quantitative determination of metal carbonyl species in solution or in solid polymer matrices were carried out by infrared spectroscopy. IR was used because (a) most solvents and polymers do not have strong absorption bands in the region between 1800 and 2200 cm^{-1} where metal carbonyls absorb (if a solvent or polymer does absorb in this region it can be compensated with a reference), (b) the carbonyl bands of metal carbonyls, both terminal and bridging, are very sharp and well contoured in the 1800-2200 cm^{-1} region and permit an accurate evaluation of concentration, and (c) the infrared spectra of a great number of metal-carbonyls and their hydride species including $Co_2(CO)_8$ and $Fe(CO)_5$, are well known (92,103,113). Moreover, the influence of various factors on the spectra (such as solvent effects, temperature or substituting ligands) have been considered in the literature (24,92,113), and therefore permit evaluation of changes in the spectra of the metal-poymer composite films.

The infrared spectra of $Fe(CO)_5$ in a hydrocarbon solvent and in a polystyrene matrix are shown in Figures 25 and 26, respectively. There are two strong bands at 2019 and 1996 cm^{-1} and a weak band at 645 cm^{-1}. The two main absorption bands (C-O stretching) are retained also in the infrared spectra of $Fe(CO)_5$ in the various other polymeric matrices. The small absorption at approximately 2100 cm^{-1} observed in the carbonyl-polymer systems, but not in solution, corresponds to an iron tetracarbonyl species (10). For $Fe_3(CO)_{12}$ in methylene chloride there are two main absorptions at 2042 and 2020 cm^{-1}. These absorptions are retained and only slightly broadened in a polymer matrix (Figure 27). These bands are observed to shift to lower wavenumbers in

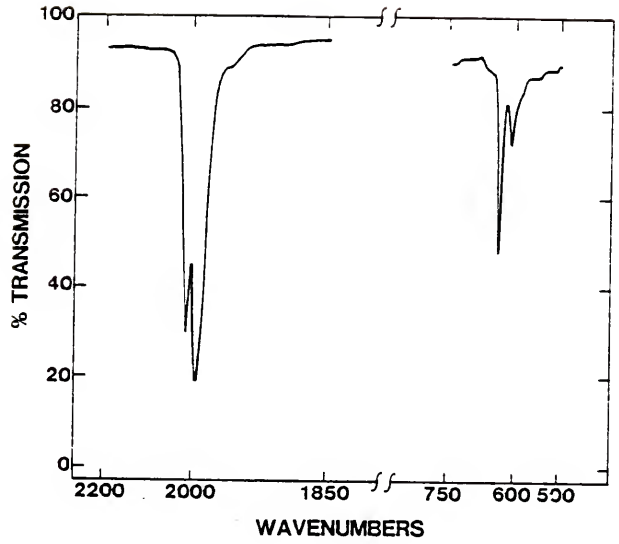

Figure 25. Infrared Spectrum of $Fe(CO)_5$ in Benzene.

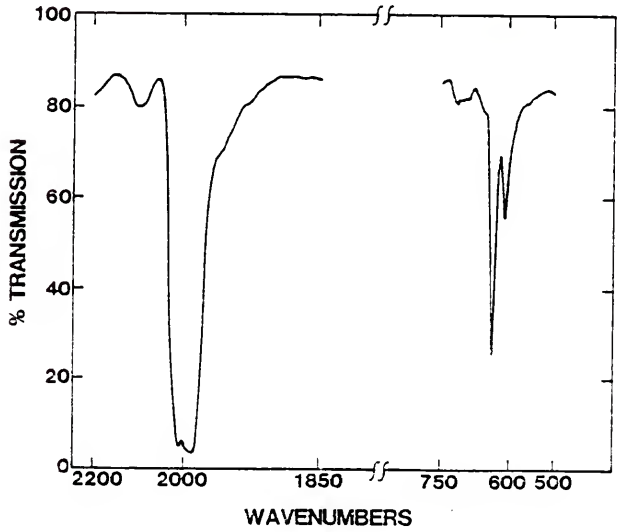

Figure 26. Infrared Spectrum of $Fe(CO)_5$-Polystyrene Film Before Decomposition of Carbonyl.

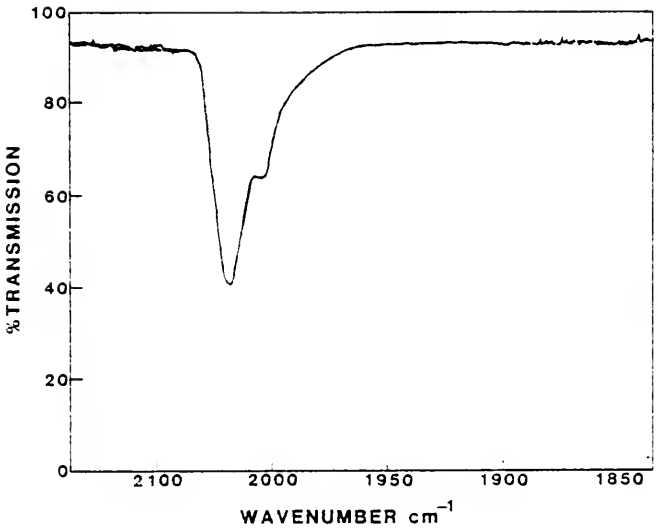

Figure 27. Infrared Spectrum of $Fe_3(CO)_{12}$ in Polycarbonate (Cast in CH_2Cl_2).

DMF (2015 and 1998 cm^{-1}, respectively), though the formation of an anionic complex is not noted (refer back to Figure 23). Similarly, strong carbonyl stretching absorptions at 2065 and 2040 cm^{-1} along with the bridging carbonyl absorption at 1860 cm^{-1} are noted for $Co_2(CO)_8$ in methylene chloride. As previously discussed, the disproportionation reaction of $Co_2(CO)_8$ in DMF to form the anionic complex is quite rapid and only the 1890 cm^{-1} carbonyl absorption is retained along with the formation of an amide stretching band at 3550 cm^{-1}. Although there is a shift to lower wavenumber and a decrease in the number of absorption bands observed for $Co_2(CO)_8$ in a polymer relative to hexane, the bridging carbonyl band is retained. One may conclude by comparing these spectra that the metal carbonyls of interest retain characteristic absorptions in solid polymer matrices and hence the spectra may be used for quantitative measurements.

4.2.1 UV-Vis Spectroscopic and Atomic Absorption Analysis to Determine Metal Concentrations

It was important to measure the actual amount of metal carbonyl retained in the final films prior to decomposition because of carbonyl volatility and reactivity. The amount of iron pentacarbonyl in the composites was determined using Vogel's 1,10-phenanthroline solution method. From UV absorptions at 396 nm and comparison to the iron standard curve (see Section 3.6.2), the actual iron concentrations in composite films were measured. The iron or cobalt concentration in $Fe_3(CO)_{12}$ or $Co_2(CO)_8$ composites was also determined using a pyrolytic technique followed by atomic absorption analysis. These carbonyls are crystalline solids and the polymeric composites of these two carbonyls were prepared in a closed CO or H_2 environment. The added metal

carbonyl content of cast films for these carbonyls was much closer to the amount initially added.

4.2.2 Determinaton of Infrared Extinction Coefficients to Correlate Metal and Metal Carbonyl Concentrations

By making the assumption that the amount of iron determined from Vogel's 1,10-phenanthroline method corresponds to the concentration of $Fe(CO)_5$ indicated by the infrared absorption in the carbonyl stretching region, infrared extinction coefficients for iron pentacarbonyls in the various polymeric systems were evaluated. This same assumption was made for $Fe_3(CO)_{12}$ and $Co_2(CO)_8$ composites analyzed for metal content by pyrolysis followed by atomic absorption. For these determinations, infrared extinction coefficients were evaluated in terms of solid polymer volume. Thus for each system, a cast film density was determined and used (see Appendix C for sample calculation of actual iron concentrations and infrared extinction coefficients).

In 1960, Noack reported some extinction coefficient values for the main IR bands of numerous carbonyls, both in hydrocarbon and chlorinated solvents (103). Since both types of solvents were used it was of interest to compare our solution extinction coefficient values with those of Noack. Noack's values are presented adjacent to our solution extinction coefficients in Table 4. The extinction coefficients determined for the various systems studied are presented in Table 5. In polymeric composites, the carbonyl absorption bands at in the 2000 cm^{-1} region retain the same relative doublet intensitives of those produced in the solvent in which the carbonyl-polymer solution was prepared. Since methylene chloride was normally the solvent of choice, the extinction coefficients of metal carbonyls in polymers are compared to appropriate values in this solvent. In all polymeric composites, the

Table 4. IR Extinction Coefficients[a] for Metal Carbonyls in Solution

System	Extinction Coefficient	Noack's Extinction Coefficient	Wavenumber cm^{-1}
$Fe(CO)_5$-ethyl benzene	4140	---	
$Fe(CO)_5$-methylene chloride	---	8200	1996
$Fe_3(CO)_{12}$-methylene chloride	12000	18000	2047
$Fe_3(CO)_{12}$-ethyl benzene	12650	---	2047
$Co_2(CO)_8$-methylene chloride	3870	3400	2040
$Co_2(CO)_8$-methylene chloride	1000	1000	1860
$Co_2(CO)_8$-hexane	---	1200	1886

[a]Units are liter of solution/mole metal carbonyl cm

Table 5. IR Extinction Coefficients for Metal Carbonyls in Polymer Matrices

System	Extinction Coefficient[d]	Wavenumber cm^{-1}
$Fe(CO)_5$-PC[a]	2524	1996
$Fe(CO)_5$-PSF[a]	5189	1994
$Fe(CO)_5$-PS[a]	7148	1996
$Fe(CO)_5$-PMMA[b]	7458	1996
$Fe(CO)_5$-PVF_2[c]	~350	1996
$Fe_3(CO)_{12}$-PC[a]	7710	2040
$Fe_3(CO)_{12}$-PS[a]	8660	2045
$Co_2(CO)_8$-PS[a]	825	2035
	281	1860

a. Films cast from methylene chloride solution
b. Films cast from benzene solution
c. Films cast from dimethylformamide
d. Units are liters of film/mole metal carbonyl cm

extinction coefficient for the ~2000 cm^{-1} band was observed to be lower than in solution, even when taking into consideration the solvent effect on this value. The same phenomenon was also observed in the case of $Co_2(CO)_8$ in polystyrene. It is likely that the polymeric matrix may impose restrictions on the vibrational degrees of freedom of the metal carbonyl resulting in bands of lower intensity. This is supported by the fact that extinction coefficients in the amorphous polymers (PSF, PS and PMMA) are higher suggesting that there is greater freedom (stretching, bending) in an amorphous structure than in the highly ordered crystalline morphology of polyvinylidene fluoride (105,114).

4.3 Decomposition of Metal Carbonyls in Polymer Matrices

The decomposition kinetics for metal carbonyls in solution were of interest to this study for comparison with the kinetics observed in polymeric matrices. The experimental procedure for evaluating solution kinetics is described in Section 3.10. The kinetic data for solution decompositions are presented in the following discussion of appropriate polymeric systems. The first-order rate law may be represented as:

$$\text{Ln } A = kt + \text{constant}$$

where A = concentration of reactant A
t = time (sec.)

Thus, a plot of Ln A vs t gives a straight line of slope equal to -k, where k is the rate constant. In the case where the reaction rate is proportional to A^2 or to (A)(B), second-order kinetics is said to be

observed. The rate constant k now has units of concentration^{-1} sec.$^{-1}$ and the equation becomes:

$$\text{Ln}\ \frac{(B_o)(A)}{(A_o)(B)} = [(A_o)-(B_o)]\ kt$$

where A_o and B_o = initial concentration of reactants of A and B

where A and B = concentration of A and B at time t

This is often the case where intermediate products form and accumulate in a reaction.

4.3.1 Kinetics of Thermal Decomposition for Iron Carbonyls in Polymeric Matrices

Metal carbonyl thermal decompositions in various polymeric matrices were studied at different temperatures and carbonyl concentrations. The actual concentrations of carbonyls present in the polymeric matrices are given in Table 2, section 4.1.1.

Polydimethylsiloxane (PSi) was observed to retain very little iron pentacarbonyl even prior to heat treatment as noted both from the lack of a characteristic color and from the iron analysis. The addition of small amounts of DMF to the PSi-$Fe(CO)_5$-methylene chloride solutions to produce the anionic species did little to improve this retention. Silicone elastomers are high molecular weight polymers, usually polydimethylsiloxanes. The room-temperature vulcanizing (RTV) silicone elastomers are cured by crosslinking linear or slightly branched siloxane chains with reactive end groups such as silanols which are activated by atmospheric moisture to yield the Si-O-Si link with

production of HCl (105). It is probable that during the preparation of the PSi-$Fe(CO)_5$ solutions for film casting, there was sufficient exposure to light to produce some $Fe(CO)_4^{-2}$ which could form iron hydride (24). This pale yellow solid (the color noted for these films) is stable only at very low temperature and in the liquid state begins to decompose above -10°C. It is relatively more stable in the gas phase when diluted with carbon monoxide. Thus, it would seem we have achieved nearly complete volatilization of $Fe(CO)_5$ under the conditions existing in the polydimethylsiloxane-$Fe(CO)_5$ system.

A typical series of infrared spectra corresponding to two $Fe(CO)_5$ decomposition experiments are presented: Figure 28 shows the thermal decomposition of $Fe(CO)_5$ in PSF at 118°C; Figure 29 shows the thermal decomposition of $Fe(CO)_5$ in PVF_2 at 140°C. The $Fe(CO)_5$-PVF_2 system is presented separately because the films intended for decomposition studies were initially prepared by "cold" casting and hence there was a disproportionation reaction involving $Fe(CO)_5$ and DMF. All kinetic calculations for the various systems were done using the 1996 cm^{-1} IR carbonyl band. In all cases, the $Fe(CO)_5$ thermal decomposition follows first order reaction kinetics (see Figures 30 and 31).

From the slopes shown, the rate constants for the thermal decompositions were calculated for each system at each decomposition temperature. Table 6 shows these values at 125°C and 140°C (see Appendix D for calculation of rate constants). This table also includes the decomposition rate constant for a solution of $Fe(CO)_5$ in ethyl benzene. Note that the decomposition in a polymer matrix is faster than in solution. This fact agrees with our observations in systems containing cobalt where the decomposition and oxidation of $Co_2(CO)_8$ was

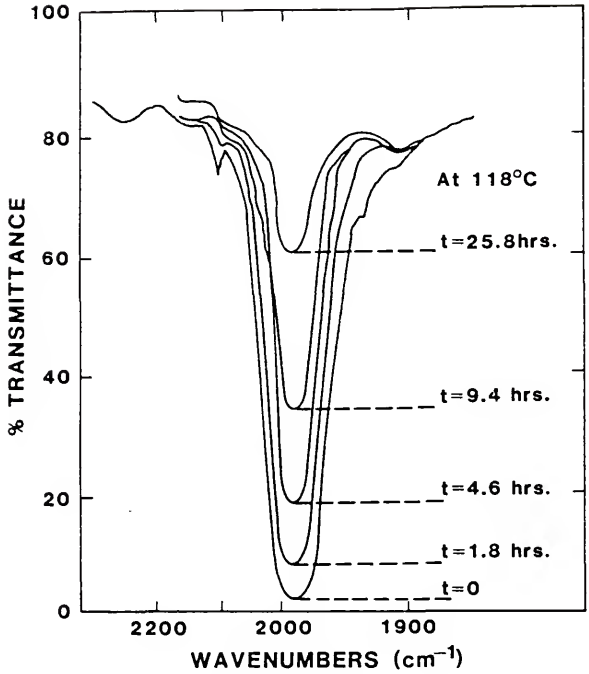

Figure 28. Thermal Decomposition of $Fe(CO)_5$ in PSF at 118°C.

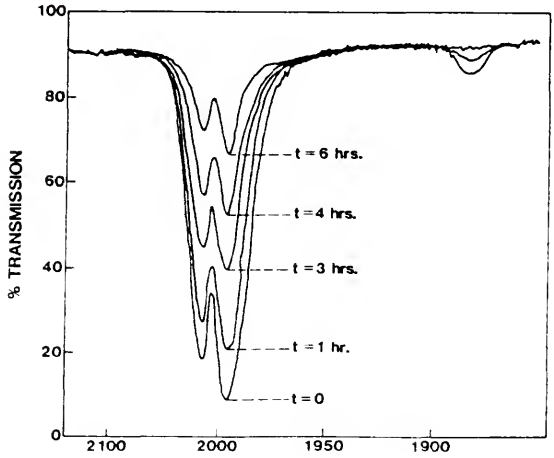

Figure 29. Thermal Decomposition of $Fe(CO)_5$ in PVF_2 at 140°C.

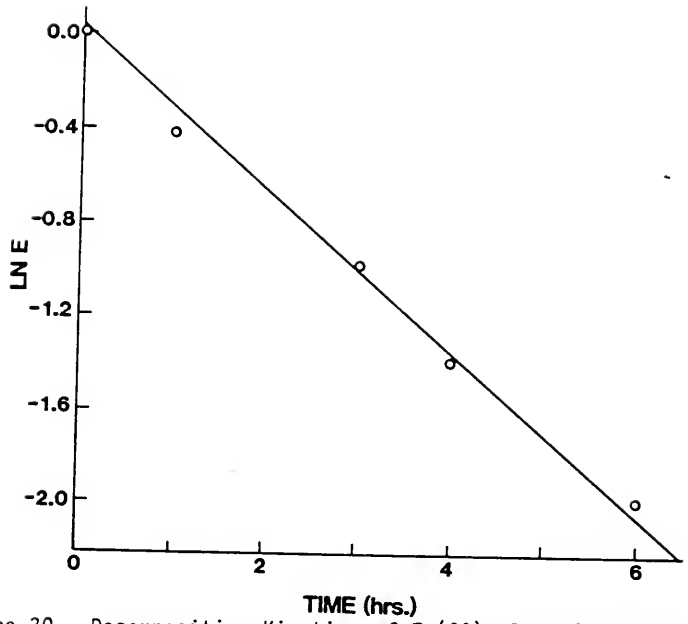

Figure 30. Decomposition Kinetics of $Fe(CO)_5$-PVF_2 Composites at 140°C.

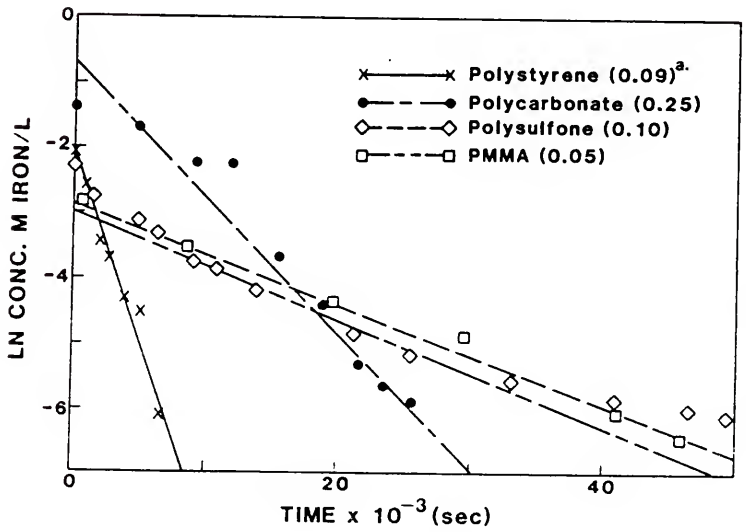

Figure 31. Decomposition Kinetics of $Fe(CO)_5$-Polymer Systems at 132°C.
a. Moles $Fe(CO)_5$ per liter of film at time = 0 seconds.

Table 6. Observed Rate Constants For The Thermal Decomposition of $Fe(CO)_5$-Polymer Composites.

Polymer Composite	Rate Constant at 125°C (sec^{-1})	Rate Constant at 140°C (sec^{-1})
Prepared in Air		
6.8% $Fe(CO)_5$-PC	3.11×10^{-5}	2.57×10^{-4}
1.8% $Fe(CO)_5$-PSF	3.90×10^{-5}	3.13×10^{-4}
1.6% $Fe(CO)_5$-PS	5.18×10^{-4}	6.69×10^{-4}
0.9% $Fe(CO)_5$-PMMA	5.48×10^{-5}	1.82×10^{-4}
4.6% $Fe(CO)_5$-PVF_2	---	9.12×10^{-4}
1.0% $Fe(CO)_5$-ethyl benzene	6.71×10^{-5}	8.69×10^{-5} [a]
Prepared in H_2		
0.9% $Fe(CO)_5$-PS	4.09×10^{-5}	---
0.7% $Fe(CO)_5$-PSF	1.14×10^{-5}	---

[a] Rate constant for $Fe(CO)_5$-ethyl benzene thermal decomposition at 130°C.

found to be two orders of magnitude faster in a solid polymeric matrix than in solution.

This may be attributed to the fact that the metal carbonyl is embedded in a thin polymer film, thus its exposure to O_2 is more extensive than in solution. The decomposition rates of $Fe(CO)_5$ in polymer samples prepared in a 10 wt. % H_2-argon environment were slightly slower than those prepared in air. This same trend is observed in comparing the $Co_2(CO)_8$-polystyrene samples prepared under H_2 and CO. This may be attributed to the slightly lower concentrations used in those iron-polymer systems prepared in an H_2-argon environment. Also, inert argon gas was used as the carrier gas for the H_2 in film preparation and storage, thus largely eliminating the incorporation of oxygen into the polymer film. The fact that argon is a relatively heavy molecule also slows down its migration and displacement in a film matrix as well. The combination of these factors could produce this trend in reaction rate.

The thermal decompositions were performed at 118°C, 125°C, 132°C and 142°C. The rate constants were plotted versus temperature as shown in Figure 32 and activation energies were calculated from the slopes (Table 7). The activation energy for the solid state decomposition of $Fe(CO)_5$ in a polycarbonate matrix was observed to be higher than that of other systems studied. From the viscosity measurements, extensive molecular weight breakdown is noted, suggesting attack on the polycarbonate backbone. The mechanism of this attack is proposed to be anionic attack at the ester group on the polycarbonate backbone - a chemical bond requiring higher energy to dissociate than the metal carbonyl bond itself. A higher activation energy also is noted for the

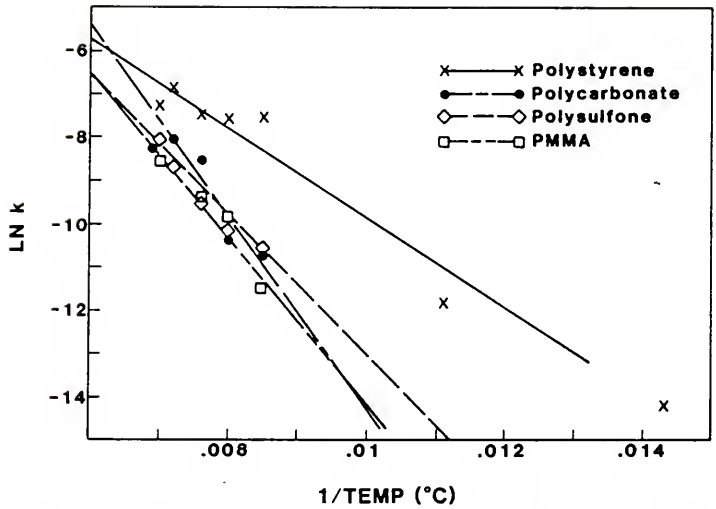

Figure 32. Arrhenius Plot for Thermal Decomposition of $Fe(CO)_5$-Polymer Composites.

Table 7. Thermal Activation Energies For The Decomposition of $Fe(CO)_5$-Polymer Composites

Composite System	Activation Energy ($\frac{Kcal}{mole}$)
$Fe(CO)_5$-PC	45.1
$Fe(CO)_5$-PSF	30.2
$Fe(CO)_5$-PS	29.0
$Fe(CO)_5$-PMMA	35.4

solid state decomposition of $Fe(CO)_5$ in polymethylmethacrylate. The appearance of a hydroxyl stretching absorption was observed upon thermal treatment of $Fe(CO)_5$-PMMA films suggesting similar anionic attack to that proposed for PC systems. PMMA also contains an ester group, though not in the main chain, thus little change is observed in the molecular weight. Activation energies observed for both the PC and PMMA systems were higher than those for polymeric systems not containing an ester group. This suggests that activation energies for the $Fe(CO)_5$-polymer systems increase as the degree of interaction with the polymer increases.

4.3.2 Kinetics of Thermal Decompositions for Triiron Dodecacarbonyl in Solid Polymer Matrices

The comparision of kinetics and decomposition products of the $Fe_3(CO)_{12}$ systems with respect to the $Fe(CO)_5$-polymer systems is useful in understanding the chemistry of the solid-state decompositions. The effect of semi-immobilization of the larger triiron carbonyl complex in a polymer matrix is demonstrated by the decomposition species formed (as followed via IR spectroscopy) and the reaction rates for the carbonyl decomposition.

Comparison of spectra for the $Fe_3(CO)_{12}$-polymer systems prepared in air versus those prepared in CO (Figure 33, a and b) indicate the effect of an oxidative atmosphere upon the decomposition of $Fe_3(CO)_{12}$ to other carbonyl species during thermal treatments. A much simpler spectra is obtained from $Fe_3(CO)_{12}$ polymer films prepared under CO. Once within the solid polymeric matrix, the $Fe_3(CO)_{12}$ is relatively stable even upon exposure of the composite film to light and air. This indicates that the polymer matrix acts as a barrier to oxidative processes upon the

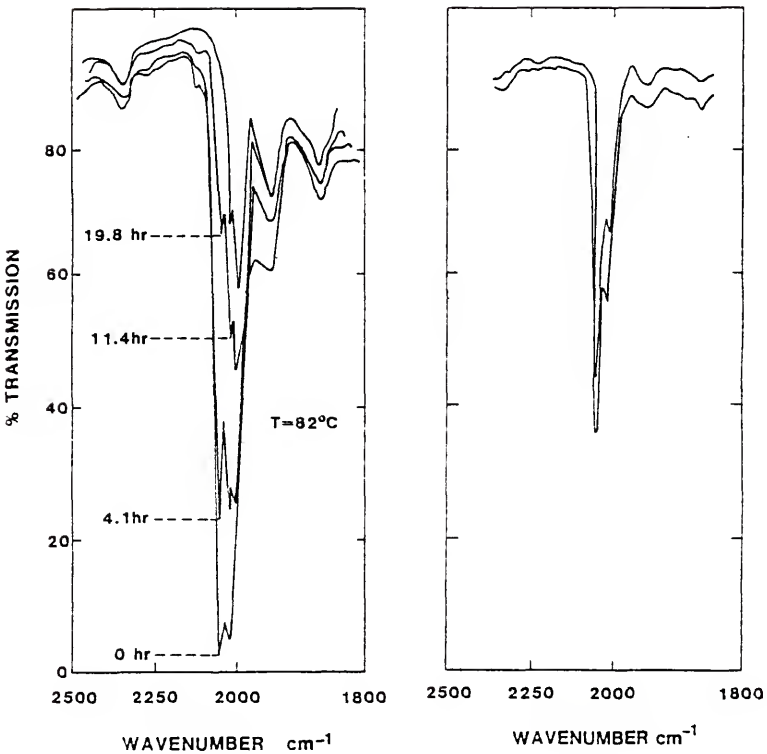

Figure 33. Infrared Spectra Showing Thermal Decomposition of $Fe_3(CO)_2$ in Polystyrene Prepared and Stored in Air (a) and in CO (b).

$Fe_3(CO)_{12}$. However, there was an observed, though quite slow, decomposition of the carbonyl band with prolonged exposure to air indicating the slow diffusion of air into the polymer matrix.

The 2045 cm^{-1} band was used in this study to determine the kinetics for the decomposition of $Fe_3(CO)_{12}$ in solution and in a polymer matrix. Table 8 shows the observed rate constants for the various systems studied. Solution decomposition kinetics are also presented to compare with solid state decompositions. Low concentrations of $Fe_3(CO)_{12}$ were necessary in order to follow the kinetics of decomposition via IR spectrophotometry.

The kinetics for thermal decomposition of $Fe_3(CO)_{12}$ in ethyl benzene in air proceeds via intermediate formation of $Fe(CO)_5$ and thus follows a second-order rate law. This is evident in the appearance of the characteristic IR absorption 1996 cm^{-1} (see Figure 34) and in the color change from green triiron dodecacarbonyl to brown iron pentacarbonyl. This reaction occurs almost immediately at 110°C decompositions, but can be easily followed at 82°C.

For neutral molecules, bridging CO groups absorb in the 1700-1860 cm^{-1} and terminal ones generally absorb at higher frequencies, 1850-2125 cm^{-1} (24). The initial solution spectra for $Fe_3(CO)_{12}$ show two terminal CO stretching vibrations at 2045 and 2016 cm^{-1}. Thus, it seems that initially there are no bridging CO's present. Wender and Pino also confirm this for $Fe_3(CO)_{12}$ in solution (32). The $Fe_3(CO)_{12}$ structure is a highly unsymmetrical one and the most stable conformations are those in which bridges are incompletely formed. With heating, a decrease in the 2045 cm^{-1} absorption is accompanied by the appearance and increase of the characteristic $Fe(CO)_5$ band at 1996 cm^{-1}. The 2016 cm^{-1}

TABLE 8. Observed Rate Constants for the Thermal Decomposition in Air of $Fe_3(CO)_{12}$-Polymer Composites and Solutions

Polymer Composite	Rate Constant (sec^{-1})	Temperature °C	Activation Energy Kcal/mole
0.5% $Fe_3(CO)_{12}$-PC	1.90×10^{-3}	110°C	
	1.30×10^{-4}	82	22.2
	7.86×10^{-7}	30	
0.7% $Fe_3(CO)_{12}$-PS	1.78×10^{-4}	110°C	
	1.56×10^{-4}	82	20.1
	2.65×10^{-7}	30	
0.4% $Fe_3(CO)_{12}$- ethyl benzene	[a]	110°C	
	7.13×10^{-2}	82 [b]	---

[a] Decomposition of 2045 cm^{-1} IR adsorption too rapid to follow.
[b] Decomposition of $Fe_3(CO)_{12}$ in ethyl benzene follows second-order rate law thus units become liter/mole sec.

absorption remains essentially constant until the 2045 cm^{-1} band has disappeared. As the 1996 cm^{-1} band is increasing, there is also the very brief appearance of a bridging CO species at 1865 cm^{-1} [suggested by Wender and Pino (32) to be due to bridging carbonyls in $Fe_3(CO)_{12}$ or $Fe_2(CO)_9$] and a terminal CO stretching region at 1942 cm^{-1}. During this thermal decomposition, the solution is observed to change from the brilliant $Fe_3(CO)_{12}$ green color to a brown solution with a dark precipitate indicative of iron oxides eventually forming.

In the polymer films, first-order decomposition kinetics are observed. Only the 2045 and 2016 cm^{-1} absorptions are observed and they both decrease simultaneously with thermal treatment. This is most

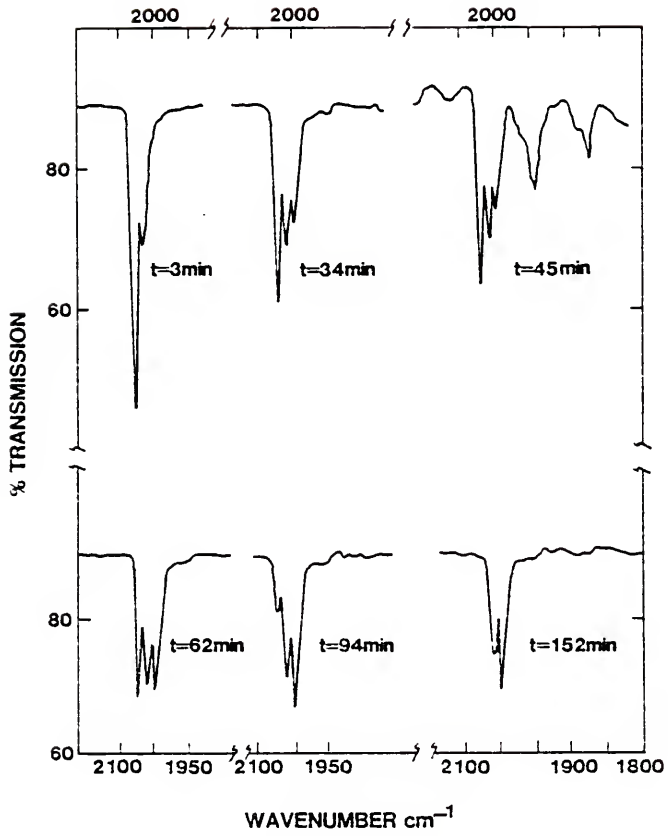

Figure 34. Thermal Decomposition of $Fe_3(CO)_{12}$ in Ethyl Benzene at 82°C in Air.

probably due to the restrictions in mobility placed upon the large $Fe_3(CO)_{12}$ molecule by the solid polymer matrix and upon the fact that the diffusion of oxygen into the polymer matrix is slower than in solution. The fact that hte solution decomposition kinetics of $Fe_3(CO)_{12}$ follows a second-order rate law while solid state decomposition kinetics is first-order makes rates difficult to compare.

4.3.3 Kinetics of Thermal Decomposition of Cobalt Carbonyl in Solid Polymer Matrices

The decomposition kinetics for $Co_2(CO)_8$ in solution and in a polystyrene matrix are somewhat more complex than those observed for iron carbonyls because the order of reaction is a function of the environment in which it occurs. The atmospheric decomposition of $Co_2(CO)_8$ in hexane is shown to follow first order kinetics (Figure 35) whereas decomposition under N_2 in toluene proceeds by second-order kinetics to form $Co_4(CO)_{12}$ (Figures 36 and 37). Dr. Tannenbaum is acknowledged for these solution studies.

Figures 38 and 39 show the thermal decomposition in air of $Co_2(CO)_8$ in a polystyrene matrix prepared under two different environments. Though both reactions follow first-order decomposition kinetics, those films prepared in CO decompose at a faster rate than those prepared in H_2 (see Table 9). Carbon monoxide tends to stabilize the $Co_2(CO)_8$ species (115) whereas in high H_2 pressures it is known to react in heptane as follows (116).

$$Co_2(CO)_8 + H_2 \xrightarrow[\text{heptane}]{25^0C} HCo(CO)_4$$

Though those $Co_2(CO)_3$-PS films prepared in 10% H_2-argon were pink in color, no anions were observed in the IR spectra for these systems.

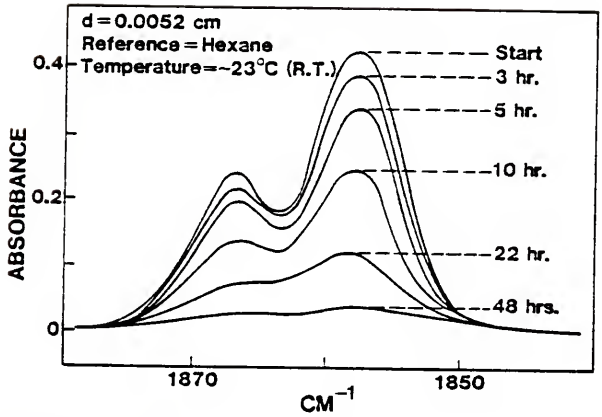

Figure 35. Decomposition in Air of 4.76×10^{-2} M/L $Co_2(CO)_8$ in Hexane.

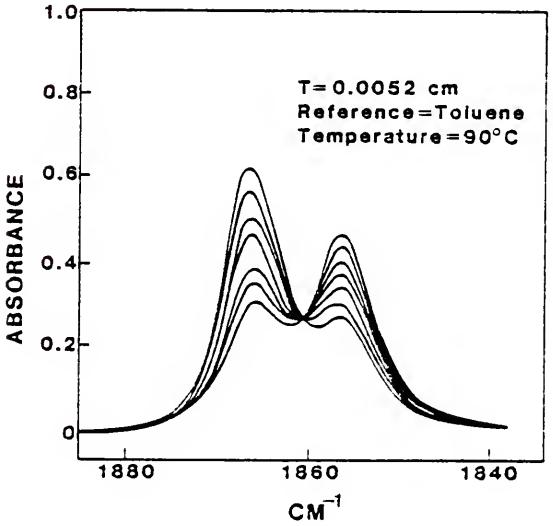

Figure 36. Decomposition in N_2 of 5.53×10^{-2} M/L $Co_2(CO)_8$ in Toluene.

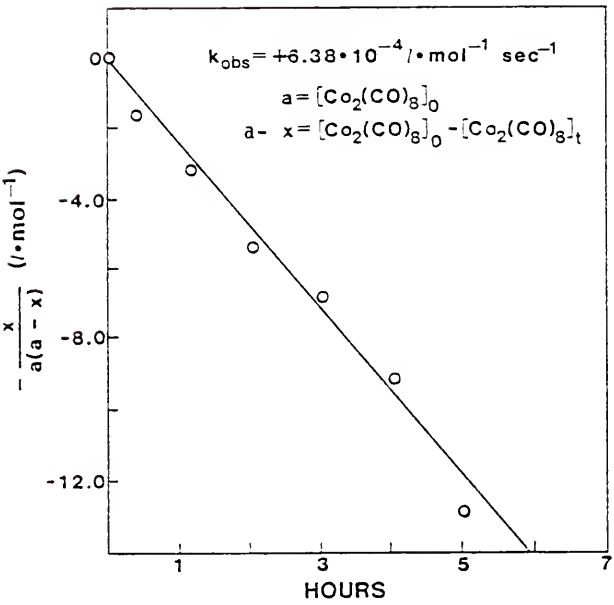

Figure 37. Second-Order Decomposition of $Co_2(CO)_8$ to $Co_4(CO)_{12}$ in Toluene at 90°C in Inert Atmosphere.

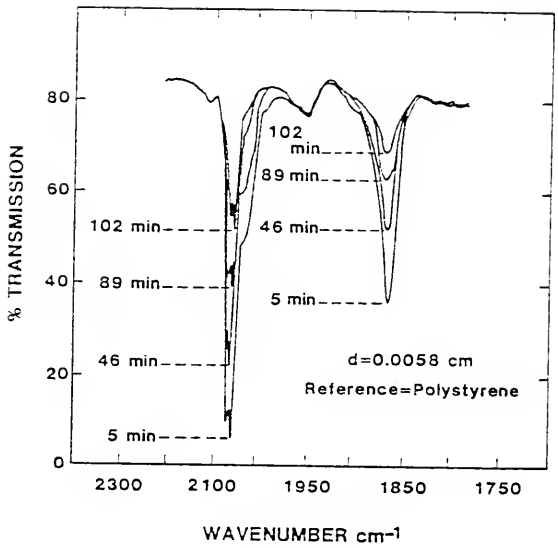

Figure 38. Infrared Spectra of the Decomposition of $Co_2(CO)_8$-Polystyrene (Cast from CH_2Cl_2 in H_2 at 36°C in Air.

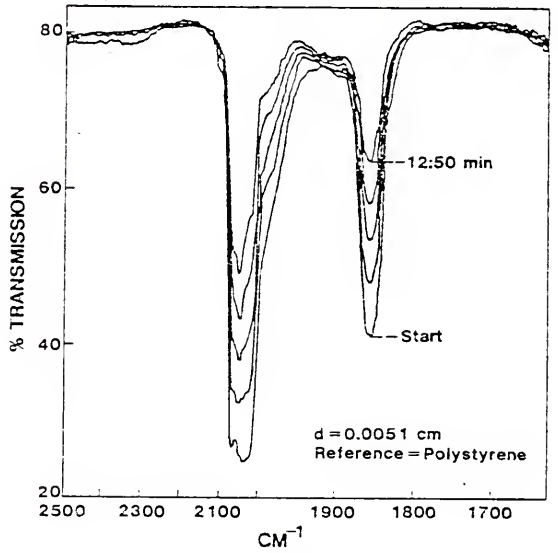

Figure 39. Infrared Spectra of the Decomposition of $Co_2(CO)_8$-Polystyrene (Cast from CH_2Cl_2 in CO) at 36°C in Air.

TABLE 9. Observed Rate Constants for the Thermal Decomposition of $Co_2(CO)_8$ in Solution and in Polstyrene

System	Prep/Storage	Rate Constant	Decomposition Conditions	IR cm^{-1}
2.1% $Co_2(CO)_8$-Toluene	CO/--	6.38×10^{-4}a	N_2/90°C	1867
8.0 % $Co_2(CO)_8$-Polystyrene	CO/CO	5.27×10^{-6}a	N_2/90°C	1858
2.0% $Co_2(CO)_8$-Hexane	CO/--	1.54×10^{-5}	Air/36°C	1858
0.4% $Co_2(CO)_8$-CH_2Cl_2	CO/--	2.75×10^{-4} 3.14×10^{-4}	Air/36°C	2050 1858
8.6% $Co_2(CO)_8$-Polystyrene	H_2/H_2	2.58×10^{-4} 2.17×10^{-4}	Air/36°C	2050 1858
6.5% $Co_2(CO)_8$-Polystyrene	CO/CO	1.08×10^{-3} 1.33×10^{-3}	Air/36°C 1858	2050
1.1% $Co_2(CO)_8$-Polystyrene	CO/CO	3.22×10^{-3} 1.86×10^{-3}	Air/28°C	2050 1858
0.9% $Co_2(CO)_8$-Polystyrene	CO/CO	3.45×10^{-3} 2.61×10^{-3}	Air/28°C	2050 1858

[a] Second-order decomposition kinetics with formation of $Co_4(CO)_{12}$ (units = liter/mole·sec). First order decomposition kinetics observed for other systems (units = $sec.^{-1}$).

The rate of oxidation of $Co_2(CO)_8$ is observed to be one to two orders of magnitude higher in polystyrene than in solution, depending on the solvent. Since $Co_2(CO)_8$ is embedded in a thin and amorphous polystyrene film, its exposure to O_2 is more extensive than in solution. Support for this hypothesis is provided by the "protective layers" experiments. In these experiments, polystyrene protective layers were cast over each side of a $Co_2(CO)_8$-polystyrene film, like the "bread" of a sandwich (see Figure 7, Section 3.3.3). The thickness of this protective layer was varied to effect a change in the thickness of the O_2 barrier. Figure 40 shows the thermal decomposition of a "protected" sample. First order decomposition kinetics in air were maintained. Figure 41 clearly shows that increasing the O_2 barrier thickness of polystyrene significantly slowed the oxidation reaction of $Co_2(CO)_8$.

Second-order decomposition kinetics of $Co_2(CO)_8$ to $Co_4(CO)_{12}$ in an N_2 atmosphere were observed in both solution and in a polystyrene matrix (Figure 42). The decomposition of $Co_2(CO)_8$ in an inert atmosphere $Co_4(CO)_{12}$ and further to CoO and Co is governed primarily by diffusion. This is supported by the fact that the rate of decomposition in N_2 is two orders of magnitude higher in solution than in the polystyrene matrix. In the later case, the solid state nature of the system considerably slows down the diffusion of the bulky $Co_2(CO)_8$ cluster through the matrix.

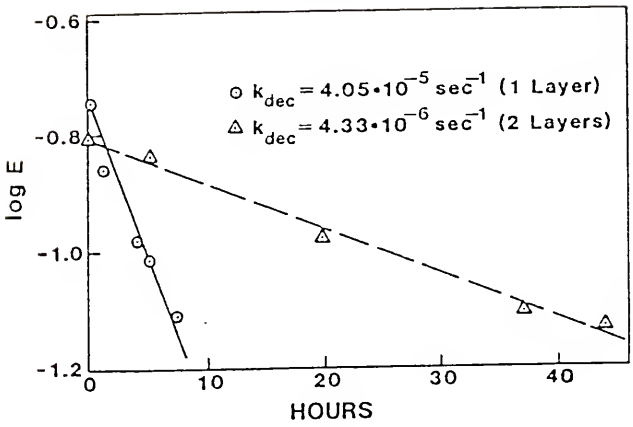

Figure 40. Decomposition of "Protected" Sample: $Co_2(CO)_8$ in Polystyrene-Effect of Increasing O_2 Barrier Film Thickness.

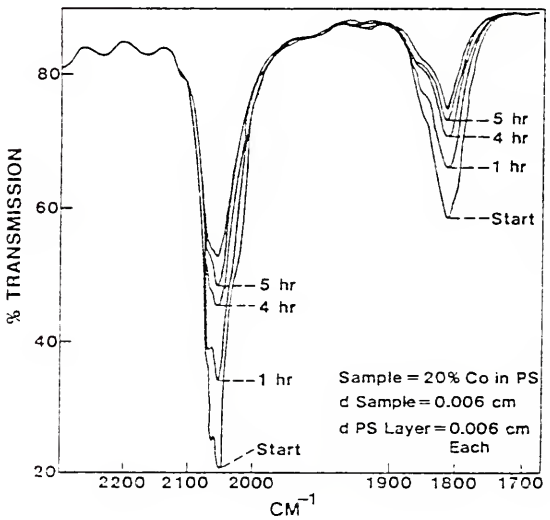

Figure 41. First-Order Decomposition in Air of $Co_2(CO)_8$-Polystyrene Film With Polystyrene Protective Layers at Room Temperature.

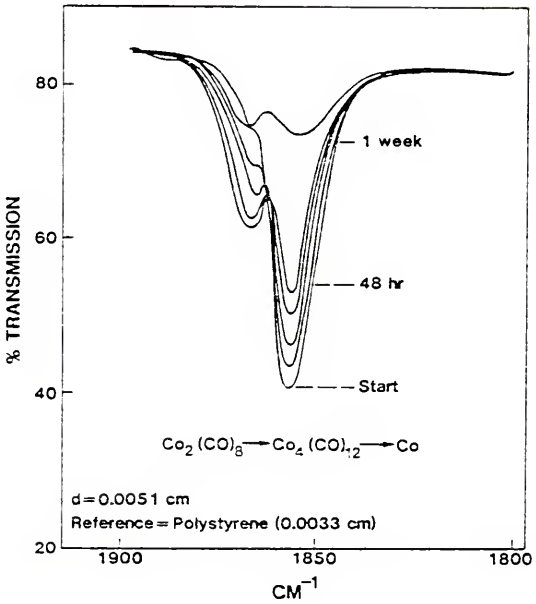

Figure 42. Second-Order Decomposition of $Co_2(CO)_8$ to $Co_4(CO)_{12}$ in Polystyrene Matrix in Inert Atmosphere at 90°C.

4.3.4 Kinetics of Photolytic Decomposition of Iron Carbonyls in Solid Polymer Matrices

In addition to thermal decompositions, photolytic decompositions were also performed on the iron carbonyl-polymer composites. It is not uncommon to find energies required for photochemical change to be higher than those for corresponding thermal reactions (110). Only those molecules which absorb the incident light can undergo primary excited-state events. This represents one of the real advantages in photoinduced chemical reactions when compared to heat driven reactions. It therefore is possible to selectively excite certain absorbing substances in the presence of other molecules which are transparent to the incident irradiation (117). De Paoli (10) applied this law in using polymers as matrices to study the photochemistry of metal carbonyls. He assumed that since polymers do not absorb the radiation used to induce the photochemical reactions of metal carbonyls, they would not enter into the reaction and thus not be degraded. Saturated hydro- and fluorocarbon polymers meet these requirements.

A primary method for the photochemical preparation of metal carbonyl derivatives involves ultraviolet radiation of a solution of the metal carbonyl in the presence of a donor D and resultant liberation of CO. Strohmeier carried out this type of solution preparation for metal carbonyls under nitrogen or argon because metal carbonyl derivatives are sensitive to oxidation. This problem is somewhat remedied by our method of iron carbonyl decomposition in a solid polymer matrix which tends to protect the iron carbonyl from rapid oxidation. In fact, the rate of $Co_2(CO)_8$ decomposition in a polystyrene matrix was studied with respect to the thickness of this boundary layer. Strohmeier also noted that the

choice of a suitable solvent is of vital importance to the yield and isolation of pure products.

Metal carbonyl complexes presently comprise the most important class of organometallic substances which have been the object of photochemical studies. Metal carbonyls are among the most photoreactive transition-metal complexes. All the $M(CO)_5$ complexes (M = Fe, Ru, Os) are photosensitive with respect to substitution of CO.

$$M(CO)_5 \xrightarrow{h\nu} [M(CO)_5]^* \longrightarrow M(CO)_4^- + CO$$

$$Fe(CO)_5 \xrightarrow{h\nu} Fe(CO)_4^- + CO \xrightarrow{Fe(CO)_5} Fe_2(CO)_9$$

The work of Clark and co-workers provides the now familiar result that ligands (L) most like CO will be incorporated to the highest degree (118). Excited-state reactions of polynuclear iron carbonyls includes both substitution and declusterifiation:

$$Fe_2(CO)_9 \xrightarrow[\text{Argon}]{h\nu,\ L} Fe_2(CO)_8^- + CO$$

$$Fe_2(CO)_9 \xrightarrow[\text{room temp.}]{h\nu,\ 2L} 2\ Fe(CO)_4L + CO$$

$Fe_3(CO)_{12}$ clusters have also received some attention and a variety of confusing observations made. Photodeclusterification involving the ring opening conversion of the trinuclear carbonyls to dinuclear and mononuclear species is likely to occur as represented below (117).

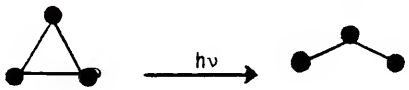

The UV decomposition reactions were of particular interest in the iron pentacarbonyl systems since it is well known that $Fe(CO)_5$ is converted to $Fe_2(CO)_9$ upon irradiation (28, 111) and hence may provide a different mechanistic pathway for the decomposition of $Fe(CO)_5$. These decompositions were also followed by means of infrared spectroscopy, but the characteristic bands for $Fe_2(CO)_9$ at 2066, 2038, 1855 and 1851 cm^{-1} (119) were not observed. Since the conversion of $Fe(CO)_5$ to $Fe_2(CO)_9$ is diffusion dependent and since the experiment was performed in air, it is required that the rate of diffusion of $Fe(CO)_5$ through the polymeric matrix be greater than the oxidative decomposition rate. From preliminary experiments, this did not seem to be the case.

First order decomposition kinetics were observed for the photochemical decomposition of iron pentacarbonyl in polymer matrices (see Figure 43). From the slopes shown, the rate constants for the photolytic decompositions were calculated and are summarized in Table 10 along with values determined by De Paoli for $Fe(CO)_5$ in a polyethylene (PE) matrix (10). From his work, he suggests that the photochemical decomposition reaction of $Fe(CO)_5$ in solution (with argon bubbled through to remove CO) is much slower than that observed in a polymer matrix. This trend was also observed in both our thermal and photolytic decomposition studies and lends support to the theory that metal carbonyls supported in thin films have increased exposure to oxygen (relative to solution) and thus decompose more rapidly.

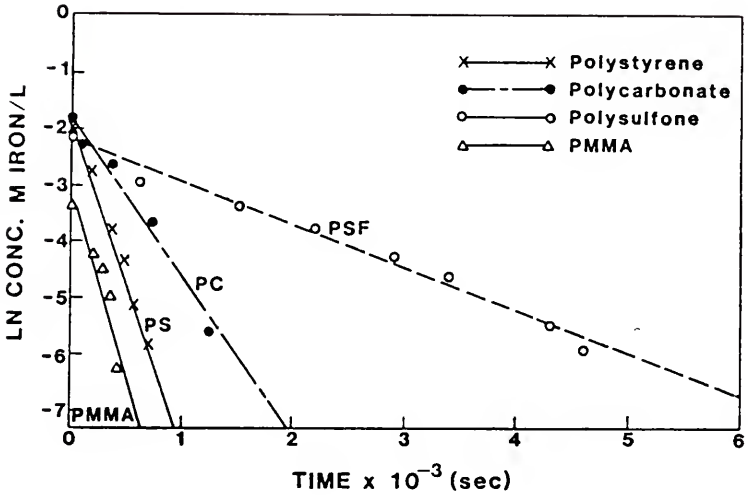

Figure 43. Photolytic Decomposition of $Fe(CO)_5$-Polymer Systems at 38 Nanoamperes.

TABLE 10. Observed Rate Constants for the Photolytic Decomposition of Iron-Polymer Systems

Polymer System	Rate Constant ($sec.^{-1}$)	Energy at Sample (nanoamps)[b]
6.8% $Fe(CO)_5$-PC	2.89×10^{-3}	37.7×10^3
1.8% $Fe(CO)_5$-PSF	7.51×10^{-4}	37.0×10^3
1.6% $Fe(CO)_5$-PS	5.70×10^{-3}	36.5×10^3
0.9 $Fe(CO)_5$-PMMA	7.10×10^{-3}	40.0×10^3
0.2 $Fe_3(CO)_{12}$-PS	2.19×10^{-4}	----
$Fe(CO)_5$-PE	6.5×10^{-3} [a]	----
$Fe(CO)_5$-PE	2.5×10^{-3} [a]	----
1.0%$Fe(CO)_5$-ethyl benzene	2.8×10^{-5}	---

[a] Values reported by De Paoli (10) for broad band UV light irradiation of $Fe(CO)_5$ in polyethylene films at ν_{2063} cm^{-1} and ν_{1973} cm^{-1} corresponding to $Fe(CO)_3$ and $Fe(CO)_4$, respectively.

[b] Decompositions were done at ~50 cm from source (radiometer/photometer not available to measure energy at sample for $Fe_3(CO)_{12}$-PS and $Fe(CO)_5$-ethyl benzene).

4.3.5 Kinetics of Gamma Radiation Decompositions of Iron Carbonyls in Solid Polymer Matrices

Gamma radiation was also used to decompose iron carbonyls in solid polymer matrices. Ionizing radiation, such as gamma radiation, have in fact been used to initiate chain polymerizations (114). Molecular excitation may occur with subsequent formation of radicals in the same manner as photolysis, but ionization of a compound is more probable due to the higher energies of this radiation compared to visible or

ultraviolet light. Ionizing radiations have particle or photon energies in the range of 10 KeV - 100 MeV compared to 1 - 6 eV for visible ultraviolet photons.

With the knowledge that gamma radiation facilitates chemical reactions through the formation of radical and ionic species, it was of interest to explore the possibilities for the solid state decomposition of metal carbonyls in a polymeric matrix via gamma radiation. The literature gives no report of any related studies. For our purpose, a Co-60 source was used to irradiate samples (approximately 0.1 g). At a distance of 2 inches from the cobalt source, the dose rate was 0.021 krad/sec.

Decomposition rates for the metal carbonyl-polymer systems treated with gamma radiation proceeded quite slowly (Table 11). This may be attributed to the fact that the dryness of the reaction system and absence of other species which can react with ions (either those formed in radiolytic reactions or in the ionic propagating species) are critical. No particular care was taken to eliminate moisture, oxygen, monomer or remnant solvent from films for radiation treatment, and thus the presence of these compounds may have scavenged many of the ionic species formed. It is of interest, however, that radiolytic decomposition proceeded much more rapidly in systems containing $Fe_3(CO)_{12}$ than those with $Fe(CO)_5$--which does not appear to decompose at a dose of 1.8 Mrad. Triiron dodecacarbonyl clusters have the structure shown in Figure 5 (Section 2.5.2) and may be undergoing radiolytic decluster-fication via ring opening of the trinuclear complex to produce reactive di- and mononuclear species. These species may then proceed to loose their CO via substitution reactions to form various iron oxide compounds.

Table 11. Observed Rate Constants for Gamma Radiation Decomposition of $Fe_3(CO)_{12}$-Polymer Composites

Polymer Composite	Rate Constant (sec^{-1}) At 2.1×10^{-5} $\frac{megarads}{sec}$
0.5% $Fe_3(CO)_{12}$-PC	1.11×10^{-5}
0.2% $Fe_3(CO)_{12}$-PS	5.67×10^{-6}
6.8% $Fe(CO)_5$-PC	no decomposition observed after 24 hour treatment

Though the polystyrene matrix was somewhat yellowed by a 5.4 Mrad gamma radiation treatment, qualitative mechanical properties seemed to be retained. The polycarbonate-$Fe_3(CO)_{12}$ composite became dark purple in color, quite similar to the polycarbonate-$Fe(CO)_5$ samples following thermal and photolytic decomposition treatments. This suggests the final products formed may be similar in these two systems: γ-Fe_2O_3 and β-FeOOH.

The possiblity that radiolytic decomposition of metal carbonyls may be achieved within certain polymer matrices without significant degradation of these matrix, suggests an interesting area for further research in the selective solid state decomposition of metal carbonyls.

4.4 Characterization of Metal Polymer-Composites

The characterization of the composite morphology (particle size, shape and chemical composition) are of interest to more completely understand the chemistry of these novel metal-polymer systems. To do this, extensive studies using transmission electron microscopy (TEM) and small angle x-ray scattering studies were pursued. Electron energy dispersive spectra (EEDS) was used in the TEM studies to positively identify metal containing morphologies. Magnetic susceptibility measurements were made on the Guoy balance to identify those systems of special interest for magnetic applications. Many systems were studied were numerous and much still needs to be done to understand the controlling factors and resulting products in these metal-polymer composites.

4.4.1 Microparticles Observed To Be Formed Within Polymer Matrices

The solid state decomposition of metal carbonyls in polymers generally produces heterophase metallic domains, some of which are a function of the matrix polymer. The nascent metal species created by UV photolysis or by thermal decomposition of metal carbonyls are highly reactive. In the presence of a polymer matrix, these reactive species may attack the polymer to crosslink or degrade it. The chemistry of the system is determined primarily by the nature of the polymer matrix, the decomposition atmosphere, reactivity of the metal species and the rate of the decomposition process.

4.4.1.1 Transmission electron microscopy with electron energy dispersive spectra: characterization of chemical composition of particles formed by solid state decomposition of metal carbonyls in polymer matrices

Figures 44 and 45 are a typical TEM photomicrograph showing particles formed by thermal decomposition of $Fe(CO)_5$ in a polycarbonate matrix. Figure 46 shows an SEM photomicrograph of a liquid nitrogen fracture surface of this iron-PC composite. Note that the phase separated particles are in clusters enclosed by the polymer matrix. Upon thermal treatment, the initially clear $Fe(CO)_5$-PC films became dark purple in color (higher carbonyl loadings producing darker pigmentation). Electron diffraction patterns for the $Fe(CO)_5$-PC composite product (Figure 47) are indicative of γ-Fe_2O_3 and β-FeOOH. Reaction of the passive γ-Fe_2O_3 particles with water is well known and has been discussed by Griffith et al. (70). It should be noted, however, that it is the α-polymorph of FeOOH which is normally formed. The β-structure has been observed to form only during the breakdown of α-Fe_2O_3 in the presence of chlorinated solvents. Thus, it is suggested

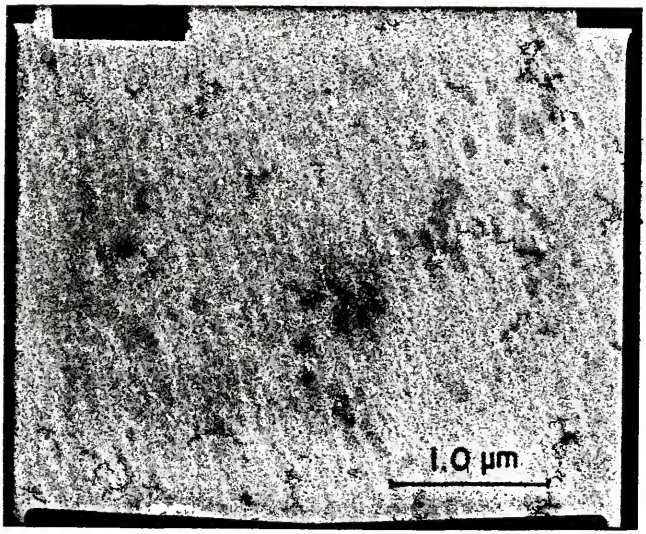

Figure 44. TEM Photomicrograph Showing Particles Formed by Thermal Decomposition of $Fe(CO)_5$ in a Polycarbonate Matrix.

Figure 45. TEM Photomicrograph (Higher Magnification and Higher Carbonyl Loading) Showing Particles Formed by Thermal Decomposition of $Fe(CO)_5$ in a Polycarbonate Matrix.

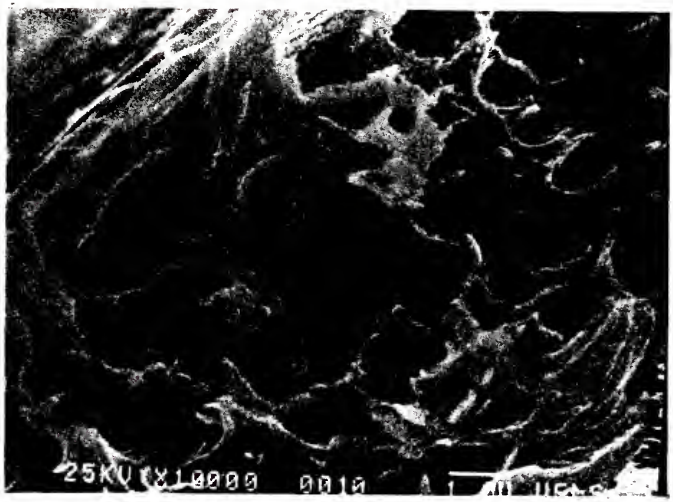

Figure 46. SEM Photomicrograph of a Liquid N_2 Fracture Surface Showing Iron Clusters by Polycarbonate Matrix.

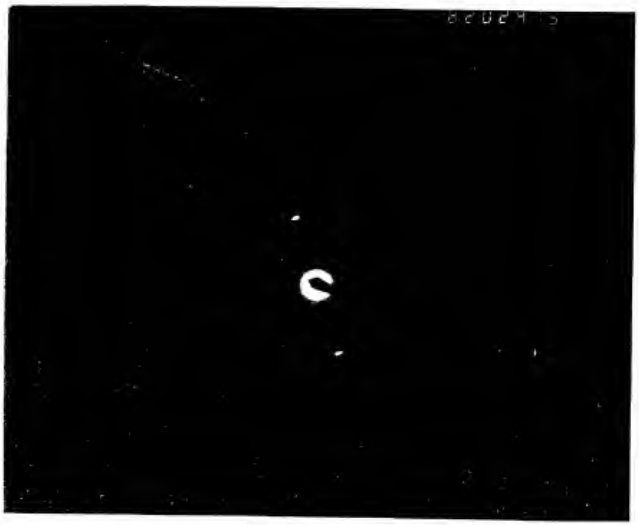

Figure 47. Electron Diffraction Pattern for Iron-PC Composite Indicative of γ-Fe_2O_3 and β-FeOOH.

that traces of CH_2Cl_2 present in the PC (supported by electron energy dispersive spectra shown in Figures 48 and 49) and atmospheric moisture are responsible for this reaction.

$$Fe_2O_3 + H_2O \rightleftharpoons 2FeOOH$$

The formation of metallic iron particles must also occur even though the concentration of the α-Fe particles is low due to the oxidative atmosphere in which the decompositions were conducted. In an inert atmosphere, these species could become the dominant particles, as observed for decompositions of $Co_2(CO)_8$ in N_2 which yield α-Co particles almost exclusively in our studies.

Figure 50 shows the chains of metal/metal oxide particles formed in the "cold cast" $Fe(CO)_5$-PVF_2 system suggesting magnetic interaction between the particles (69,70). S. Reich (97) also observed this encapsulation and chain-like morphology in iron-PVF_2 composites prepared by the "hot method". TEM photomicrographs of polysulfone (Figure 51) and of iron-polysulfone composites (Figures 52, 53 and 54) demonstrate the lack of this chain morphology in polysulfone composites. The formation of FeS particles in the PSF system and FeF_2 particles in the PVF_2 system indicate an interaction between the $Fe(CO)_5$ and polymer with abstraction of S or F. Initially light yellow and translucent $Fe(CO)_5$-PSF films became nearly opaque and a rich brown color upon decomposition treatments. However, the iron-PVF_2 composites remained translucent upon decomposition of the carbonyl though also becoming a rich yellow-brown color. The electron diffraction analyses for FeS and FeF_2 are presented in Table 12. EEDS for $Fe(CO)_5$-polysulfone systems indicate

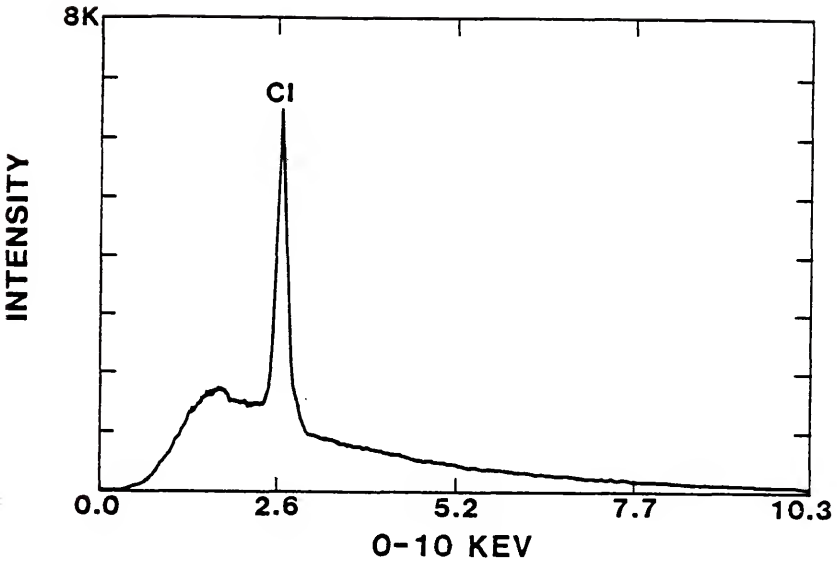

Figure 48. Electron Energy Dispersive Spectra for Polycarbonate Control Film Showing Chloride Peak (ie. Retained CH_2Cl_2).

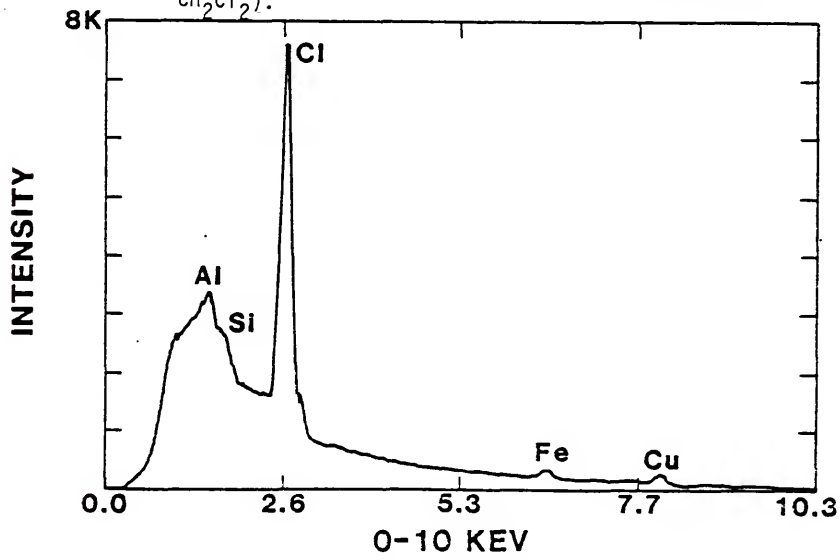

Figure 49. Electron Energy Dispersive Spectra for Iron-Polycarbonate Film Showing Chloride Peak (ie. Retained CH_2Cl_2).

Figure 50. TEM Photomicrograph of Chain-like Particle Morphology of "cold cast" Iron-PVF_2 Films Following Thermal Decomposition.

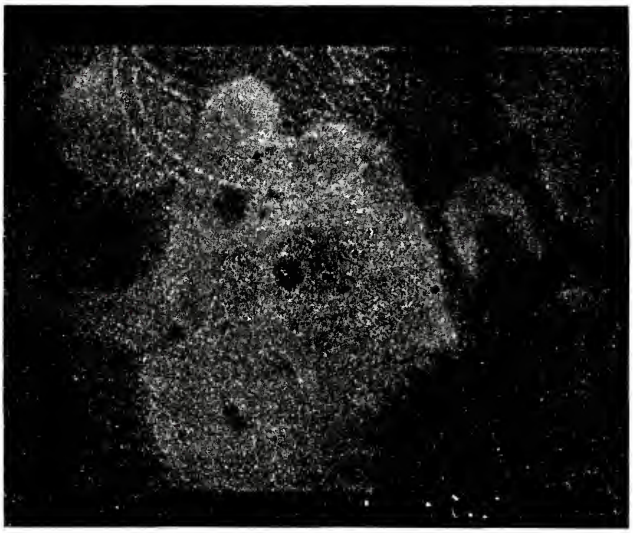

Figure 51. TEM Photomicrograph of Polysulfone Film Thermally Treated (Lighter Regions Represent Thinner Film).

Figure 52. TEM Photomicrograph of Iron-PSF Films Thermally Treated.

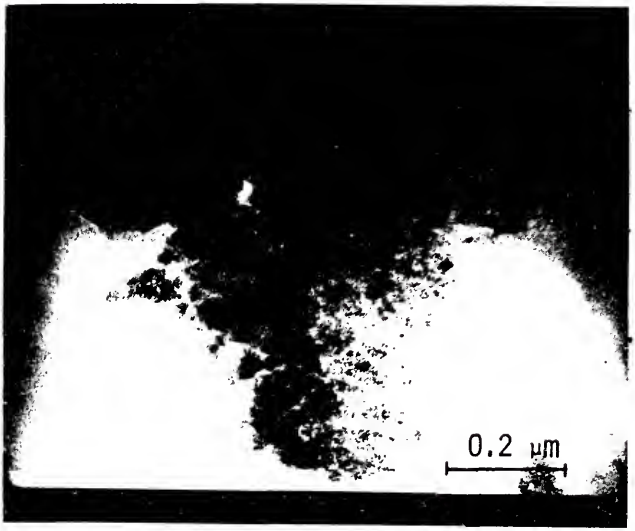

Figure 53. Higher Magnification TEM Photomicrograph of Iron-PSF Film Thermally Treated Showing Particle Morphology in Thin Film Region.

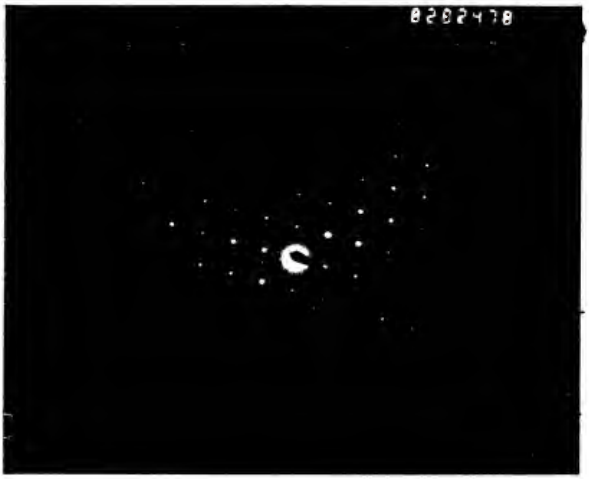

Figure 54. Electron Diffraction Pattern of Hexagonal Crystalline Morphology in Iron-PSF Composite.

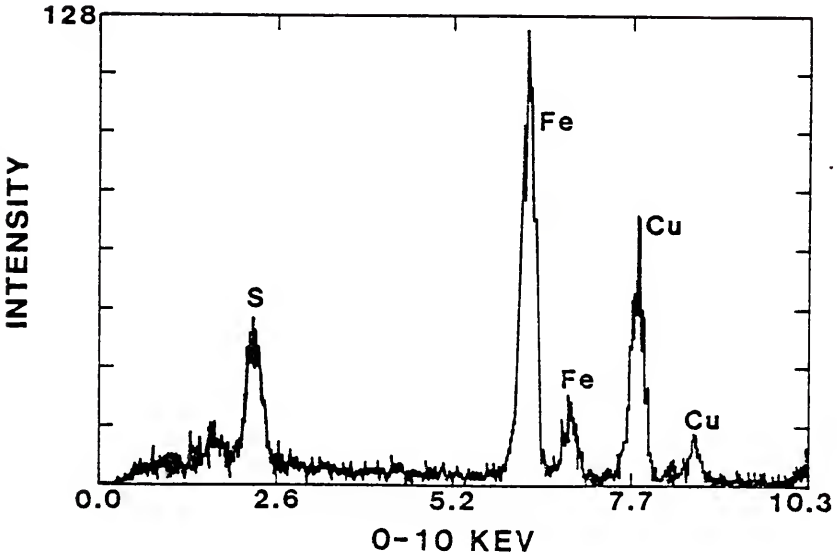

Figure 55. Electron Energy Dispersive Spectra of Crystalline Morphology in Iron-PSF Composite Indicative of Iron (Copper Peak is Due to Cu TEM Grid, S Peak to PSF).

Table 12. Electron Diffraction Analysis for FeF_2 and FeS in PVF_2 and PSF Composites, Respectively

Electron Diffraction d(Å)	FeF_2 d(Å)	Electron Diffraction	FeS d(Å)
3.31	3.32	3.59	3.65
2.67	2.70	3.01	3.24
2.33	2.34	2.87	2.84
2.09	2.10	2.53	2.59
1.76	1.73	2.45	2.44
1.64	1.66	2.07	2.11
1.48	1.49	----	1.98
----	1.48	1.81	1.75
1.41	1.42	1.64	1.63
1.36	1.39	1.51	1.50
----	1.21	1.41	1.41
1.19	1.17		
0.99	1.11		
0.92	1.05		

the absence of the chloride peak observed in polycarbonate composites (Figure 55). This is in agreement with the fact that no β-FeOOH was formed, only the δ-FeOOH polymorph.

Both polystyrene and polymethylmethacrylate composite systems showed low retention of $Fe(CO)_5$ in contrast to the polycarbonate and polysulfone systems. This was idicated not only by metal analyses and the lack of pronounced color for the polystyrene and polymethylmethacrylate composites, but also by the decrease in number of metal cluster morphological features viewed under TEM (Figures 56 and 57, respectively). Electron diffraction patterns for thermally treated $Fe(CO)_5$-PMMA films are indicative of γ-Fe_2O_3 and δ-FeOOH. The few clusters observed in thermally treated $Fe(CO)_5$-PS films made it more difficult to evaluate the morphology and composition of this system conclusively.

Polydimethylsiloxane (PSi) shows a distinct electron beam diffraction pattern and morphology which is present in the composite sample as well (Figures 58 and 59). This diffraction pattern is indicative of silicate filler making the indexing of spots difficult. However, analyses of the remaining diffraction spots in the PSi composite suggest the formation of some α-Fe and FeO particles despite the low retention of the carbonyl discussed earlier. Iron pentacarbonyl-PSF and PS films prepared and stored in 10% H_2-argon but thermally treated in air feature a morphology different from those prepared in air (Figures 60 and 61). The preparation in H_2 appears to have increased clustering of the particles. EEDS indicated the clusters indeed contained iron, but no diffraction patterns were observed from these inclusions. Dark field imaging (Figure 62) also indicates the

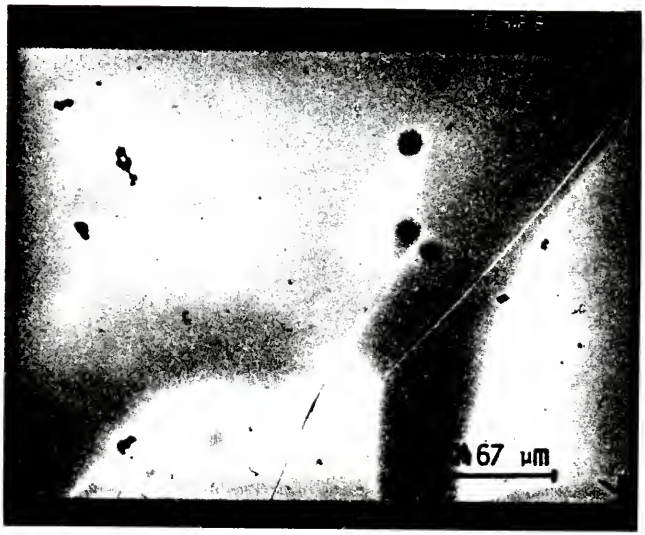

Figure 56. TEM Photomicrograph of $Fe(CO)_5$-PS Film Thermally Treated.

Figure 57. TEM Photomicrograph of $Fe(CO)_5$-PMMA Film Thermally Treated.

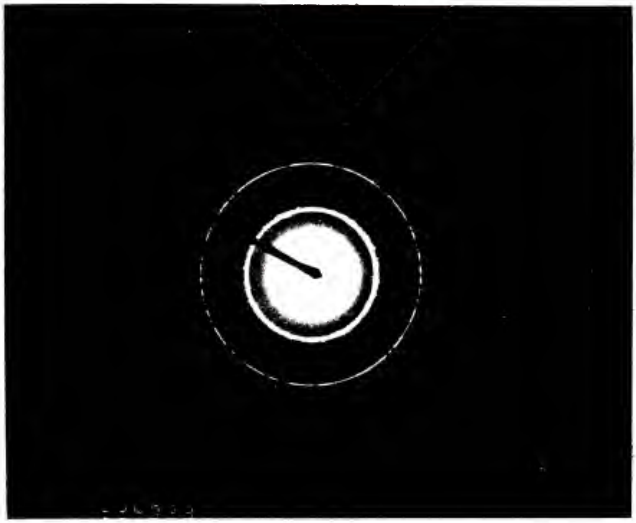

Figure 58. Diffraction Pattern of Polydimethylsiloxane Film.

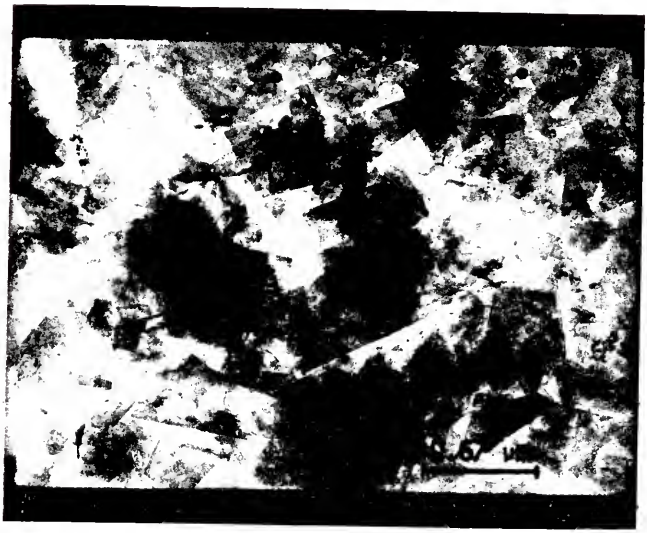

Figure 59. TEM Photomicrograph of Polydimethylsiloxane Which Shows Diffracting Morphology.

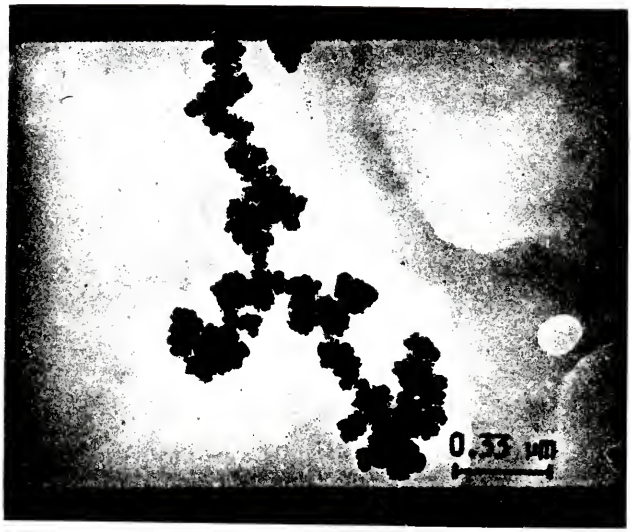

Figure 60. TEM Photomicrograph of $Fe(CO)_5$-PSF Films Prepared in H_2-Argon and Thermally Treated in Air.

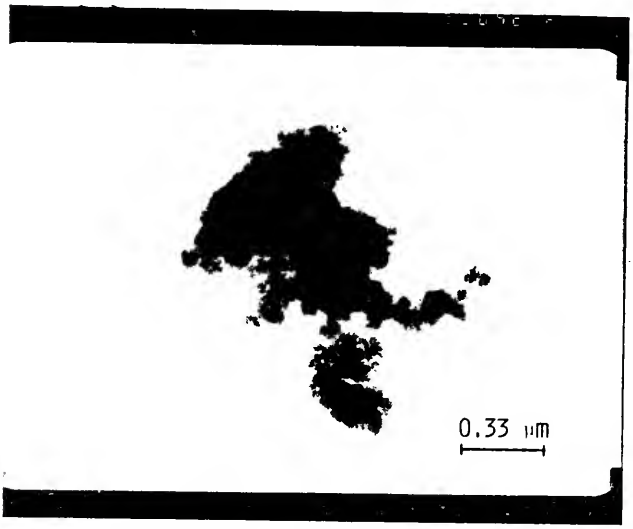

Figure 61. TEM Photomicrograph of $Fe(CO)_5$-PS Film Prepared in H_2-Argon and Thermally Treated in Air.

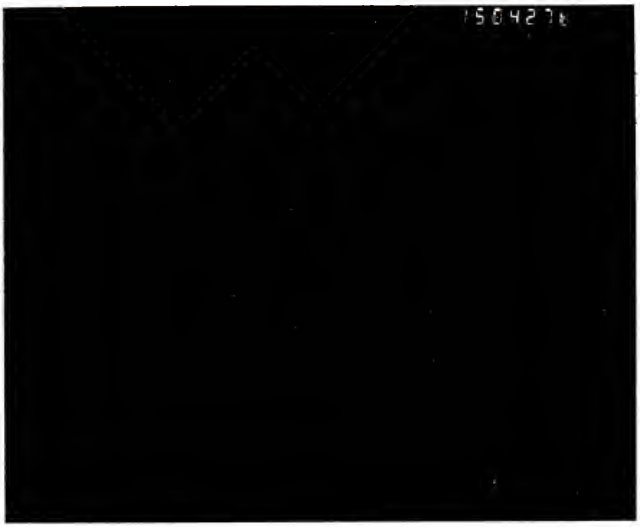

Figure 62. Dark Field TEM Photomicrograph Image of Iron Cluster in $Fe(CO)_5$-PSF Film Prepared in H_2-Argon, Thermally Treated in Air.

lack of crystalline structure suggesting these clusters to be amorphous iron. Yellow pigmentation in the iron-PS system was barely discernible, whereas the iron-PSF composite was again opaque and a rich yellow-brown color, but with a more metallic appearance than the iron-PSF films prepared in air.

Triiron dodecacarbonyl containing polycarbonate and polystyrene films prepared in CO were a brilliant forest green color prior to the solid state decomposition of this carbonyl. Upon thermal treatment the $Fe_3(CO)_{12}$-polycarbonate systems assumed a dark purple to black color (similar to $Fe(CO)_5$-PC systems after thermal treatment). The $Fe_3(CO)_{12}$-PS systems thermally treated became pale brown color. The addition of a few ml DMF to the initial methylene chloride-$Fe(CO)_5$-PS solution prior to casting with subsequent solid-state decomposition of the carbonyl produced films similar in color to the PVF_2 composite, a translucent rich brown color.

Triiron dodecacarbonyl in polycarbonate and polystyrene films prepared (no added surfactants) and dried in CO were decomposed in a reducing environment of 10% H_2-argon gas producing translucent (though dark) purple PC films and translucent brown PS composites. In a reducing atmosphere with rapid gas exchange (to remove evolved CO), primarily α-Fe is to be the expected product. Smaller clusters were observed in these composites decomposed in the solid state in an H_2 atmosphere than systems prepared in H_2 and decomposed in air. The reducing atmosphere during film preparation most probably led to clustering of iron particles [formed from reduced $Fe(CO)_5$] prior to complete solidification of the solution cast films. Conclusive identification of particles is not possible from data available at this time.

Thermally treated $Fe_3(CO)_{12}$-PSF and -PS films (both prepared with a small portion of DMF in the initial film casting solution) show strikingly different morphologies. The polysulfone composite shows the formation of numerous dark, spherical morphologies (Figure 63), many of which have dark aggregates closely associated with them. Though spherical features were noted in the $Fe(CO)_5$-PSF composites and often had metal particles associated with them, they were bright spheres - indicative of thinner film regions. EEDS indicates the $Fe_3(CO)_{12}$-PSF spheres with dark aggregates contain both sulfur and iron (those without dark aggregates show only sulfur present). $Fe_3(CO)_{12}$-polystyrene composites did not show the spherical morphologies observed in the polysulfone system, but clusters of γ-Fe, particles, γ-Fe_2O_3 and FeOOH particles (Figure 64).

The use of a Pluronic surfactant in the $Fe_3(CO)_{12}$-polysulfone systems produced a strikingly different morphology. The surfactant seems itself to phase separate in the polysulfone. The clusters resulting from decomposed triiron carbonyl are preferentially dispersed in the surfactant. At low carbonyl loadings the polyethylene oxide regions are small and incompletely "filled" with the metal/metal oxide aggregates (Figure 65). Increasing the initial $Fe_3(CO)_{12}$ loadings (from <4 to >10 wt. %) produces crystalline type morphologies which appear colloid in nature. The carbonyl seems to preferentially aggregate first to the surfactant regions and then to regions of higher carbonyl concentration in the surfactant (Figures 66, 67 and 68).

Dicobalt octacarbonyl-polystyrene and -polyvinylidene fluoride composites were also studied with electron microscopy to evaluate morphologies and chemical compositions. The decomposition products of

Figure 63. TEM Photomicrograph Showing Spherical Morphologies of Sulfur and Iron in $Fe_3(CO)_{12}$-PSF Composite (Prepared with DMF).

Figure 64. TEM Photomicrograph of Iron, Iron Oxide Clusters in $Fe_3(CO_{12}$-PS Composite (Prepared with DMF).

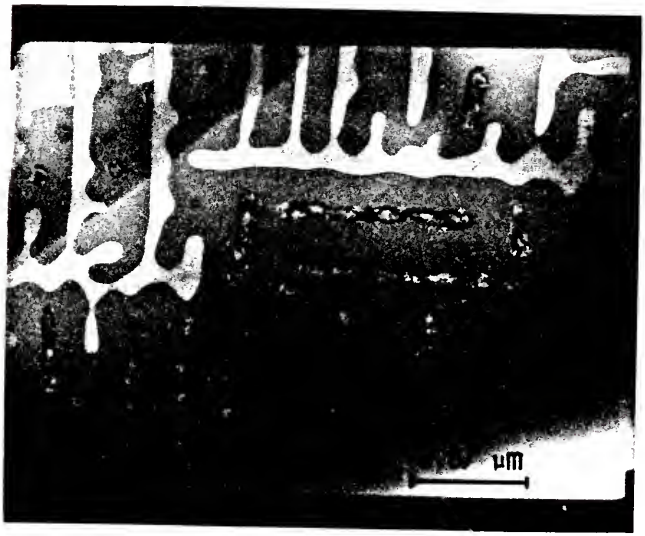

Figure 65. TEM Photomicrograph of Low Concentration $Fe_3(CO)_{12}$-PSF with Added Pluronic Surfactant.

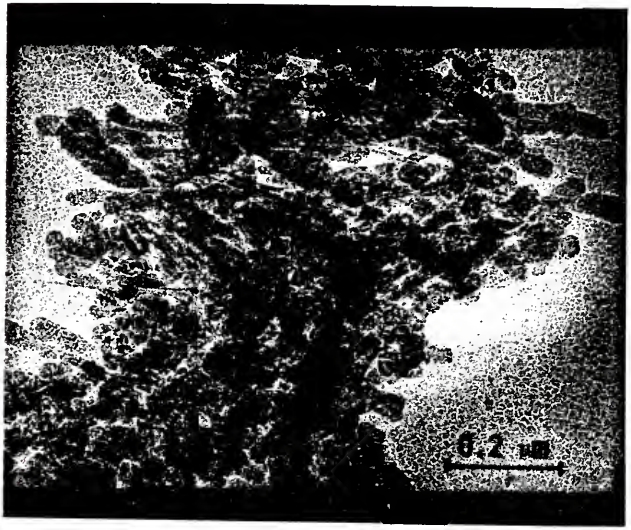

Figure 66. TEM Photomicrograph of High Concentration $Fe_3(CO)_{12}$-PSF with Added Pluronic Surfactant.

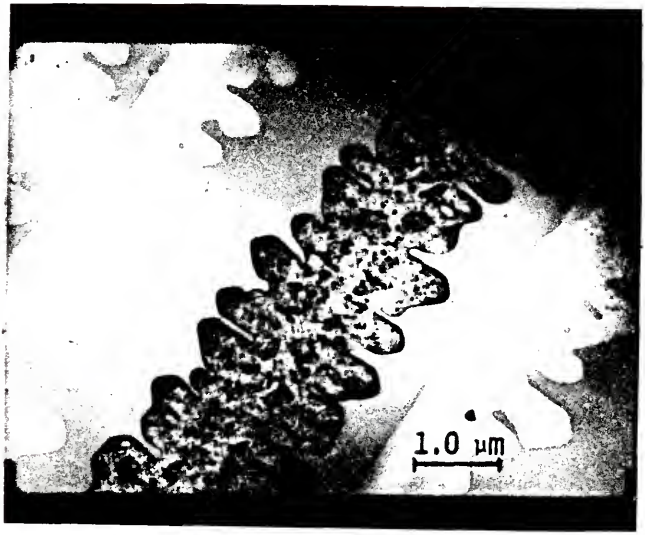

Figure 67. TEM Photomicrograph of $Fe_3(CO)_{12}$-PSF Showing Segregation of Phases.

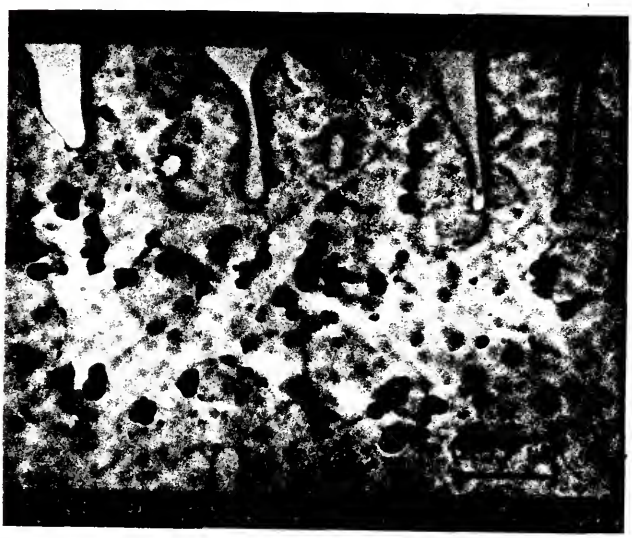

Figure 68. Higher Magnification TEM Photomicrograph of $Fe_3(CO)_{12}$-PSF Indicating Colloidal Nature of Aggregates.

$Co_2(CO)_8$-PS show a strong dependence on the atmosphere in which the reaction occurs. In an inert atmosphere (N_2), decomposition proceeds at a second-order rate with intermediate formation of $Co_4(CO)_{12}$ and onto form predominately α-Co (see Table 13). The decomposition of $Co_2(CO)_8$ in air produces a mixture of cobalt oxides: CoO and Co_2O_3. Figure 69 shows the morphology of $Co_2(CO)_8$-PS decomposed in air.

Results for dicobalt octacarbonyl in PVF_2 were similar to the $Fe(CO)_5$-PVF_2 system. $Co_2(CO)_8$ undergoes a vigorous disproportionation reaction with DMF to produce a very reactive anionic species (22). The films obtained with this system were brittle and insoluble indicating substantial polymer-carbonyl interaction. This extensive attack on the PVF_2 matrix was also noted for the mixed cobalt-iron-PVF_2 composites. Electron diffraction showed the particles formed following thermal treatment to be cobalt oxides (CoO and Co_2O_3) and CoF_2. Figure 70 shows a TEM photomicrograph of the particles formed in thermally treated $Co_2(CO)_8$-PVF_2 composites. The formation of CoF_2 in this system parallels the formation of FeF_2 in the $Fe(CO)_5$-PVF_2 system, and points to the fact that in both cases the polymer matrix was attacked by a reactive metal carbonyl species (possibly the anion produced in the disproportionation reaction). This resulted in abstraction of the fluorine atom and, in the case of cobalt, severe degradation of the polymeric matrix.

In some instances, the polymeric matrix has been observed to participate in the carbonyl decomposition reaction. This is due to the chemical structure of the polymer and/or to the solvent selected for the solution preparation of these composites. In all cases, γ-Fe_2O_3 was

Table 13. Electron Diffraction Analyses for α-Co Formed in $Co_2(CO)_8$-PS Films Thermally Treated in N_2.

ELECTRON DIFFRACTION d(A)	α-Co d(A)	hkl
2.163	2.165	100
2.024	2.023	002
1.960	1.910	101
1.167	1.252	110
1.151	1.149	103
	1.083	200
	1.066	112
1.046	1.047	201
	1.015	004

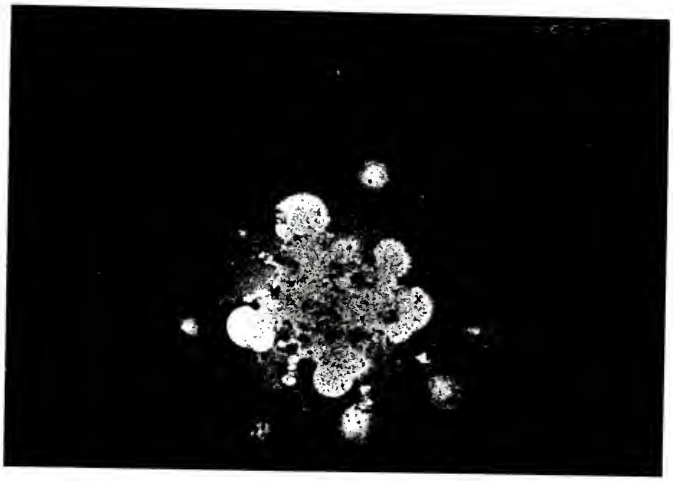

Figure 69. TEM Photomicrograph of $Co_2(CO)_8$-PS Film (Air Decomposition of Carbonyl).

Figure 70. TEM Photomicrograph of Thermally Treated $Co_2(CO)_8$-PVF_2.

produced in iron carbonyl composites formed by decompositions in air. Other particles (e.g. FeF_2, FeS, β-FeOOH) were also formed from $Fe(CO)_5$ which were dependent upon the polymer used. Particles formed by the thermal treatment of $Co_2(CO)_8$-polymer systems are observed to be not only a function of the polymer but also of the decomposition environment. A review of the particles formed in the various systems is presented in Table 14.

4.4.1.2 small angle x-ray scattering analyses to determine range of particle sizes in metal-polymer composites

Small angle x-ray scattering was originally introduced to detect large lattice spacings but has evolved to become a primary means for studying the dimensions of colloidal particles. In this manner the range of particle sizes and larger d spacings of the polymeric lattices were studied to evaluate changes in their crystalline nature upon incorporation of metal-carbonyls and consequent solid state decomposition of these carbonyls.

Of the polymers selected for study only polyvinylidene fluoride may be termed crystalline. If there is sufficient order in the crystalline phase, a lattice spacing may be evaluated by plotting angle versus intensity. A distinct SAXS peak was observed for PVF_2 corresponding to a characteristic lattice spacing of 63Å. This feature was missing from the composite sample, suggesting that the solid state decomposition of $Fe(CO)_5$ in PVF_2 disrupts the regular crystalline morphology (Figures 71 and 72). Earlier work by S. Reich (97) in this laboratory supports this conclusion. Polycarbonate (PC) is extensively attacked by the solid state decomposition of $Fe(CO)_5$, thus a change in the angle versus

TABLE 14. Particles Obtained in Various Systems[a]

System	Heterophase Particle Composition (from electron diffraction)
$Fe(CO)_5$-PC	γ-Fe_2O_3, β-FeOOH
$Fe(CO)_5$-PSF	γ-Fe_2O_3, δ-FeOOH, α-Fe, FeO, FeS
$Fe(CO)_5$-PSF[b]	Amorphous iron
$Fe(CO)_5$-PVF_2	γ-Fe_2O_3, α-Fe, FeF_2
$Fe(CO)_5$-PS	---
$Fe(CO)_5$-PS[b]	Amorphous iron
$Fe(CO)_5$-PMMA	γ-Fe_2O_3, δ-FeOOH
$Fe(CO)_5$-PSi	α-Fe, FeO
$Fe_3(CO)_{12}$-PSF (with DMF)	α-Fe_2O_3, FeS
$Fe_3(CO)_{12}$-PSF (with Pluronic)	γ-Fe_2O_3, FeS, γ-Fe_3O_4
$Fe_3(CO)_{12}$-PS (with DMF)	α-Fe_2O_3, γ-Fe, FeOOH (β or δ)
$Co_2(CO)_8$-PS[d]	α-Co
$Co_2(CO)_8$-PVF_2	CoO, Co_2O_3, CoF_2
$Co_2(CO)_8$-PS[c]	CoO, Co_2O_3

a. Preparations and decompositions in air unless otherwise noted.

b. Preparations in H_2 with decomposition in air.

c. Preparations in CO with decomposition in air.

d. Preparations in CO with decomposition in N_2.

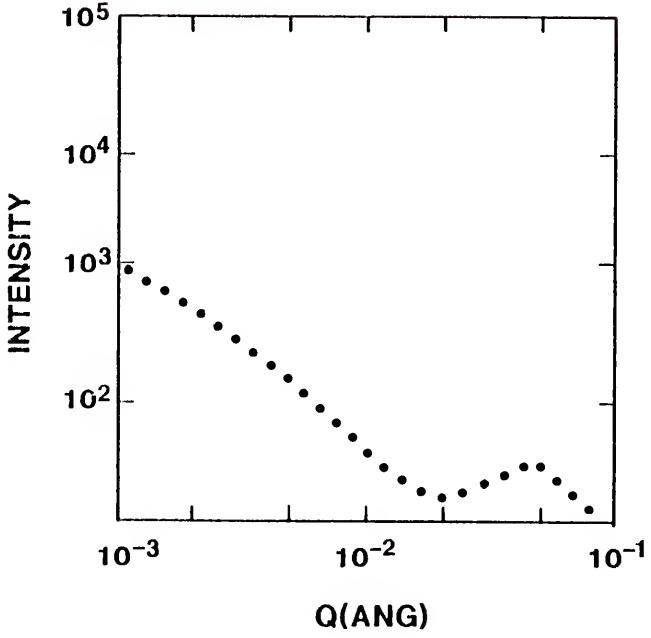

Figure 71. SAXS Intensity versus Angle Plot for PVF_2 Film Showing d Spacing of 63 Å.

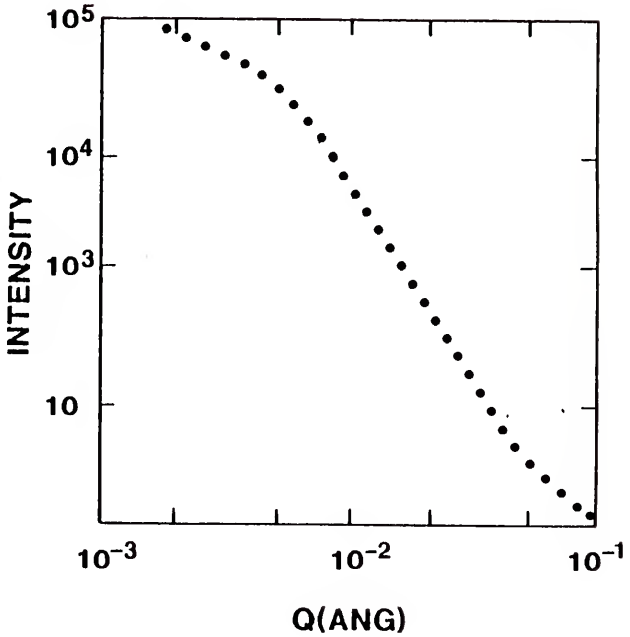

Figure 72. SAXS Intensity versus Angle Plot for Iron-PVF_2 Composite.

intensity plots might be expected in comparing PC to iron-PC composites. However, these SAXS plots show no distinctive difference between the control or composite PC sample. This most probably results from the low-order commonly observed in the polycarbonate morphology due to steric hinderances present in the chain (105). The remaining polymers studied (polystyrene, polysulfone, polydimethylsiloxane and polymethylmethacrylate) are also primarily amorphous in nature - thus no predominate lattice spacing was observed nor expected in SAXS plots of angle versus intensity.

Two-dimensional contour maps of composite materials with the appropriate polymer background subtracted were also evaluated. Composite materials how isotropic concentric circles indicating that the metal/metal-oxide particles do not have a preferred orientation (Figures 73 and 74). Phase separation was particularly evident in composites which retained larger amounts of the carbonyl as shown from TEM and SAXS studies. Guinier plots of the SAXS data (Figure 75) were used to evaluate the particle size ranges and are presented in Table 15. Particle sizes ranged from approximately 25 to 200Å. The closest size distribution was realized in PVF_2 composite films. This is most probably due to the fact that the solvent (DMF) was rapidly devolatilized by heating. This consequently allowed little diffusion time for aggregation into larger particles, despite the higher carbonyl loading. The decomposition of iron carbonyl in PVF_2 seems to have produced a species which has reacted with the fluorine atom of the polymer--thus also creating less of a tendency to cluster.

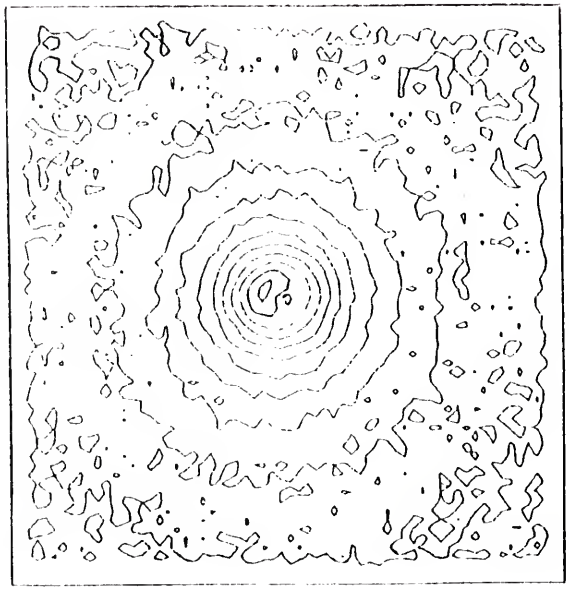

Figure 73. 2D Contour Map for SAXS Experiment in Iron-Polystyrene Films.

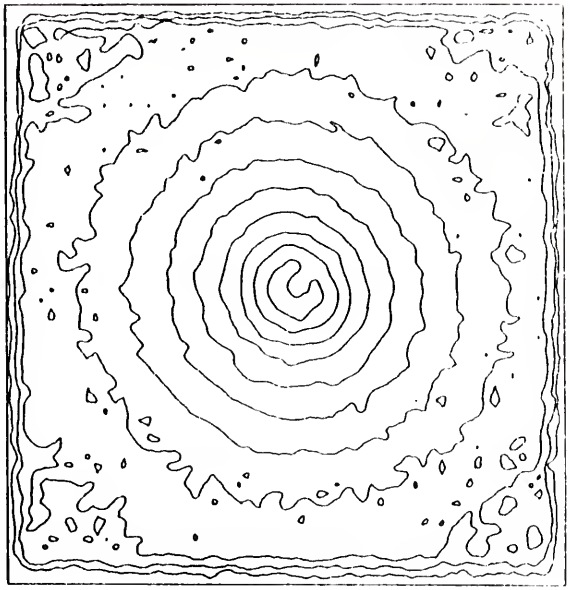

Figure 74. 2D Contour Map for SAXS Experiment in Iron-Polyvinylidene Films.

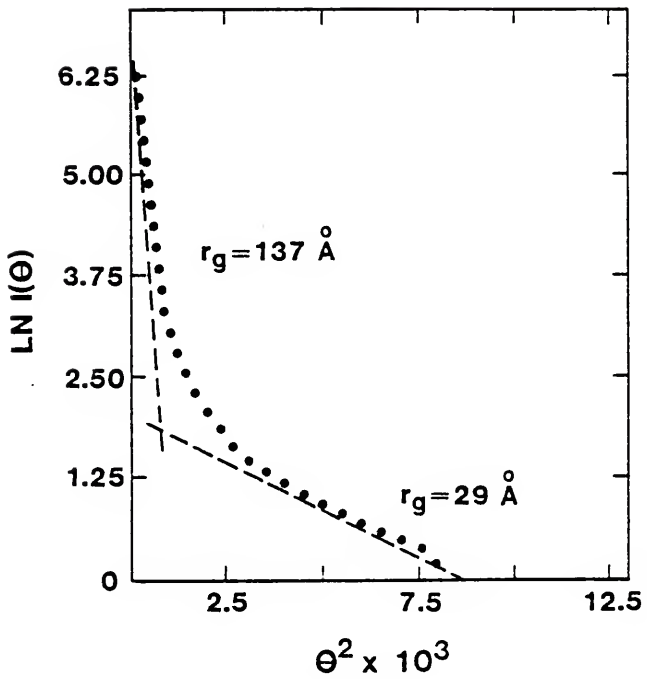

Figure 75. Guinier Plot for $Fe_3(CO)_{12}$-Polystyrene Films, Thermally Treated (SAXS Data Corrected for Background and Polystyrene Matrix Scattering).

Table 15. Range of Particle Sizes for Metal-Polymer Composite Systems

Metal Carbonyl-Polymer	Range of Particle Sizes
1.6% $Fe(CO)_5$-Polystyrene	23 - 132Å
1.8% $Fe(CO)_5$-Polysulfone	21 - 186
6.8% $Fe(CO)_5$-Polycarbonate	31 - 191
<0.1% $Fe(CO)_5$-Polysiloxane	130 - 164
4.6% $Fe(CO)_5$-Polyvinylidene Fluoride	26 - 88
0.9% $Fe(CO)_5$-Polymethyl-methacrylate	21 - 210
6.0% $Fe_3(CO)_{12}$-Polystyrene (Pluronic)	29 - 137
2.0% $Fe_3(CO)_{12}$-Polystyrene (Pluronic)	34 - 169
2.0% $Fe_3(CO)_{12}$-Polystyrene* (Pluronic)	37 - 115
2.1% $Fe_3(CO)_{12}$-Polysulfone (Pluronic)	17 - 210
4.2% $Co_2(CO)_8$-Polystyrene	14 - 257

* This sample UV treated while all others were thermally treated

Though polydimethylsiloxane retained little of the initial carbonyl loading composites. This may be explained by the complete exclusion of $Fe(CO)_5$ from the crosslinking reaction of polydimethylsiloxane. Thus, this segregates the remaining $Fe(CO)_5$ into a few areas of high concentration where the molecules may cluster during the decomposition reaction. This is evident in the inhomogeneity of the PSi-$Fe(CO)_5$ composite morphology as observed under transmission electron microscopy. It may be assumed that any particulate filler present in the siloxane coantrol was subtracted as background in the composite film and thus would not affect this value. Another interesting observation is the decrease in particle size distribution noted for samples of UV treated $Fe_3(CO)_{12}$-polystyrene composites. This may be due to the lower temperature of UV decomposition relative to thermal decompositions. Polystyrene has a glass transition temperature (Tg) of approximately 90°C. Thermal decompositions of the carbonyl were carried out at temperatures of approximately 125°C. Though this is below the melting temperature of the polymer, diffusion rates would be greatly increased through the polymer at temperatures above its Tg by virtue of the increased mobility of the amorphous polymer segments (85). This is an area requiring further study to fully evaluate the consistency of this theory and its possible usefulness.

4.4.2 Determination of Average Magnetic Susceptibility of Metal-Polymer Composites by the Guoy Method

Gases and liquids, in which the molecules are essentially random, are magnetically isotropic--magnetic susceptibility is the same in every direction. A solid whose microcrystals exhibit completely random

orientation also exhibit this characteristic. If a substance is placed in a magnetic field the intensity of magnetization may be either slightly smaller (diamagnetic), or somewhat larger (paramagnetic) than that produced in a vacuum by the same field (120).

The main transition group elements possess an incomplete inner or outer electron shell which is not effectively shielded from external influences. Ferromagnetism is the case where there is interaction between the magnetic moments of adjacent atoms due to these unpaired electrons in d or f shells (120). Fe, Co and Ni are ferromagnetic.

The magnetic anisotropy of various natural polymeric substances has been investigated by Nilakantan (121). He observed very small diamagnetic molecular anisotropy for cellulose materials with a more or less regular orientation along the fiber axis. Cotton-Feytis (122) studied the anisotropy of stretched methylmethacrylate, polyethylene terephthalate and polystyrene polymers but reported no data. They interpreted the anisotropy of the drawn polymers in terms of specific orientation of the molecular magnetic axis evaluated from magnetic and x-ray measurements. Unoriented rubber seems also to have slight anisotropy - possibly due to the direction of rolling in sample preparation. In this study, any possible anisotropy of the polymeric matrix resulting from orientation of polymeric chain during film preparation techniques was eliminated in the grinding procedure used to prepare samples for magnetic susceptibility measurements.

To determine the magnetic characteristics of these metal-polymer composites, a Guoy balance was used and is described in Section 3.13. The apparent change in sample weight was measured in applied inhomogeneous fields of 6830 gauss, 5740 gauss and 0 field environments

for both the matrix polymer and composite. Values of magnetic susceptibilities in both the matrix and composite were determined from these measured weight changes. Since gram susceptibility, X_g, is an additive property, one may assume:

$$X_{gc} = aX_{gp} + bX_{gm}$$

where X_{gc} = gram susceptibility of composite

X_{gp} = gram susceptibility of polymer

X_{gm} = gram susceptibility of metal

a = wt. fraction polymer

b = wt. fraction metal

Thus, having determined the metal content of composite samples, the gram susceptibility may be normalized to this metal content. A sample calculation of this magnetic susceptibility is shown in Appendix E.

The magnetic susceptibility data presented in Table 16 indicates that not only the metal carbonyl, but also the polymeric matrix have an effect upon the resulting magnetic characteristics of these metal-polymer composites. Both polyvinylidene fluoride and polysulfone composites prepared with $Fe(CO)_5$ demonstrated ferri- or ferromagnetic character. Iron oxide magnetite, Fe_3O_4, which has Fe^{+3} and Fe^{+2} ions distributed among the octahedral and tetrahedral voids of its spinel structure, exhibits ferrimagnetic behavior (32). Though Fe_3O_4 particles were not observed in the electron diffraction analyses, these two composites contain both α-Fe and γ-Fe_2O_3 particles which could produce

Table 16. Magnetic Susceptibility, χ, For Metal-Polymer Composites[a]

System	Particles Observed	$\chi \times 10^{+6}$ 5740 gauss	6830 gauss
0.2% $Fe(CO)_5$-PC	γ-Fe_2CO_3, β-FeOOH	-761	-633
1.1% $Fe(CO)_5$-PSF	γ-Fe_2CO_3, δ-FeOOH α-Fe, FeO, FeS	+183	+ 57
1.0% $Fe(CO)_5$-PS	---	-543	-495
0.9% $Fe(CO)_5$-PMMA	γ-Fe_2O_3, δ-FeOOH	-1440	-1340
4.6% $Fe(CO)_5$-PVF_2	γ-Fe_2O_3, α-Fe, FeF_2	+1060	+990
4.0% $Fe_3(CO)_{12}$-PS (Pluronics)	---	+61	+67
1.0% $Fe_3(CO)_{12}$-PSF	γ-Fe_2O_3, FeS, γ-Fe_3O_4	+57	+15
4.2% $Co_2(CO)_8$-PS	α-Co, CoO, Co_2O_3	+153	+105

[a] Values are corrected for percent metal in composite so that susceptibility measurements are in terms of metal content (gram susceptibilities are reported).

ferrimagnetic behavior. It is not possible to distinguish between ferri- and ferromagnetic character from the data accumulated in this study. S. Reich (97) also confirms the ferrimagnetism of the iron-PVF_2 system. Though these observed susceptibilities are low (120), it is known that supported and colloidal oxides often exhibit surprising degrees of magnetic dilutions quite probably due to lattice distortions resulting from oxygen and carbon interstituals. The remaining $Fe(CO)_5$ systems demonstrate diamagnetism. A diamagnetic material is distinguished from all the others by the fact that its susceptibility is negative. Solid-state decomposition of $Fe_3(CO)_{12}$ in a polystyrene matrix produces paramagnetic behavior, whereas a polysulfone matrix again produces what appears to be ferri-/ferromagnetic behavior. This feature is also demonstrated in the cobalt polystyrene systems. Bose and Raychaudhun (123) have found both CoO and Co_3O_4 to be paramagnetic, thus the resultant ferri-/ferromagnetic behavior must be due primarily to the α-Co.

Beischer and Winkel (124) prepared aerosols of nickel and iron by the thermal decomposition of carbonyls in a nitrogen atmosphere. They determined that particles prepared in this manner exhibited ferromagnetic character as long as the particle diameter size was greater than approximately 15Å. Magnetic properties, particularly hysteresis, are influenced by grain size and lattice orientation, which depends on the presence of impurities and on previous heat treatments (120). All systems studied contained a mixture of metal or metal oxides. Thus, it would be of interest to perform sample preparations and decompositions under closely controlled environments to increase the selectivity of the decomposition reaction to zero-valent metal or magnetic oxides and in this manner control their magnetic properties.

4.4.3 Electron Beam Decomposition of Iron Carbonyls in Solid Polymer Matrices

In the electron microscope, the primary purpose of the electron beam is to produce an image and possibly an electron diffraction pattern of the sample. For our purposes, however, a novel application is proposed--that of electron beam writing. Electron beam writing is of interest in that it suggests the feasibility of high density, high resolution information storage on these metal carbonyl-polymer systems. Electron scattering is divided into two categories elastic and inelastic scattering. When elastic scattering occurs, though the direction component of the electron's velocity is changed, the magnitude is not, so that the kinetic energy is unchanged. Less than 1 eV of energy, a negibible amount, is transferred from the beam electron to the specimen in an elastic scattering event. Elastic scattering is more probable in high atomic number materials and at low beam energy (125).

The second general category of scattering is that of inelastic scattering. During inelastic scattering, energy is transferred to the target atoms and electrons, and kinetic energy of the beam electron decreases. There are a number of possible inelastic scattering processes (126).

a) plasma excitation in which beam electrons can excite waves in the "free electron gas" which exists between the ionic cores in a solid
b) excitation of conduction electrons leading to secondary electron (low-energy) emissions
c) ionization of inner shells
d) Bremsstrahlung or continuum x-rays
e) excitation of phonons

Of primary interest to our study is e) the excitation of phonons. A substantial portion of the energy deposited in the sample by the beam electron is transferred to the solid by the excitation of lattice oscillations (phonons), i.e. heat. In thin specimens at high beam currents, significant heating may occur. For a low atomic number matrix, such as a plastic, inelastic scattering is more probable. The electrons tend to penetrate into the solid with relatively little lateral scattering initially. As they lose energy, elastic scattering becomes more probable and thus a pear shaped electron interaction volume results.

Initial electron beam decomposition studies were done on the JEOL JSM-35C SEM. Samples of PC and $Fe(CO)_5$-PC films 0.004 to 0.015 cm thick were used. Five to ten wt. % loadings of $Fe(CO)_5$ treated at a 39 mm working distance and 30 KeV for no longer than 500 seconds (magnification of 10X and aperatures out) were found to produce the best results (with respect to viewing the decompositions). Higher loadings created such a dense decomposition pattern that subsequent viewing was quite difficult. At these settings the energy absorbed by the sample was calculated to be approximately 2.1×10^{-5} joule/cm^2.

Figure 76, (a and b) shows the typical decomposition patterns obtained in the $Fe(CO)_5$-PC films. This pattern morphology is indicative of a chain or secondary reaction mechanism. This decomposition pattern was shown to increase dramatically by increasing either the loading of $Fe(CO)_5$ in the film or the exposure time. The color of these films was the same typical purple color as obtained in thermal decompositions. Extended exposures resulted in a blackening of the film and what appears

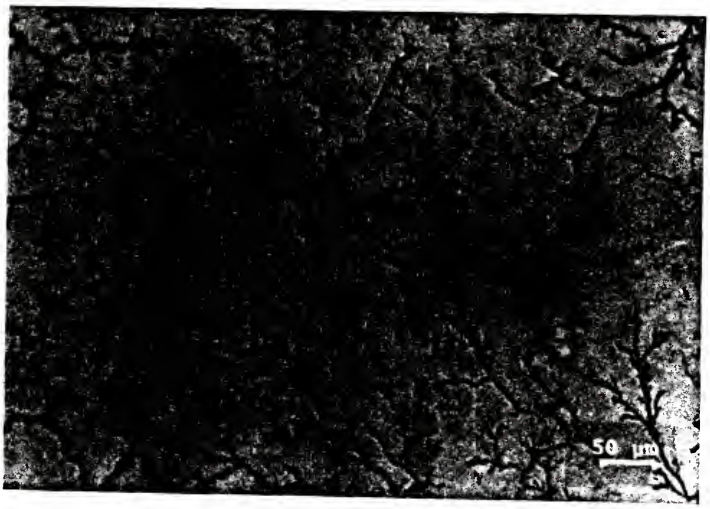

(a)

(b)

Figure 76. Optical Photomicrographs of Electron Beam Decomposition of PC-$Fe(CO)_5$ Film at 30 KeV for 500 Seconds (a and b).

to be flowing of the polymer. Thus, it may be suggested that decomposition of the $Fe(CO)_5$ is occuring via phonon interaction along the inelastically scattered electron paths within the matrix. Qualitatively, the Fe-PC composite films appeared to retain their mechanical integrity. Though the decomposed areas were quite small, an attempt was made to evaluate the solution viscosity. It appears that at exposure times of 500 seconds the polymer is not degraded. With increasing exposure to 1000 seconds, the polymer may by crosslinked somewhat followed by breakdown at longer exposures of 2000 seconds.

These preliminary studies indicated that by increasing the voltages and decreasing exposure times on thinner samples, the resolution of the decomposition pattern might be improved. Thus, exploratory work was done on the VG-HB5 STEM at the University of Illinois. Thin samples (less than 0.1 μm) of polysulfone and polysulfone-$Fe(CO)_5$ were prepared by the TEM dilution technique (section 3.8.4 and 3.11) and stored in darkness until analyses.

A polysulfone sample with no added $Fe(CO)_5$ was initially viewed at first 100 and then 60 KeV in a selected area at 100,000X magnification. No contamination (no beam damaged area) was noted in either case as shown in Figure 77. Thus, we may conclude that the development of a dark "spot" on the metal carbonyl-polysulfone grid to also not be attributable to beam contamination. A line decomposition was also tried on the PSF control at a magnification of 100,000X and 100 KeV for approximately 1.5 minutes-no line was observed to form.

Next, a $Fe(CO)_5$-PSF sample grid was viewed at 100,000X under 100 KeV on a selected area. When the magnification was lowered, a small

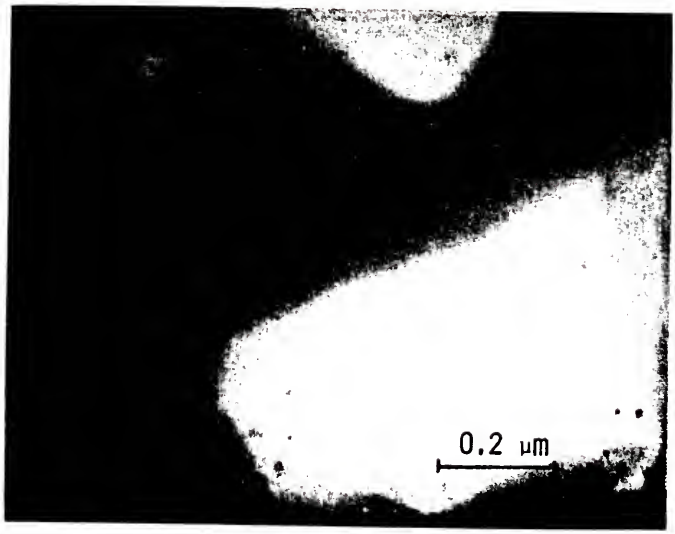

Figure 77. Control Polysulfone Sample Viewed at 100 and 60 KeV in Selected Area (Dark Regions are Dense Layers of Carbon Support Film).

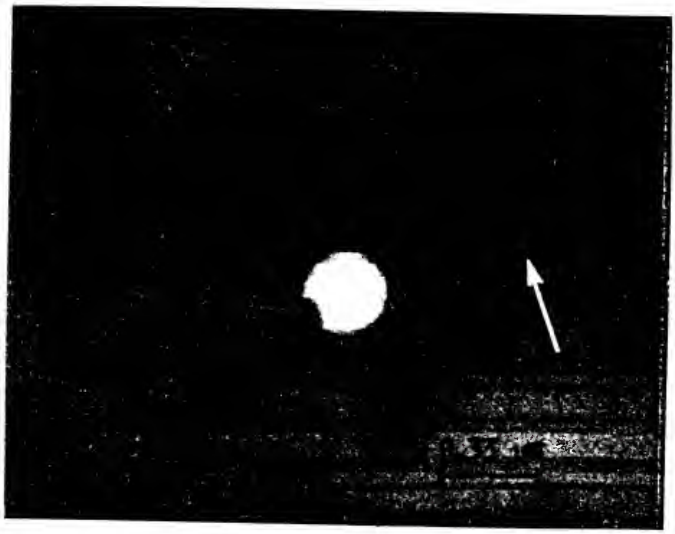

Figure 78. $Fe(CO)_5$-Polysulfone Sample Viewed at 100 KeV in Selected Area (Arrow Indicates Decomposition Region on Sample).

spot indicative of the selected area was noted (see Figure 78). Note the bright sphere located just off center-it is a thinner region of the PSF-$Fe(CO)_5$ sample. Some thinner film regions were noted in the polysulfone grid film (as well as for the $Fe(CO)_5$-polysulfone grid film)--indicative of high humidity during preparation of these samples. Several line decompositions were done at 100,000X and it was noted that thinner film regions produced less spread in the beam decomposition morphology (Figure 79). This is noted in the 75 Å decomposition line observed in thin regions increasing to 150 Å in thicker film regions.

Energy dispersive x-ray spectroscopy (EDX) was used to indicate the presence of iron in particular, but also to follow this solid state decomposition. It is interesting to note that when the electron beam focused on a new undecomposed region of the $Fe(CO)_5$-PSF sample, the initial Fe:S ratio was approximately 2:1. As electron beam exposure continued, an increase in the S was noted so that after 30 seconds of exposure an Fe:S ratio of 2:3.2 was evident. This change suggests that a chemical interaction is occurring between the sulfur and iron so that an increasing amount of sulfur becomes associated or bound to the metal atom. This is further supported from our studies of thermally treated $Fe(CO)_5$-PSF systems where the formation of FeS is observed.

From these preliminary studies, the feasibility of electron beam decomposition writing, and the possibility of data storage at a near molecular level may be suggested. It is an area which deserves further study.

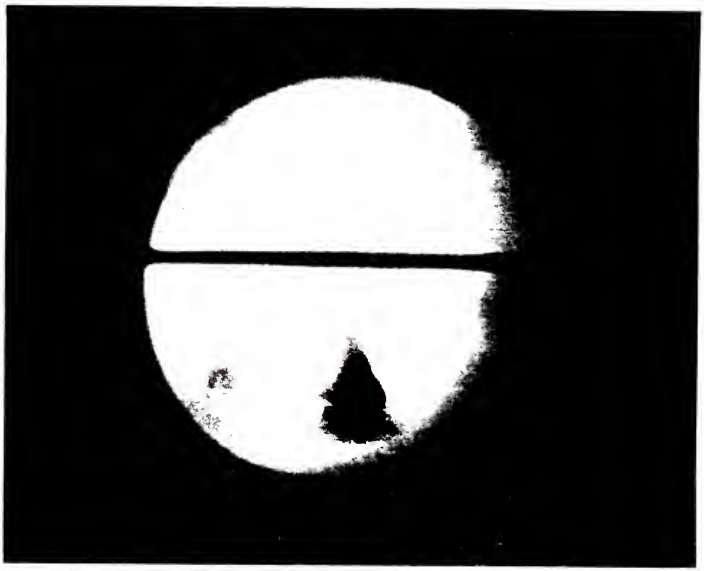

Figure 79. $Fe(CO)_5$-PSF Sample Line Decomposition at 100 KeV and 100,000 Magnification (Selected Area Decomposition Shown Above Line Decomposition).

4.5 Effect of Carbonyl Decomposition Upon Polymeric Matrix

The decomposition of metal carbonyls in polymeric matrices leads to a variety of metal containing products. It was of interest to determine the effect of these chemical interactions upon the polymer; to evaluate the extent and possibly site of attack upon the polymer chain. Viscosity molecular weight measurements were made for various composities before and after both thermal an UV treatments to quantify the degree of attack upon the various polymers. Changes in molecular weights were observed after either thermal or UV treatments for nearly all polymers. The results are summarized in Table 17.

Polycarbonate is most extensively attacked by the iron carbonyl during thermal decomposition with a large reduction in molecular weight. This fact is supported by mechanical property measurements indicating a progressive drop in ultimate tensile strength (from 9,000 to less than 100 psi) with increasing carbonyl concentration (0 to 10 wt. %). This trend was also observed in viscosity measurements of iron-polycarbonate composites. This reduction in molecular weight is accompanied by evolution of CO (see Figure 80) as well as a considerable increase in the OH stretching IR band.

The formation of β-FeOOH indicates reaction with water present during decompositions in air:

$$2FeOOH \longrightarrow Fe_2O_3 + H_2O$$

Reaction of the passive γ-Fe_2O_3 particles with water is well known and has been discussed by Griffith et al. (70). It should be noted,

Table 17. Viscosity-Molecular Weight Averages for Iron Carbonyl-Polymer Composites

Polymer[a]	Treatment None	Thermal[b]	UV[b]
Polycarbonate[c]	32,200	32,200	28,900
$Fe(CO)_5$-PC	30,500	4,400	15,000
$Fe_3(CO)_{12}$-PC	---	28,500	---
Polysulfone[c]	30,100	31,600	---
$Fe(CO)_5$-PSF	27,100	22,600	---
$Fe_3(CO)_{12}$-PSF	---	24,100	---
Polystyrene[d]	159,400	127,000	159,400
$Fe(CO)_5$-PS	123,000	80,000	66,000
Polymethyl-methacrylate[d,e]	420,000	323,400	388,000
$Fe(CO)_5$p-PMMA	318,000	211,800	302,000
Polymethyl-methacrylate[d,f]	179,000	170,000	170,000
$Fe(CO)_5$-PMMA	181,000	166,000	158,000

[a] Molecular weight values for composites are based on polymer weight (i.e. actual iron or iron pentacarbonyl weight excluded).

[b] Samples treated to completely decompose carbonyl (as indicated by infrared spectra).

[c] Ubbelohde OB viscometer; 1,4-dioxane solvent; 30°C.

[d] Ubbelohde OB viscometer; benzene solvent; 30°C.

[e] High molecular weight PMMA.

[f] Low molecular weight PMMA.

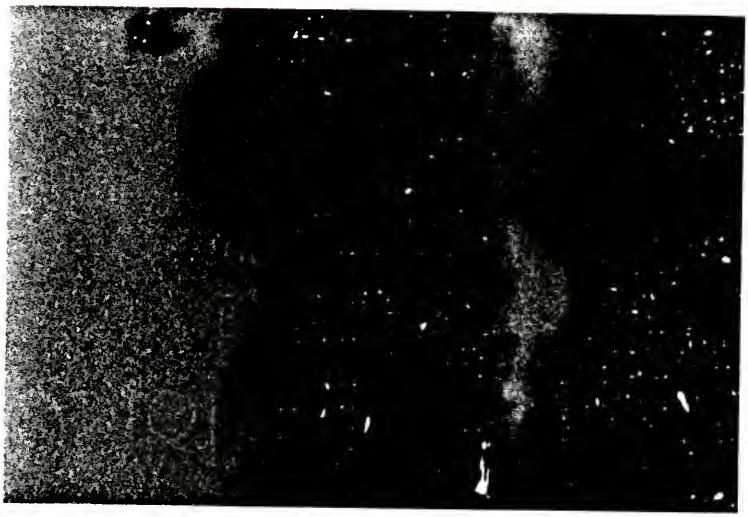

Figure 80. Thermally Treated $Fe(CO)_5$-PC Film Showing CO Evolution.

however, that it is the α-polymorph of FeOOH which is normally formed. The β structure has been observed to form only during the breakdown of γ-Fe_2O_3 in the presence of chlorinated solvents. Thus, it is suggested that traces of CH_2Cl_2 present in the PC and PSF systems (supported by electron energy dispersive spectra) and atmospheric moisture are responsible for this reaction.

The formation of metallic iron particles must also occur even though the concentration of the a-Fe particles is low due to the oxidative atmosphere in which the decompositions were conducted. In an inert atmosphere, these species could become the dominant particles, as indicated by studies reported elsewhere in this study for decompositions of $Co_2(CO)_8$ in N_2 which yield α-Co particles almost exclusively. A drop in molecular weight was also noted for UV treated $Fe(CO)_5$-PC films. Increasing exposure time lead to increased molecular weight breakdown, limited by the amount of carbonyl present in the matrix. Increasing this concentration lead to more extensive attack on the polycarbonate. Photolytic decompositions of $Fe(CO)_5$-PC films, however, did not produce the CO evolution morphology nor the extensive attack on the main chain in polycarbonate. This evident not only in viscosity and mechanical property measurements but also in the increased solubility of the attacked polycarbonate matrix in a semi-solvent such as benzene (see Figures 81 and 82).

In the PSF systems, a slight change in molecular weight was observed. This decrease in accompanied by a transformation from translucent film (though slightly brown pigmented) to a dark yellow-brown color which became opaque with increased carbonyl loadings. This

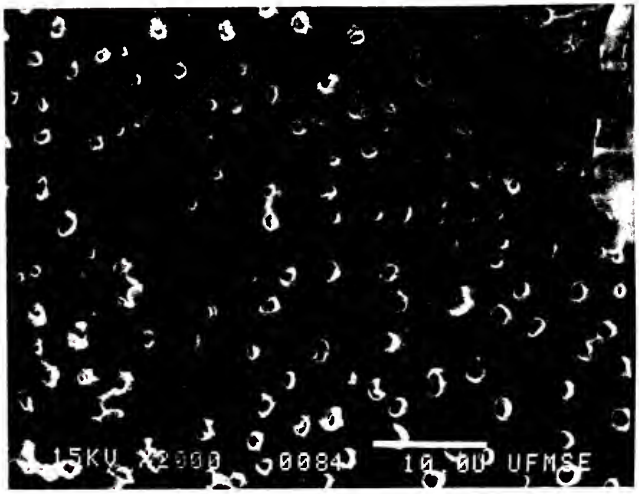

Figure 81. SEM Photomicrograph of Untreated $Fe(CO)_5$-PC Film Solvent Etched in Benzene (a Semi-Solvent).

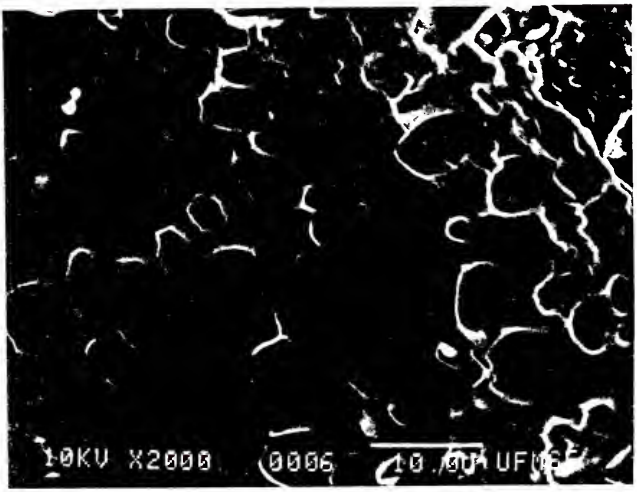

Figure 82. SEM Photomicrograph of UV Treated $Fe(CO)_5$ Film Solvent Etched in Benzene (a Semi-Solvent).

opacity is not accompanied by crystallization or apparent crosslinking of the polymer as evidenced by SAXS plots of intensity versus angle and the ready solubility of the PSF composite. At higher loadings the polymer matrix was apparently saturated. Limited degradation of the polymer chain occurs inspite of the formation of FeS.

One of the most conspicous features of ferric iron in aqueous solution is its tendency to hydrolyze and/or to form complexes (102). Iron (III) has its greatest affinity for ligands that coordinate by oxygen. At this point, a more appropriate mechanism cannot be proposed only the suggestion that limited nucleophilic attack by $Fe(CO)_5$ and/or water (or a more reactive iron species formed as a first step upon exposure to thermal treatment) on sulfur or oxygen of the sulfone group within the polymer backbone must occur and some recombination of polymeric phenylene species may result in substantial maintenance of polymer chain length (via formation of biphenylene or phenyl ether linkages). Nucleophile attack on the sulfone group is relatively hindered, however, and involves the temporary attachment or association of a fifth group.

For the PMMA composite, some reduction in molecular weight was also noted upon thermal or photolytic decomposition of $Fe(CO)_5$. This was accompanied by the appearance of a 2940 cm^{-1} IR band corresponding to a formation of carboxylic acid groups. The involvement of H_2O is also indicated by the formation of δ-FeOOH. $Fe(CO)_5$ attack on PMMA must also occur at the ester bond. In this case, unlike the PC system, the ester group is not a part of the polymer backbone, but only a side group. Therefore, the integrity of the PMMA chain was not directly affected.

In the polystyrene systems, a drop in molecular weight was observed through the mechanism of carbonyl reaction with the main chain is unclear. Though the molecular weight decreased, the polymeric integrity was primarily retained. This was also qualitatively observed in the $Co_2(CO)_8$-PS systems.

PVF_2 composites were insoluble thus viscosity measurements of the cast and thermally treated samples were not possible. However, viscosity measurements were made on the original casting solutions of PVF_2-DMF and $Fe(CO)_5$-PVF_2-DMF. Both were maintained at ~90°C for three days to allow reaction of the $Fe(CO)_5$ anionic species on the PVF_2 chain. Viscosity measurements indicated only a slight drop in intrinsic viscosity (from 1.28 for the PVF_2 control to 1.11 for the composite). Films cast (using the "hot" method) from the $Fe(CO)_5$-PVF_2-DMF solution seven days after solution preparation still formed intact films, but quantitatively were much more brittle than films cast immediately after preparation of solutions.

Results for dicobalt octacarbonyl in PVF_2 were similar to the $Fe(CO)_5$-PVF_2 system. $Co_2(CO)_8$ undergoes a vigorous disproportionation reaction with DMF:

$$3\ Co_2(CO)_8 + 12\ DMF \longrightarrow 2\ Co^{II}(DMF)_6\ [Co(CO)_4]_2^{-1} + 8\ CO$$

The reaction is several orders of magnitude faster than with $Fe(CO)_5$ and the resulting $Co(CO)_4$ anion is a very reactive species. The films obtained with this system were brittle and insoluble indicating substantial polymer-carbonyl interaction. The formation of CoF_2 in

this system parallels the formation of FeF_2 in the $Fe(CO)_5$-PVF_2 system, and points to the fact that in both cases the polymer matrix was attacked by a reactive metal-carbonyl species (perhaps the anion formed during the disproportionation reaction). This resulted in abstraction of a fluorine atom, and in the case of cobalt, severe degradation of the polymeric matrix. The faster reaction rates for cobalt systems may be expected since cobalt carbonyls are known to be more sensitive to oxidative environments than iron carbonyls.

Qualitative evaluation of SEM electron beam treated $Fe(CO)_5$-PC films indicated similar mechanical properties to the control polycarbonate film. This maybe due to the finely localized region of decomposition produced by the electron beam, though the possibility exists that the mode of decomposition in this technique is different from thermal or photolytic decompositions. Larger areas of film must be treated in order to quantify this observation.

4.6 Mechanistic Aspects

The results of this study permit a general mechanistic view of the thermal decomposition of metal carbonyls in polymeric matrices. For polycarbonate the molecular weight is drastically reduced. The appearance of an OH stretching IR band at 3510 cm^{-1} indicates the formation of hydroxyl functions accompanying polycarbonate chain degradation. A possible mechanism for the decomposition of $Fe(CO)_5$ in PC is given in Figure 83. It seems reasonable to assume that attack by an iron carbonyl on the ester function of the polymer leads to chain scission of the polymer. The C=O carbon is the probable site of a nucleophilic attack. A molecule of water must also be involved in

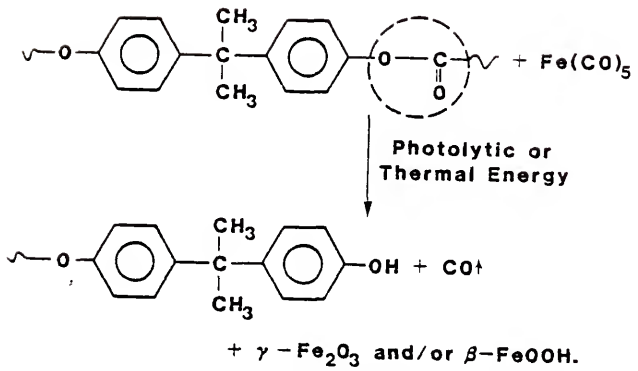

Figure 83. Proposed Mechanism for Decomposition Reaction of $Fe(CO)_5$ in a Polycarbonate Matrix.

$$Fe(CO)_5 + DMF \longrightarrow (DMF)\ Fe(CO)_4 + CO$$

$$(DMF)Fe(CO)_4 + (R - C\begin{matrix}F\\F\end{matrix}) \longrightarrow FeF_2 + R^1$$

Figure 84. Proposed Mechanism for Decomposition Reaction of $Fe(CO)_5$ in a Polyvinylidene Fluoride Matrix.

this esterolytic process giving rise to the OH groups. The presence of H_2O was also shown by the formation of β-FeOOH in the presence of chlorinated solvents.

Electron beam decomposition of $Fe(CO)_5$ in polycarbonate seems to proceed by a highly localized thermally induced reaction (i.e. phonon interaction with carbonyl molecules), thus the bulk of the polymer remains intact and unaffected by carbonyl interaction. The solid state decompositions of metal carbonyls appears in general to be highly dependent upon diffusion of the carbonyl species through the matrix. Thus, decompositions not requiring heating of the bulk (ie. electron beam, UV or gamma radiation treatment) tend to decrease the mobility of the carbonyl species and thereby limit attack upon the polymer.

Photolytic decompositions quite obviously occur at lower temperatures than the thermal decompositions of $Fe(CO)_5$. Also, evidence for the formation of $Fe_2(CO)_9$ from the photolytic treatment of $Fe(CO)_5$ in a solid polymer matrix was not observed. Formation of the diiron species requires diffusion of the carbonyl species through the solid matrix, a process which would be slower for room temperature photolytic decompositions. Photolytic reactions thus generally appear to occur with less degradation of polymer. This view is supported by retention of good mechanical properties for composites prepared by photolysis or radiolysis to decompose the carbonyl.

It is quite interesting that the decomposition of $Fe_3(CO)_{12}$ in a PC matrix was not accompanied by the extensive molecular weight breakdown observed in the $Fe(CO)_5$-PC composite. The thermal decomposition of $Fe_3(CO)_{12}$ in ethyl benzene solution was shown to follow second-order

kinetics with intermediate formation of $Fe(CO)_5$ which further decomposes to iron oxides with continued heating. Unlike solution decomposition, the solid state decomposition of $Fe_3(CO)_{12}$ does not proceed via intermediate formation of $Fe(CO)_5$ but decomposes directly to iron oxides (Fe_2O_3). Also, no IR absorption was apparent in the 3500 cm^{-1} region to indicate the formation of hydroxyl functions during the thermal decomposition of $Fe_3(CO)_{12}$-PC systems. The steric hindrances imposed by the solid polymer matrix upon the bulky $Fe_3(CO)_{12}$ significantly decreases the decomposition reaction rate as compared to a solution.

In the PMMA system, the appearance of a 2940 cm^{-1} IR band corresponding to a carboxylic OH group indicates formation of carboxylic groups. The involvment of H_2O is also indicated by the formation of δ-FeOOH. $Fe(CO)_5$ attack on PMMA must also occur via an anion at the ester group. In this case, unlike the PC system, the ester group is not a part of the polymer backbone, but only a side group. Therefore, the integrity of the PMMA chain should not be affected. In both PMMA and PC composites, the formation of γ-Fe_2O_3 and FeOOH was accompanied by diamagnetic behavior.

The formation of FeS and various iron oxides was observed for thermally decomposed $Fe(CO)_5$ and $Fe_3(CO)_{12}$-PSF composites and was accompanied by ferri/ferromagnetic behavior and a slight decrease in molecular weight (see Table 8). EDX data for $Fe(CO)_5$-PSF samples also indicate that upon electron beam decomposition of the carbonyl, more sulfur becomes associated with iron. Though the mechanism of attack is unclear, only limited degradation of the polymer chain occurs in spite of the formation of FeS. The appearance in the IR spectra of a broad OH

stretching group (possibly phenol) at 3460 cm^{-1} with solid state thermal decomposition of $Fe(CO)_5$ suggests this degradation may also proceed by reaction with an oxygen group. In polysulfone, there are both main chain oxygens (between phenyl groups) and side group oxygens on the sulfone function. The formation of FeS suggests this attack may proceed at the sulfone functional group. Limited nucleophilic attack by a carbonyl anion and/or water (or a more reactive iron species formed as a first step upon exposure to thermal treatment) on sulfur or oxygen of the SO_2 group within the polymer backbone must occur and some recombination of polymeric phenylene species may result in substantial maintenance of polymer chain length (via formation of biphenylene or phenyl ether linkages).

Polydimethylsiloxane (PSi) retained only small amounts of $Fe(CO)_5$ even prior to heat treatments. Room-temperature vulcanizing silicone elastomers are cured by crosslinking of siloxane chains with reactive end groups. These end groups are activated by atmospheric moisture to yield Si-O-Si links and the by product HCl. It appears the HCl reacts with an $Fe(CO)_4^{-2}$ species to produce the hydride and that in the presence of the CO environment, the hydride rapidly volatilizes.

In the PVF_2 system, two events may explain the formation of γ-Fe_2O_3 and FeF_2. PVF_2 films prepared by the "hot" casting technique were observed to be insoluble and therefore crosslinked. This suggests that at elevated temperatures (114°C) and in the presence of DMF, an aprotic solvent, the fluoride atom is abstracted from the polymer via reaction with DMF. This reaction may also proceed, though more slowly, even at room temperature. Secondly, $Fe(CO)_5$ was observed to disproportionate in DMF (see Figure 17) and produce very reactive anionic species of the

type $Fe^{II}(DMF)_b[Fe_3(CO)_{12}]^{-2}$. Since the $Fe^{II}(DMF)_6$ iron atom is cationic and can readily react with fluorine of PVF_2 to form FeF_2. It appears that not only does DMF abstract fluorine atom from PVF_2 at elevated temperatures, but that the reactive anionic carbonyl species formed in DMF was capable of abstraction even at room temperature. This does not happen in DMF alone, because PVF_2 films cast at room temperature were not crosslinked. Therefore composite systems of $Fe(CO)_5$-PVF_2 must involve a DMF-carbonyl complex as suggested in Figure 84. No infrared evidence was found for the formation of a $(DMF)Fe(CO)_4$ complex. For films cast by the "hot" method, the anionic carbonyl pathway may occur very rapidly at the elevated temperature as well as the reaction in Figure 84. Results for $Co_2(CO)_8$ in PVF_2 were similar for the $Fe(CO)_5$-PVF_2 systems. $Co_2(CO)_8$ disproportionates even more vigorously than $Fe(CO)_5$ in DMF. Thus, the PVF_2 matrix was even more extensively crosslinked.

In general, it appears metal carbonyl interactions occur in polymer systems with reactive functionality often leading to changes in molecular weight and branching or crosslinking of the polymers. Metal binding to polymer is also likely in some cases. The magnetic properties of the heterophase in thse composites appear also to be a function of the polymeric matrix as well as the decomposition environment.

5. CONCLUSIONS

The metal carbonyl-polymer systems discussed in this dissertation indicate the complexity of the decomposition of organometallic compounds in solid polymer matrices and the potential for preparing new and interesting metal-polymer composites. In general, this approach to metal-polymer composite preparation appears to afford a unique method by which metal and/or metal-oxide microparticles may be incorporated into a solid matrix. This study has demonstrated the feasibility of this novel preparative technique and opportunities for future investigation. The following are major conclusions of this research.

1. Solvent effects were significant. Solvents that react with the carbonyl to produce an anionic (carbonyl) species produced composites with more metal carbonyl in the cast films. The triiron and cobalt carbonyls were retained in the polymeric matrix more strongly than $Fe(CO)_5$ when no interaction occured with the polymer.

2. In methylene chloride, no disproportionation reactions occur for the iron or cobalt carbonyls. $Fe(CO)_5$ undergoes a disproportionation reaction in DMF and the resulting anionic species reacts with the fluorine atom of the PVF_2.

3. The disproportionation reaction of $Co_2(CO)_8$ with DMF is more vigorous than that of $Fe(CO)_5$. Thus, anionic degradation of a reactive polymer can be more extensive.

4. $Fe_3(CO)_{12}$ was not observed to undergo disproportionation in DMF but exhibited low solubility in organic solvents (i.e., 3.4 g $Fe_3(CO)_{12}$/liter CH_2Cl_2). Pluronic surfactant produced $Fe_3(CO)_{12}$ dispersions in polysulfone.

5. Iron carbonyls retain their characteristic IR carbonyl stretching absorptions in solid polymer matrices though a shift to lower wavenumber and broadening is often observed due to the solid matrix. Fewer IR absorption bands were observed for cobalt carbonyl spectra in a polymer when compared to that in hexane solution. Two primary bands, a terminal CO stretch at 2040 cm^{-1} and a bridging CO stretch at 1860 cm^{-1}, are exhibited both in solution and a polymeric matrix.

6. In all metal carbonyl-polymeric composites, the extinction coefficients for the ~2000 cm^{-1} band (IR carbonyl stretching) were observed to be lower than in solution. It is likely that the polymeric matrix may impose restrictions on the vibrational degrees of freedom of the metal carbonyl resulting in bands of lower intensity. This view is supported by the fact that extinction coefficients in the amorphous polymers were higher suggesting greater freedom in an amorphous structure than in the highly ordered crystalline morphology of a polymer such as polyvinylidene fluoride.

7. Iron pentacarbonyl remains quite sensitive to light, even when somewhat protected from oxidation in a polymer matrix. On the other hand, $Fe_3(CO)_{12}$ in a polymer matrix exhibited a greatly reduced oxidation rate compared to crystalline $Fe_3(CO)_{12}$ in air. Surprisingly, the oxidative decomposition of cobalt and iron pentacarbonyls may proceed faster in a polymeric matrix than in solution. The difference

between the decomposition rates in solution and in the solid state were larger for $Co_2(CO)_8$ than for $Fe(CO)_5$ apparently because the cobalt carbonyl is more sensitive to O_2 than $Fe(CO)_5$. $Fe_3(CO)_{12}$ decomposition in solution followed second-order decomposition, thus comparison to the first-order kinetics observed in a polymer was not possible.

8. The rate of oxidation of $Co_2(CO)_8$ was observed to be one to two orders of magnitude faster in polystyrene than in solution, depending on the solvent. $Co_2(CO)_8$ is embedded in a thin amorphous polystyrene film, may be more extensively exposed to O_2 than in solution. Support for this hypothesis was provided by the oxygen barrier experiment.

9. The atmospheric decomposition of $Co_2(CO)_8$ in hexane follows first-order kinetics whereas decomposition of a $Co_2(CO)_8$-toluene solution in N_2 proceeds by second-order kinetics to form $Co_4(CO)_{12}$. Second-order decomposition of $Co_2(CO)_8$ to $Co_4(CO)_{12}$ in an N_2 atmosphere was observed in both solution and in polystyrene. The rate of decomposition in N_2 was two orders of magnitude faster in solution than in polystyrene probably because this nonoxidative decomposition was probably $Co_2(CO)_8$ diffusion controlled.

10. The thermal decomposition of $Fe_3(CO)_{12}$ in ethyl benzene in air proceeds via intermediate formation of $Fe(CO)_5$ and is second-order. However, in a polymeric matrix first-order kinetics was observed. This may result primarily from the slower diffusion of the larger $Fe_3(CO)_{12}$ complex through the solid matrix which thereby limits the formation of $Fe(CO)_5$ and also from exclusion of the oxidative atmosphere within the polymer.

11. The activation energy for the solid state decomposition of $Fe(CO)_5$ in a polycarbonate matrix was observed to be higher than that of other systems studied. This is accompanied by extensive molecular weight breakdown in the polycarbonate and probably results from anionic attack at the ester group of the polymer backbone. This requires more energy to dissociate than the metal carbonyl bond. A higher activation energy is also noted for PMMA systems - the polymer again containing an ester group (though as a side function) which may facilitate association of the carbonyl.

12. Although photolytic solution decomposition of of $Fe(CO)_5$ proceeds via the formation of $Fe_2(CO)_9$, this is not observed in solid polymer matrices. The conversion of $Fe(CO)_5$ to $Fe_2(CO)_9$ is carbonyl diffusion dependent and since the experiment was carried out in air, it is required that the rate of diffusion of $Fe(CO)_5$ through the polymeric matrix to form $Fe_2(CO)_9$ be greater than the oxidative decomposition rate of $Fe(CO)_3$. It appears that the oxidation of $Fe(CO)_5$ is the favored reaction pathway because $Fe(CO)_5$ diffuses too slowly through the solid matrix to form $Fe(CO)_9$.

13. Gamma radiation decomposition of the metal carbonyl-polymer systems was relatively slow. This may be due to impurity effects (i.e., oxygen, monomer, moisture, remnant solvent). Radiolytic decompositions of $Fe_3(CO)_{12}$ systems proceeded much more rapidly than those with $Fe(CO)_5$. Gamma decompositions of metal carbonyl were achieved without significant degradation of the polymer matrix.

14. Electron beam decompositions of $Fe(CO)_5$ in a polycarbonate matrix (samples ~0.01 cm thick) were achieved in an SEM using a 30 KeV beam (approximately 1 μm beam size at sample). This decomposition

produced a "tree-like" morphology approximately 2 μm wide suggesting a thermal decomposition pathway via phonon interaction along the inelastically scattered electron paths within the matrix. Qualitatively the Fe-PC composite films prepared in this manner appear to show little polymer degradation and retain their mechanical integrity.

High energy electron beams (100 KeV and 12 Å beam size) demonstrated high resolution "writing" capability on thin $Fe(CO)_5$-polysulfone samples (~0.1 μm thick). Composite films treated in this manner produced fine lines ~50Å wide. Thinner film regions produced finer line decomposition patterns.

EDX data suggests the electron beam formation of FeS in PSF films, consistent with electron diffraction data for thermally treated $Fe(CO)_5$-PSF samples. Less polymer degradation was apparent in $Fe(CO)_5$ films treated with an electron beam relative to thermally decompositions.

15. The thermal decomposition of $Fe(CO)_5$ in polycarbonate leads to a heterophase containing γ-Fe_2O_3 and β-FeOOH (the latter resulting from the presence of chloride ions and atmospheric moisture in the system) accompanied by extensive degradation of the polycarbonate. Other polymers investigated were much more stable.

16. Though the thermal treatment of $Fe(CO)_5$ and $Fe_3(CO)_{12}$-PSF films leads to the formation of FeS (as well as α-Fe and iron oxides), only a slight decrease in molecular weight was observed. This suggests that there is limited attack by reactive iron carbonyl species on the sulfur or oxygen of the sulfone group within the polymer backbone. Some recombination of polymeric phenylene species may result in substantial maintenance of polymer chain length.

17. Much less degradation was observed for thermally treated polycarbonate films containing $Fe_3(CO)_{12}$ rather than $Fe(CO)_5$. This same trend was also demonstrated, though not so dramatically, for polysulfone composites.

18. Thermal decomposition of $Fe(CO)_5$ in a PC matrix leads to more extensive attack on the solid matrix than UV, gamma or electron beam treatments. Similarly, thermally treated $Fe(CO)_5$-PMMA films also show greater degradation of the polymer. The diffusion of reactive species created by thermal treatment of films may be enhanced by the increased temperatures making attack on the polymer more extensive as well as increasing oxidative reactions. In both PC and PMMA composites, γ-Fe_2O_3 and FeOOH particles were observed to form in thermally treated films.

19. Microparticle morphology and size appears to be a function of the polymer matrix and method of carbonyl decomposition used. Spherical morphologies of microparticles observed in PVF_2 and PC-$Fe(CO)_5$ composites are accompanied by interaction of the metal carbonyl with the polymer (ie. crosslinking or degradation). A smaller particle size range was observed in some PVF_2-$Fe(CO)_5$ composites suggesting that rapid decomposition at higher temperatures prevented clustering of the particles. SAXS also suggested that smaller particle size ranges may be achieved by photolytic than by thermal decomposition of carbonyl in polystyrene. The mobility of carbonyl species through the polymer to produce clustering is lower at the lower temperature used during photolysis than in thermal treatments.

20. Preparations in a reducing environment to prevent oxidation (H_2) produced amorphous iron clusters in PS and PSF-$Fe(CO)_5$ composites. For PSF-$Fe(CO)_5$ composites prepared in air, there appears to be an association of the iron species and sulfur. The thermal decompositions in a N_2 environment of $Co_2(CO)_8$ in PS produced α-Co predominantly.

21. The solid state decomposition of metal carbonyls in polymer matrices produces materials with diverse magnetic properties which are dependent upon the carbonyl and polymer. PC, PS and PMMA-$Fe(CO)_5$ composites containing γ-Fe_2O_3 and FeOOH microparticles exhibit diamagnetic behavior whereas PS-$Fe_3(CO)_{12}$ composites (with higher carbonyl and Pluronic surfactant additions) demonstrated paramagnetic behavior. In general, PSF-$Fe(CO)_5$ or $Fe_3(CO)_{12}$ composites were ferri-/ferromagnetic. Ferri/ferromagnetic properties were also observed in PVF_2-$Fe(CO)_5$ and $Co_2(CO)_8$ composites. In the PVF_2 systems both α-Fe and α-Co microparticles were observed. Normally these species demonstrate ferrimagnetic behavior though the M_2O_3 oxides (where M=Fe or Co) were also present in these composites.

22. In $Fe(CO)_5$-PVF_2 systems, the formation of γ-Fe_2O_3 and FeF_2 suggests dissplacement of the fluorine by reactions involving anionic species formed from $Fe(CO)_5$ and DMF. PVF_2 crosslinking was noted with DMF (heat treated to volatilize the solvent) even in the absence of the metal carbonyl. Thus, fluorine displacement can occur via reactions between the polymer and DMF.

23. Attempts to prepare polydimethylsiloxane films with $Fe(CO)_5$ produced composites with only a trace of metallic product due to volatilization of the carbonyl. This apparently proceeds by hydride formation resulting from $Fe(CO)_4$ reaction with HCl produced in the vulcanization of the siloxane. The volatile hydride leaves only small amounts of carbonyl decomposition products in the polysiloxane. Other siloxane curing systems may produce more satisfactory composites.

24. Thermal decompositions with $Co_2(CO)_8$ demonstrate the effect of oxygen upon the products. α-Co was predominantly formed in N_2 atmosphere whereas oxidation leads to CoO and Co_2O_3 in the presence of air. In a PVF_2 matrix, $Co_2(CO)_8$ decomposition leads to extensive crosslinking and the formation of CoF_2. In an O_2 free environment, the formation of predominantly α-Fe rather than oxide microparticles has also been indicated.

25. A major objective of this research, to produce fine metal dispersions in polymers, was achieved. Metal and/or metal oxide particles 25-200Å in size were produced in many systems as indicated by SAXS studies.

6. FUTURE RESEARCH

Specific recommendations for future research are presented below. These suggestions include not only interesting research areas showing particular promise but also recommendations to improve the simplicity of sample preparation and analytical techniques for various studies.

6.1 Preparation Techniques to Limit Metal Carbonyl Decomposition Prior to Incorporation into Polymer Thus Controlling Product Purity

A. Preparation of $Fe(CO)_5$-polymer systems should be done under inert atmospheres (i.e. within the glove box) to limit volatilization and decomposition of $Fe(CO)_5$. Volumes may be measured with calibrated pipettes and confirmed via atomic absorption analyses.

B. Preparation of $Co_2(CO)_8$ and $Fe_3(CO)_{12}$-polymer systems should be done within the glove box under inert atmospheres (including the weighing of the carbonyls) to prevent decomposition of the carbonyl prior to incorporation into polymer. Alternatively, various estimated amounts of carbonyl may be added to systems and quantitatively determined later via atomic absorption analyses.

6.2 Metal Carbonyl-Polymer Systems

A. Further studies with the carbonyl-polysulfone system are of interest in view of the facts that polysulfone retains much of its mechanical integrity following the decomposition reaction and that the decomposition products demonstrate ferri/ferromagnetic behavior.

B. Tetrahydrofuran should be evaluated as a solvent for the $Fe_3(CO)_{12}$-polymer systems as a means to improve the solubiity of this carbonyl.

C. The solubility of $Fe_3(CO)_{12}$ in Pluronics surfactant should be evaluated and a compatible polymer found to be used as the matrix polymer to maximize carbonyl loadings.

D. Viscosity studies are of interest to evaluate the extent (if any) of attack upon the polymer matrix in the solid state decomposition of $Fe_3(CO)_{12}$ in polycarbonate.

E. Metal products formed in decompositions of carbonyls in reducing environments are of interest. The concept of metal carbonyl decompositions in a reducing atmosphere coupled with higher carbonyl loadings may offer materials with unique magnetic behavior.

F. A more complete study of mixed metal carbonyl systems [ie. $Fe(CO)_5$-$Co_2(CO)_8$] should be pursued to determine possible chemical interactions occurring between the carbonyls and its effect upon the matrix material.

6.3 Decomposition Treatments

A. Photolytic and gamma radiation treatments should be pursued to verify that smaller particle sizes of the metal clusters may be obtained in this manner.

B. Gamma radiation polymerization of methyl methacrylate and styrene in the presence of $Fe_3(CO)_{12}$ or $Co_2(CO)_8$ is of interest. Monomers and solvents for these studies should be purified by distillation techniques to eliminate compounds which could react with the reactive carbonyl species created by the gamma radiation. Preparation of the samples should be done in CO or N2 environments

and sealed in tubes, thus eliminating air which could lead to oxide products. Prior to sealing of tubes, H_2 gas could be introduced. This preparation and consequent gamma radiation decomposition and polymerization could lead to metal incorporation into the polymer chain and/or metal in the zero valent state within the polymer.

C. Electron beam decomposition studies on these metal carbonyl-polymer systems should be pursued to more completely evaluate the limiting factors of metal carbonyl selected, carbonyl concentration, sample morphology (thickness), electron beam energy and mode of energy input. A finder TEM grid is recommended to locate decomposition areas for later study and characterization of decomposition products.

6.4 Analytical Techniques Recommended

A. A vibrating sample magnetometer or induction method is recommended to determine magnetic susceptibility of composite samples. A simple effective induction method is described by Barnett (127) and Elmore (128). These techniques would not only be more rapid, but also eliminate changes in magnetic properties resulting from the freeze-grinding procedure used to prepare samples for the Guoy balance.

B. Microtoming of embedded composite samples is preferred for TEM characterization studies. Though this technique is more tedious and time consuming, a more representative view of the composite morphology is provided. The most successful embedding and microtoming procedure is that described in Section 3.12.

C. Atomic absorption analyses is recommended for quantifying metal content of composites. This eliminates the problem that some metal may be retained within the precipitated polymer obtained in Vogel's 1,10-phenanthroline method.

APPENDIX A

CALCULATION OF ENERGY ABSORBED BY SAMPLE DURING ELECTRON BEAM DECOMPOSITIONS

I. In discussing with Dr. Bates the energetics of electron beam decompositions under the scanning electron microscope, it was concluded that there is negligible backscattering of electrons. This is based on:

η_{Fe} = backscattering coefficient of Fe = 0.3

$\eta_{polymer} = 0.05 = \eta_p$

and

$\eta_{alloy} = \Sigma W_i \eta_i$

where W_i = weight fraction of i component

then

$\eta_{alloy} = \eta_p (0.97) + \eta(0.03)$

(for a 15 wt. % $Fe(CO)_5$ composite)

$\eta_{alloy} = 0.038$

Thus we may assume that the specimen current is indicative of the entire beam energy (101).

II. At 25 KeV, an average specimen current of 4.18×10^{-8} amps (4.18×10^{-8} coulombs/sec) was recorded. We know there are 1.6×10^{-19} coulombs/eV (eV = electron charge), so the energy absorbed by the sample becomes:

$$4.18 \times 10^{-8} \quad \frac{\text{coulombs}}{\text{sec}} \times \frac{\text{eV}}{1.6 \times 10^{-19} \text{ coulombs}}$$

$$= 2.61 \times 10^{11} \frac{\text{eV}}{\text{sec}}$$

We also know 1 eV = 1.602×10^{-19} joules

so $2.61 \times 10^{11} \frac{\text{eV}}{\text{sec}} \times 1.602 \times 10^{-19} \frac{\text{joules}}{\text{eV}}$

$= 4.18 \times 10^{-8} \frac{\text{joules}}{\text{sec}}$ which is the energy absorbed by the sample during electron beam decomposition.

APPENDIX B

INTRINSIC VISCOSITY MEASUREMENTS AND CALCULATION OF VISCOSITY-AVERAGE MOLECULAR WEIGHT

I. Sample Preparation

A. Concentration C = 0.5 - 1.0g/100 ml

B. Enough sample to prepare a concentration in above range is weighed out exactly. The sample is then dissolved in an appropriate solvent (see Polymer Handbook) in a volumetric flask. Because at least 8 ml is needed for the measurement, the volume of solution should be greater than 10 ml (20-25 ml is recommended).

C. The solution should be filtered with a solvent-resistant filter prior to measurement.

II. Thermostat for Constant Temperature Bath

The temperature should be set at the appropriate temperature (according to the Polymer Handbook); Fluctuation of temperature should be within ± 0.01°C.

III. Viscometer

A. It should be kept clean and free from dust.

B. Cleaning Procedure

1. Chromerge cleaning solution can be used for cleaning
2. Rinse
3. Dry with vacuum aspirator. Do Not Heat in drying oven.

IV. Viscosity Measurement

A. Viscometer must be set exactly perpendicular

B. Solvent Viscosity:

1. 10 ml of the chosen solvent is added to the dry viscometer
2. Solvent flow time should be measured after equilibration of solvent temperature (at least 15 minutes)
3. Solvent flow time should be over 100 seconds. If times are less than 100 seconds, then a viscometer of a thinner capillary should be used.
4. The flow time fluctuation of three serial measurements should be within ± 0.1 seconds. (If not, check for dust in the capillary and temperature fluctuation in the constant temperature bath).

C. Sample Viscosity

1. First step
   a. 10 ml sample solution is added to the dry viscometer.
   b. Sample flow time should be measured after temperature equilibration.
   c. Three serial flow times should be measured. Fluctuation must be within 0.1 seconds (if not see IV-B(4)).
2. Second step
   a. 3 ml of solvent is added to viscometer to dilute sample solution. It should be mixed completely with sample solution.

b. Prior to measurement, capillary should be washed three times with the mixed solution.

c. Repeat IV-C(1)b and IV-C(1)c.

3. Third step

a. Repeat IV-C(2).

4. Fourth step

b. Repeat IV-C(2).

D. Calculations

1. Definitions

a. t_o = solvent flow time

b. t_1 = sample flow time

c. C = concentration in grams per deciliter

d. η_{rel} = relative viscosity

e. η_{sp} = specific viscosity

f. η_{red} = reduced viscosity

g. $\eta_{rel} = \frac{t_1}{t_o}$

h. $\eta_{sp} = \frac{t_1}{t_o}$

i. $\eta_{red} = \frac{\eta sp}{C}$

j. $[\eta]$ = intrinsic viscosity (I.V.)

2. Determination of I.V.

   a. Use linear curve fitting to extrapolate to zero

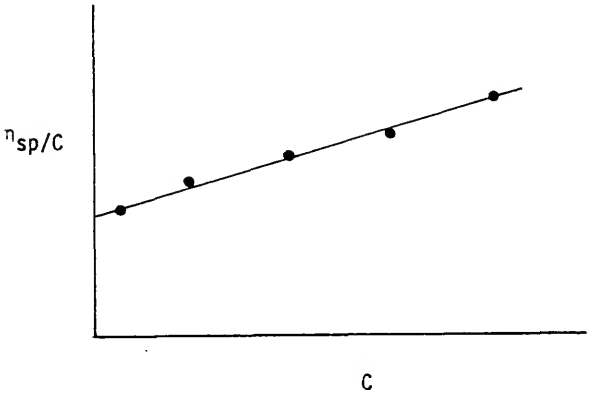

E. Then using the Mark-Houwink Equation (103), the appropriate values for K and a constants (35) and the determined [η], the viscosity - average molecular weight, $\bar{M}_v$, was calculated:

$$[\eta] = K\bar{M}_v^a$$

Nota Bene: Consult Polymer Handbook, Chapter IV-1, before starting for theory and selection of proper solvent.

APPENDIX C

DETERMINATION OF EXTINCTION COEFFICIENTS IN A POLYMERIC MATRIX

I. For 0.0684 gr PC-$Fe(CO)_5$ film solvated in 50 ml Vogel's 1,10-phenanthroline solution:

a. Absorbance (UV 396 nm) = A ≡ 0.143

b. Path length = d = 1.0 cm

c. Extinction Coefficient for iron in Vogel's solution (see standard curve Section 3.6):

$$\varepsilon_{UV} = 53.7 \frac{\text{ml soln}}{\text{mg Fe cm}}$$

So using Beer-Lambert's Law: $A = \varepsilon_{UV} d c_a$

where c_a = actual iron concentration in mg Fe/ml film.

and density of PC cast film = 0.89 $\frac{\text{gr film}}{\text{ml film}}$

$$c_a = \frac{A}{\varepsilon_{UV} d} = \frac{0.143 \text{ (50 ml)} \; 0.89 \frac{\text{gr film}}{\text{ml film}}}{53.7 \frac{\text{ml soln}}{\text{mg Fe cm}} \text{ (0.00684 gr film)}}$$

$$= 17.235 \frac{\text{mg Fe}}{\text{ml film}} = 0.3102 \frac{\text{M } Fe(CO)_5}{\text{L film}}$$

This calculation was done for a series of sequential $Fe(CO)_5$ concentrations in PC matrices.

II. Infrared absorptions at 1996 cm^{-1} were recorded for these same sequential $Fe(CO)_5$ concentrations in PC matrices.

Thus, plotting c_a as X and infrared absorbance as Y (providing all films are of uniform thickness d) a linear curve fit provides the best approximation for the slope of the curve: a value for ε_{IR} x d.

i.e.

c_a	Abs.
0.3102 $\frac{M\ Fe(CO)_5}{L\ film}$	2.0521
0.0601	0.8717
0.0207	0.5119
0	0

So $\frac{\varepsilon_{IR} x\ d}{d} = \varepsilon_{IR} = 2524\ \frac{L}{M\ Fe\ cm}$

APPENDIX D

CALCULATION OF RATE CONSTANTS FOR DECOMPOSITION REACTION OF METAL CARBONYLS IN A POLYMER MATRIX

I. Absorbance at 1996 cm^{-1} was measured at various times during thermal decomposition at 118°C for a PC-$Fe(CO)_5$ film 0.0042 cm thick (reference PC film of same thickness). Concentration of the metal carbonyl was determined using the Beer-Lambert law:

$A = \varepsilon dc$ where A = the measured IR absorbance at 1996 cm^{-1}

ε = observed extinction coefficient of carbonyl in polymer matrix

$= 2524 \quad \frac{\text{liter}}{\text{mole cm}}$ for a PC-$Fe(CO)_5$ film

d = film thickness = 0.0042 cm

c = concentration in moles $Fe(CO)_5$/liter

Absorbance A IR 1996 cm^{-1}	Concentration C moles/liter	Ln C	Time (sec)
1.949	0.184	-1.693	0
1.949	0.184	-1.693	2310
1.946	0.183	-1.698	11550
0.342	0.032	-3.433	78870
0.224	0.021	-3.856	92970
0.166	0.016	-4.155	101670
0.066	0.006	-5.073	168150

Using x = time (sec) and y = Ln C, a linear curve fit was done so that the statistically evaluated slope is the rate constant (with units of sec^{-1}). The rate constant k at 118°C for PC-$Fe(CO)_5$ was 2.20×10^{-5} sec^{-1}.

APPENDIX E.

CALCULATION OF MAGNETIC SUSCEPTIBILITY OF COMPOSITES BY THE GUOY METHOD

I. Given:

$$X_g = \frac{2g\Delta w' l}{H^2 M_s}$$

where X_g = gram magnetic susceptibility

g = gravitational constant

= 980.521 cm/sec^2

$\Delta W'$ = change in weight of sample upon application of magnetic field

l = length of sample (cm)

H = applied magnetic field (gauss)

M_s = sample mass (g)

Assume that:

a. the atmosphere surrounding the sample has negligible susceptibility.

b. $\Delta W' = W_f - W_o$

where W_f = weight of sample in applied field

W_o = weight of sample in absence of applied field

II. Then, since magnetic susceptibilities are additive:

X_{gc} = gram susceptibility of composite

X_{gp} = gram susceptibility of polymer

X_{gm} = gram susceptibility of metal

a = wt % polymer

b = wt. % metal (as determined from Vogel's method or atomic absorption analyses)

and a + b = 1

So that for $Fe(CO)_5$-PC

$Xgc = 0.976\ X_{gc} + 0.024\ X_{gm}$

REFERENCES

1. K. J. Wynne, "Conducting Polymers", N. R. Reviews, p. 38-47, (Spring 1981).

2. Encyclopedia of Polymer Science and Technology", Editors H. F. Mark, N. G. Gaylord and N. M. Bikales, Interscience Publishers, Vol. 11, p. 318 (1969).

3. Chemical and Engineering News "Organometallics Useful in Organic Synthesis", p. 34 (April 19, 1982).

4. R. B. King, Prog. Inorg. Chem., 15, p. 287 (1972).

5. T. Kitamura and T. Joh, J. Organometal. Chem., 65, p. 235 (1974).

6. J. K. Burdett, Coord. Chem. Rev., 17, p. 1 (1978).

7. A. J. Downs and S. C. Peake, Molecular Spectroscopy (Specialist Periodical Reports), The Chemical Society, London, 1, p. 523 (1973).

8. K. P. C. Vollhardt, J. E. Bercaw and R. G Bergman, J. Organometal. Chem., 97, p. 283 (1975).

9. J. B. Roucis and J. G. Ekerdt, J. Catalysis, 86, p. 32 (1984).

10. Marco-A De Paoli, J. Macromol. Sci.-Chem., A16(1), p. 251 (1981).

11. Marco-A. De Paoli, S. M. De Oliveira, F. Galembeck, J. Organometallic Chem., 193, p. 105 (1980).

12. Gyorgy Bor, URS K. Dietler, Piero Pino, A. Poe, J. Organometallic Chem., 154, p. 301 (1978).

13. M. D. Rausch, D. W. Macomber, K. Gonsalves, F. G. Fang, Z. R. Lin and C. U. Pittman, Proceedings of the ACS Division of Polymeric Materials Sci. and Engr., Washington DC, 49, p. 358, (August 1983).

14. C. T. Lynch and J. P. Kershaw, Metal Matrix Composites, published by CRC Press, Chpts. 1, 16 and 17 (1970).

15. A. E. Corradi, IEEE Trans. on Magnetics, MAG-14, p. 655 (1978).

16. G. Bates, J. Appl. Physics, 52(3), p. 2447 (March 1981).

17. K. T. Klabunde and Y. Tanaka, Proceedings of the 57th Colloid and Surface Science Symp., Abstract No. 30 (1983).

18. C. Flenniken, R. Tannenbaum and E. P. Goldberg, paper in preparation (1984).

19. E. Koerner von Gustorf, F. W. Grevels, Fortsch. Chem. Forsch., 13, p. 366 (1969).

20. W. Strohmeier, Angewandte Chemie (English Edition), 3, p. 730 (1964).

21. P. H. Hess and P. H. Parker, Jr., J. Appl. Poly. Sci., 10, p. 1915 (1966).

22. I. Wender, H. W. Sternberg and M. Orchin, J. Am. Chem. Soc., 74 (1), p. 1216 (1952).

23. W. Hieber and R. Werner, Chem. Ber., 90 p. 290 (1957).

24. F. A. Cotton and G. Wilkinson, Advanced Inorganic Chemistry, 3rd Edition, John Wiley and Sons, (1972).

25. J. A. Roth, P. Wiseman and L. Ruszala, J. Organometallic Chemistry, 240 p. 271 (1983).

26. J. P. Yesinowski and T. L. Brown, Inorg. Chem., 10 (5), p. 1097 (1971).

27. S. F. A. Kettle and L. E. Orgel, Chem. & Ind. (London), p. 49 (1960).

28. G. O. Schenck, E. K. von Gustorf and Mon-Jon Jun, Tetrahedron Letters, No. 23, p. 1054 (1962).

29. A. R. Luxmoore and M. R. Truter, Proc. Soc. Chem., p. 466 (1962).

30. L. Kirch and M. Orchin, J. Am. Chem. Soc., 81, p. 3597 (July 1959).

31. R. A. Dubois, P. E. Garrou, J. Organometallic Chem., 241, p. 69 (1983).

32. I. Wender, and P. Pino, Organic Synthesis via Metal Carbonyls, Vol. I, InterScience Publishers (1967).

33. G. F. Emerson, W. P. Ehrlich, W. P. Giering and D. Ehntholt, Trans. N.Y. Acad. Sci., 30(7), p. 1001 (1968).

34. T. A. Manuel, J. Org. Chem., 27, p. 3941 (1962).

35. H. W. Sternberg, R. Markby and I. Wender, J. Am. Chem. Soc., 78, p. 5704 (1956).

36. H. W. Sternberg, R. Markby and I. Wender, J. Am. Chem. Soc., 79, p. 6116 (1957).

37. R. F. Heck and D. S. Breslow, J. Am. Chem. Soc., 83, p. 4023 (1961).

38. I. Wender, S. Methlen, S. Ergun, H. W. Sternberg and H. Greenfield, J. Am. Chem. Soc., 78, p. 5401 (1956).

39. H. Reihlen, A. Gruhl, G. Hessling and O. Pfrengle, Ann. Chem., 482, p. 161 (1930).

40. W. Reppe and H. Vetter, Ann. Chem., 582, p. 133 (1953).

41. B. F. Hallam and P. L. Pauson, J. Chem. Soc., p. 642 (1958).

42. H. Adkins and G. Krseki, J. Am. Chem. Soc., 71, p. 3051 (1944).

43. J. E. Arnet and R. Pettit, J. Am. Chem. Soc.-Communications to the Editor, 83, (July 5, 1961).

44. R. B. King, T. A. Manuel and F. G. A. Stone, J. Inorg. and Nucl. Chem., 16, p. 233 (1961).

45. T. H. Whitesides and J. P. Neilan, J. Am. Chem. Soc., 95, p. 5811 (1973).

46. H. D. Murdoch and E. Weiss, Helv. Chem. Acta, 45(1), p. 1156 (1962).

47. R. F. Heck, C. R. Boss, J. Am. Chem. Soc., 86, p. 2580 (1964).

48. H. J. Dauben and D. J. Bertelli, J. Am. Chem. Soc., 83, p. 497 (1961).

49. A. Davison, M. L. H. Green and G. Wilkinson, J. Chem. Soc., Part 3, p. 3172 (1961).

50. H. J. Dauben, Jr., L. R. Honner and D. J. Bertilli, 15th Southwest Regional meeting ACS, Baton Rouge, LA., Abstracts, p. 89 (December 1959).

51. H. J. Dauben, Jr., and L. R. Honnen, J. Am. Chem. Soc., 80, p. 5570 (1958).

52. J. J. Lagowski, Quart. Revs. Chem. Soc., 13, p. 233 (1959).

53. R. Pettit and G. F. Emerson, Advances in Organometallic Chemistry, Vol. 1, p. 1, Academic Press, N.Y. (1964).

54. A. J. Birch, P. E. Cross, J. Lewis, D. A. White and S. B. Wild, J. Chem. Soc., Part A, p. 332 (1968).

55. C. E. Coffey, J. Am. Chem. Soc., 83, p. 1623 (1961).

56. G. F. Emerson, L. Watts and R. Pettit, J. Am. Chem. Soc., 87, p. 131 (1965).

57. J. Lewis and R. Whyman, I. Chem. Soc., p. 6027 (1965).

58. D. M. Adams, D. J. Cook and R. D. W. Kemmit, Chem. Comm., p. 103 (1966).

59. P. P. Singh, R. Rivest, Canadian, J. Chem., 46, p. 1773 (1968).

60. R. J. Angelici, Organometal. Chem. Rev., 3, p. 173 (1968).

61. A. J. Lovinger, Science, 220 (No. 4602), p. 1115 (June 1983).

62. R. G. Ford, High-Tech Materials Alert, No. 4 ed., publisher K. A. Kovaly (April 1984).

63. H. Tabei, S. Nara and K. Matsuyana, Japanese Patent No. 114,370 (1973).

64. I. S. Jacobs and C. P. Bean, Phys. Review, 100 (4), p. 1060 (November 1955).

65. R. W. Chantrell, J. Sidhu, P. R. Bissell and P. A. Bates, J. Appl. Phys., 53 (11), p. 8341 (November 1982).

66. R. Kaiser, G. Miskolczy, J. Applied Phys., 41(3), p. 1064 (March 1970).

67. R. Moskowitz and R. E. Rosenweig, Appl. Phys. Lett., 11, p. 301 (1967).

68. F. R. Eirich, F. Rowland, R. Bulas and E. Rathstein, Am. Chem. Soc., Editor S. Ross, Ed. p. 109, ACS Washington D.C. (1965).

69. J. R. Thomas, J. Appl. Phys., 37, p. 2914 (1966).

70. C. H. Griffiths, M. P. O'Horo and T. W. Smith, J. Appl. Phys., 50(11), p. 7108 (1979).

71. T. W. Smith and D. Wychick, J. Phys. Chem., 84, p. 1621 (1980).

72. M. Berger, and T. A. Manuel, J. Poly. Sci., 4(A-1) p. 1509 (1966).

73. R. R. Hampton, Analytical Chem., 21(8), p. 923 (1949).

74. R. W. Chantrell, J. Popplewell and W. S. Charles, IEEE Transactions on Magnetics, Vol. MAG-14 (5), p. 975 (September 1978).

75. B. Delmon and G. J. Jannes, Catalysis: Heterogeneous and Homogeneous, Elsevier Amsterdam (1975).

76. E. G. Derouane and J. B. Nagy, J. Catalysis, 46, p. 434 (1977).

77. C. U. Pittman, Jr., Polymer Supported Reactions in Organic Synsthesis, Editors P. Hodge and D. C. Sherrington, John Wiley and Sons, New York (1980).

78. C. U. Pittman, Jr., Organometallic Reactions and Structure, 6, p. 1 (1977).

79. G. Strukul, P. D' Olimpio, N. Bonevento, F. Pinna and M. Graziani, J. Mol. Catal., 2, p. 179 (1977).

80. J. Manassen and Y. Dror, J. Mol. Catal., 3, p. 227 (1977/78).

81. A. Gayot, C. H. Graillat and M. Bartholin, J. Mol. Catal., 3, p. 39 (1977/78).

82. A. L. Lyman and F. W. Kavanagh, Proc. Am. Petrol. Inst., Sect. III, 39, p. 296 (1959).

83. B. J. Fontana and J. R. Thomas, J. Phys. Chem., 65, p. 480 (1964).

84. B. J. Fontana, J. Phys. Chem., 67, p. 2360 (1963).

85. Introduction to Polymer Science and Technology, Editors H. S. Kaufman and J. J. Falcetta, Wiley-Interscience (1977).

86. Modern Plastics Encyclopedia, McGraw-Hill (1983-84).

87. W. Schnabel, Polymer Degradation-Principles and Practical Applications, MacMillan Publishing Co., Inc., N.Y., Hander International (1981).

88. F. Galembeck, C. C. Ghizoni, C. A. Ribeiro, H. Vargas and L. C. M. Miranda, J. Appl. Poly. Sci., 25, p. 1427 (1980).

89. F. Galembeck, E. Galembeck, H. Vargas, L. A. Ribeiro, L. C. M. Miranda and C. C. Glizoni, Surface Contamination, Vol. 1, Editor K. L. Mittal ed., Plenum Press (USA), p. 57 (1979).

90. T. Cassen, N. Geacintov and G. Ostei, Nature, 196, p. 1089 (1962).

91. R. B. Hitam, R. H. Hooker, K. A. Mahmoud, R. Narayanaswamy and A. J. Rest, J. Organometal. Chem., 222(C9) (1981).

92. R. H. Hooker and A. J. Rest, J. Organometallic Chem., 249, p. 137 (1983).

93. J. A. McIntyre, J. Phys. Chem., 74, p. 2403 (1970).

94. A. G. Massey and L. E. Orgel, Nature, 191, p. 1387 (1961).

95. C. L. Flenniken, S. Reich, M. Levy and E. P. Goldberg, Proceedings of 57th Colloid and Surface Sci. Symp, Abstract No. 33 (1983).

96. C. L. Flenniken and E. P. Goldberg, paper in prep.

97. S. Reich and E. P. Goldberg, J. Poly. Sci.: Polymer Physics Edition, 21, p. 869 (1983).

98. Vogel's Textbook of Quantitative Inorganic Analysis, 4th ed., Revised J. Bassett, R. C. Denney, G. H. Jeffery and J. Mendham, Longman Grp. Ltd., p. 742 (1978).

99. M. Block, Handbook of Decomposition Methods, International, London (1979).

100. Feldman Christian, AA Spectroscopy, Wiley, New York (1970).

101. B. D. Cullity, Elements of X-ray Diffraction, 2nd Ed., Addison Wesley Publishing Company, Inc. (1978).

102. R. T. Morrison and R. N. Boyd, Organic Chemistry, 2nd Ed., Allyn and Bacon, Inc. (1971).

103. von K. Noack, Helvetica Chimica Acta, XLV, Fasciculus VI (No. 216), p. 1847 (1962).

104. A. W. Adamson A Textbook of Physical Chemistry, Academic Press, Inc., p. 106 (1973).

105. F. W. Billmeyer, Introduction to Polymer Science and Technology, Wiley-Interscience (1977).

106. W. Hieber, N. Kahlin, Chem. Ber., 91 p. 2223 (1958).

107. P. Chini and V. Albano, J. Organometallic Chem., 15, p. 433 (1968).

108. J. C. Gressier, G. Levesque, H. Paten and F. Varret, Proceedings of the ACS Division of Polymeric Materials Sci. and Engr., Washington DC, 49, p. 358 (Aug. 1983).

109. J. Kleinberg, Inorganic Synthesis Vol. VIII, Chpt. VII, Triiron Dodecacarbonyl, McGraw Hill Publishers, p. 93 (1953).

110. H. W. Thompson, and A. P. Garrett, J. Chem. Soc., London, 28(2), p. 524 (1934).

111. E. Speyer and H. Wolf, Chem. Ber., 60, p. 1424 (1927).

112. Bor Gyorgy, URS K. Dietler, J. Organometallic Chem., 191, p. 295 (1980).

113. P. S. Braterman, Metal Carbonyl Spectra, Academic Press (1975).

114. G. Odian, Principles of Polymerization, 2nd edition, John Wiley and Sons (1981).

115. Merck Index, 9th Edition, Editors M. Windholz, S. Budavari, Merck & Co., Inc. (1976).

116. F. Unguory and L. Marko, J. Organometallic Chem., 71, p. 283 (1974).

117. G. L. Geoffroy, M. S. Wrighton, Organometallic Photochemistry, Academic Press (1979).

118. H. C. Clark and C. J. Willis, J. Am. Chem. Soc., 82, p. 1888 (1960).

119. M. Poliakoff and J. J. Turner, J. Chem. Soc., Part A, p. 2403 (1971).

120. P. W. Selwood, Magnetochemistry, 2nd Ed., Interscience Publishers, Inc. (1956).

121. P. Nilakantan, Proc. Indian Acad. Sco., 7, p. 38 (1938).

122. E. Cotton-Feytis, E. Faure-Fremiet, Compt. Rend., 214, p. 996 (1942).

123. A. K. Bose and D. P. Raychaudhuri, Science and Culture, 3, p. 246 (1937).

124. D. Beischer and A. Winkel, Naturwissenschaften, 25, p. 420 (1937).

125. L. V. Azaroff and J. J. Brophy, Electronic Processes in Materials, McGraw Hill Book Company (1963).

126. J. I. Goldstein, D. E. Newbury, P. Echlin, D. C. Joy, C. Fiori, E. Lifshin, Scanning Electron Microscopy and X-Ray Microanalysis, Plenum Press, New York and London (1981).

127. S. J. Barnett, J. Appl. Phys., 23, p. 975 (1952).

128. W. C. Elmore, Phys. Rev., 54, p. 1092 (1938).

BIOGRAPHICAL SKETCH

Cindy Lou Flenniken was born Friday the 13th, June, 1952 in the agricultural community of Bement, Illinois. She was educated in Bement and graduated from Bement High School in 1970.

Following graduation, the author studied at the University of Illinois and in May of 1974 received her Bachelor of Science Degree with honors in Food Science. She then pursued a career in the Detroit, Michigan area briefly with Detroit Public Schools Food Science Management, but primarily as a Materials Chemist with Energy Development Associates - a Gulf and Western subsidary researching a zinc chloride battery for load leveling and electric vehicle applications. During this time she attended night school at Oakland University (Rochester, Michigan), Lawrence Institute of Technology and Wayne State University.

In 1979, she entered graduate school in the Department of Materials Science and Engineering, University of Florida. While in graduate school, the author was a graduate research associate and president of the Society of Plastics Engineers and member of the Experimental Aviation Association.

I certify that I have read this study and that in my opinion it conforms to acceptable standards of scholarly presentation and is fully adequate, in scope and quality, as a dissertation for the degree of Doctor of Philosophy.

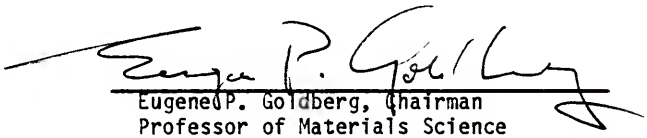

Eugene P. Goldberg, Chairman
Professor of Materials Science
and Engineering

I certify that I have read this study and that in my opinion it conforms to acceptable standards of scholarly presentation and is fully adequate, in scope and quality, as a dissertation for the degree of Doctor of Philosophy.

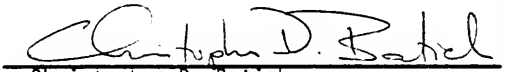

Christopher D. Batich
Associate Professor of Materials Science
and Engineering

I certify that I have read this study and that in my opinion it conforms to acceptable standards of scholarly presentation and is fully adequate, in scope and quality, as a dissertation for the degree of Doctor of Philosophy.

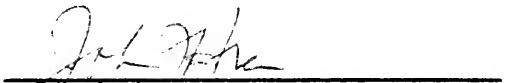

John J. Hren
Professor of Materials Science
and Engineering

I certify that I have read this study and that in my opinion it conforms to acceptable standards of scholarly presentation and is fully adequate, in scope and quality, as a dissertation for the degree of Doctor of Philosophy.

George Butler
Professor of Chemistry

This dissertation was submitted to the Graduate Faculty of the College of Engineering and to the Graduate Council, and was accepted as partial fulfillment of the requirements for the degree of Doctor of Philosophy.

Decmeber, 1984

Hubert A. Beves
Dean, College of Engineering

Madelyn Lockhart
Dean for Graduate Studies and Research